REMODELING ANTIBODIES FROM THE INSIDE OUT: FUNCTIONAL ENGINEERING OF FULL-LENGTH ANTIBODIES IN THE CYTOPLASM OF BACTERIA

A Dissertation

Presented to the Faculty of the Graduate School

of Cornell University

In Partial Fulfillment of the Requirements for the Degree of

Doctor of Philosophy

by

Michael-Paul Robinson

December 2017

REMODELING ANTIBODIES FROM THE INSIDE OUT: FUNCTIONAL ENGINEERING OF FULL-LENGTH ANTIBODIES IN THE CYTOPLASM OF LIVING BACTERIA

Michael-Paul Robinson, Ph. D.

Cornell University 2017

Antibodies are indispensable tools in many research, diagnostic, and clinical applications. Current methods for producing immunoglobulin G (IgG) antibodies in engineered cells often require refolding steps or secretion across one or more biological membranes. In this work, we describe a robust expression platform for biosynthesis of full-length IgG antibodies in the *Escherichia coli* cytoplasm. IgGs with clinically relevant antigen- and effector-binding activities are readily produced in the *E. coli* cytoplasm by grafting antigen-specific variable heavy and light domains into a cytoplasmically stable framework and remodeling the fragment crystallizable domain with amino acid substitutions that promote binding to Fcγ receptors. The resulting cytoplasmic IgGs —named "cyclonals"— effectively bypass the potentially rate-limiting steps of membrane translocation and glycosylation. Standard antibody discovery techniques often require multiple labor intensive and technically challenging steps that limit the pace at which valuable antibodies can be developed. We addressed this challenge by adapting the cyclonal platform for identification of specific antibody-antigen binding by implementing two different survival selections. Finally, we describe isolation of high-affinity full-length IgGs from combinatorial libraries after just a single round of selection. Taken together, these results show that our *E. coli*-based platform constitutes a simple yet powerful alternative for rapidly engineering full-length IgG antibodies.

BIOGRAPHICAL SKETCH

Michael-Paul Robinson grew up in Cleveland, OH, where he attended John F. Kennedy High School. After graduating, he attended Case Western Reserve University where he performed research in the lab of Professor Daniel J. Lacks. In 2009, he graduated from Case Western Reserve with a Bachelor of Science in Chemical Engineering. The same year, he began his graduate studies at Cornell University. There, he joined the lab of Professor Matthew P. DeLisa in February 2010. While at Cornell, Michael-Paul Robinson was awarded a Sloan/Colman Fellowship. He was also awarded a National Science Foundation Graduate Research Fellowship (NSF-GRFP) and a Ford Foundation Predoctoral Fellowship in 2011. In 2016, Michael-Paul was inducted into the Edward A. Bouchet Graduate Honor Society. Michael-Paul earned his Doctor of Philosophy in Chemical and Biomolecular Engineering in August 2017.

To my grandmother who believed in me when I did not believe in myself

You “thought I could”, You “knew I could”, I did

To Professor Emeritus Robert V. Edwards who saw potential in me and inspired me to pursue a PhD

ACKNOWLEDGMENTS

I must first acknowledge my thesis advisor and mentor Professor Matthew DeLisa whose guidance has been invaluable throughout my graduate studies. I acknowledge past and present members of the DeLisa research group for enlightening discussions, their indispensable insights, and vital feedback. I thank Dr. Mehmet Berkmen and his lab at New England Biolabs for their efforts on this project. I am also eternally grateful for the support that I received from Diversity Programs in Engineering (DPE). Much of the work in this dissertation would not have been possible without the contributions of the outstanding students I had the pleasure of mentoring throughout my graduate studies. Those students; namely, Alana Szkodny, Xiaolu Wen, Christen Peterson, Matthew Chang, and Daniel Tien all made significant contributions to this work while in the lab. Finally, I thank my family for their unwavering support and encouragement throughout this entire process.

This work was supported by the National Institutes of Health grant # AI092969-01A1 (to M.P.D. and M.B.), a Ford Foundation Predoctoral Fellowship (to M.-P.R.), and a National Science Foundation Graduate Research Fellowship (to M.-P.R.).

TABLE OF CONTENTS

LIST OF FIGURES

LIST OF TABLES

CHAPTER 1

CHALLENGING THE BOUNDARIES OF MONOCLONAL ANTIBODY ENGINEERING

Introduction

Over the last century researchers have sought to develop technologies and applications using the special properties of antibodies. As a tool for molecular detection and identification, antibodies have virtually unmatched diversity and can possess exquisite specificity. Specificity, immunological function, and the ability to modulate these characteristics continue to increase the importance of antibodies to modern therapeutics. The widespread use and continued growth of these antibody-based applications continues to drive innovation in antibody discovery, antibody engineering, and antibody production. In this chapter, the basic principles of antibodies will be introduced and the seminal advances in antibody-based technology will be presented. The groundbreaking research that provides the theoretical context for the work in this dissertation will also be reviewed. Additionally, the current challenges facing antibody engineering and discovery will be assessed providing motivation for the chapters to follow.

Natural antibodies

Natural antibodies, also known as immunoglobulins or Ig, are globular proteins that are produced by a host's immune system to help eliminate pathogens. Antibodies bind to unique molecules called antigens, such as membrane proteins or oligosaccharides, to elicit an immune response[1]. The specific part of an antigen that an antibody recognizes is called the epitope. Antibodies can confer immunity by preventing pathogens from interacting with host cells, targeting pathogens to immune cells called phagocytes for destruction, or activating complement pathways that enhance immune responses[2, 3].

Antibodies are found in two forms; as membrane bound antigen receptors (BCRs) on B lymphocytes or B cells, and as soluble proteins secreted by terminally differentiated B cells known as plasma B cells. Polyclonal antibodies are those produced in response to pathogens and have been secreted by many different B cell clones[1]. These antibodies recognize a number of different epitopes. Monoclonal antibodies are those that are produced from one single B cell clone. Monoclonal antibodies (mAbs) recognize only one particular epitope[2].

All immunoglobulins are constructed similarly from paired heavy and light polypeptide chains. There are two types of light chains, λ and κ, that are functionally identical and can pair with any of the 5 isotypes of heavy chain[2]. However, any particular immunoglobulin can only have one type of light chain. There are 5 different classes or isotypes of Igs, namely IgA, IgD, IgE, IgG, and IgM. These isotypes differ by the identity of their heavy chains. IgG is the isotype generated with the highest specificity. IgGs are extremely effective opsonins, molecules that mark pathogens for phagocytosis. IgGs are also effective at activating the complement pathway. As a result, IgGs provide the main source of antibody based immunity and thusly are the isotype used in most mAb therapeutic formulations.

Immunoglobulin G antibodies, or simply IgG, are the most abundant antibody class found in mammalian serum. The IgG class accounts for about ~75-80% of circulating antibody and is one of the most abundant proteins in the blood serum [1, 4].

IgGs are assembled from two light chains and two heavy chains. Two disulfide bonds covalently link the two heavy chains in the hinge region. A light chain is covalently linked to each heavy chain by an inter-chain disulfide bond forming a tetrameric full-length IgG antibody (**Figure 1.1a**). The IgG light chain (LC) is composed of two domains: a variable light (V_L) domain located at N terminus, and a

constant light domain (C_L) located at the C terminus (**Figure 1.1a**). The IgG heavy chain is composed of 4 domains: the variable heavy domain (V_H), at the N terminus, and 3 constant domains (V_H-C_H1-C_H2-C_H3) (**Figure 1.1a**). The heavy chain C_H1 domain is connected to the C_H2 domain by a flexible linker region called the hinge. The light chain (V_L-C_L) together with the V_H and C_H1 domains form a fragment known as the antigen-binding fragment (Fab) ((**Figure 1.1b**). A homodimer of the C_H2 and C_H3 domains form the Fc or crystallizable fragment. In mammalian cells, an oligosaccharide is covalently linked to a conserved asparagine residue (N297) in C_H2, a post-translational modification called glycosylation (**Figure 1.1b**) [5]. Glycosylation in the Fc fragment is integral for an IgG to be recognized by cells of the immune system (effector cells) through binding of the Fc by Fc receptors displayed on the surface of these cells [2]. Fc receptor binding can initiate phagocytosis, antibody-dependent cell-mediated cytotoxicity (ADCC), and complement dependent cytotoxicity (CDC). ADCC and CDC are two mechanisms by which antibodies facilitate the destruction of pathogen-infected and abnormal host cells. Evidence suggests that therapeutic IgG antibodies also utilize the ADCC and CDC mechanisms to potentiate the destruction of tumor cells [5].

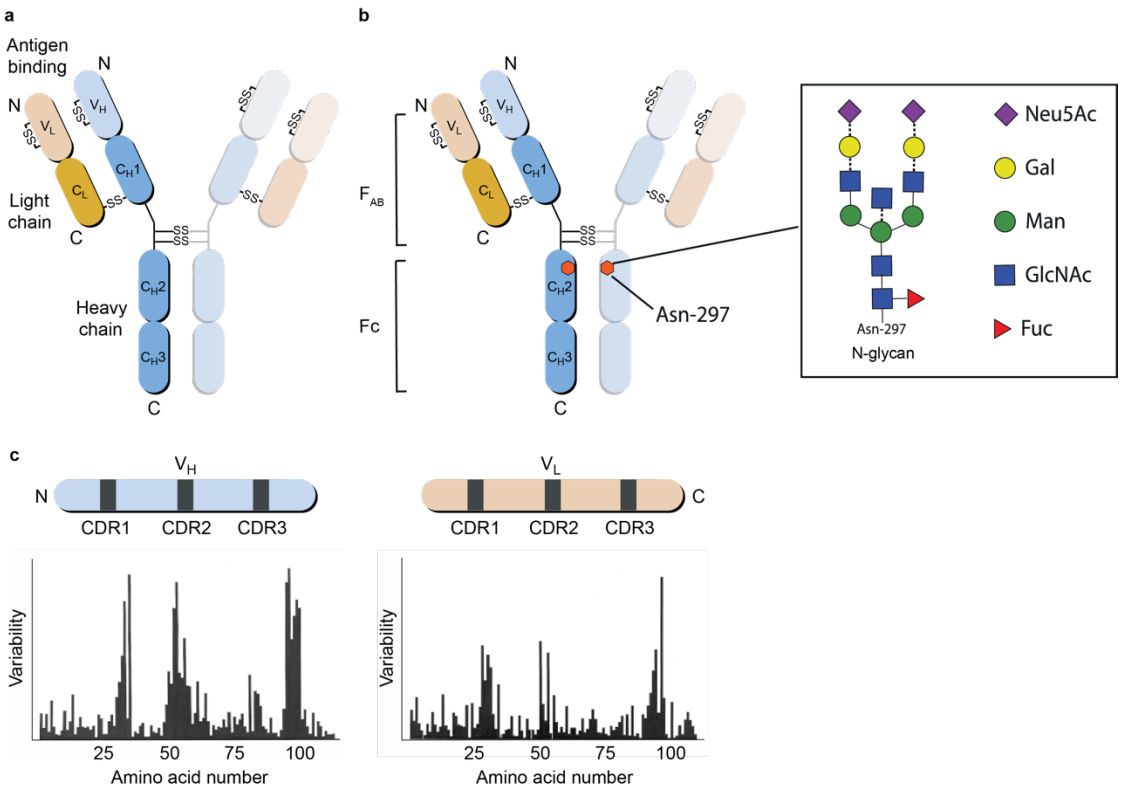

.0

Figure 1.1. Structure of a Full-length IgG antibody. (a) Antibodies are comprised of two identical heavy (H) chains (blue) and two identical light (L) chain (orange), linked by interchain disulfide bonds (-SS-). Intradomain disulfide bonds are also indicated for the variable regions of the H and L chains (V_H and V_L), which carry the antigen-recognition regions of the antibody (the antibody combining site). The L chains possess one constant (C_L) domain and the H chains contain three. (b) Schematic indicating the Fab (V_H-C_H1 of the heavy chain; V_L-C_L of the light chain) and Fc regions (C_H2-C_H3) of the antibody. Glycosylation sites at asparagine 297 (Asn-297) in C_H2 domains are indicated by hexagons. The general structure of N-linked glycosylation is shown inset; core structures indicated by solid lines and variable structures by dotted lines comprising of Fucose (Fuc), N-Acetylglucosamine (GlcNAc), Mannose (Man), Galactose (Gal) or N-Acetylneuraminic acid (Neu5Ac). (c) Linear depiction of the V_H and V_L domains. The three CDRs of each domain are the hypervariable sequences that are the key contributors to antibody diversity. Images adapted from Lobato and Rabbitts[6] and Elgundi[7].

The antigen binding properties of IgGs are localized within the V_L and V_H domains of the antibody (**Figure 1.1c**). The amino acid sequence varies the greatest between IgGs in these domains. However, within both the V_H and V_L domains, the sequence varies the greatest within three flexible loops. These loops are commonly

called the complementarity determining regions (CDRs) or hyper variable regions (HVs). The V_L and V_H CDRs that are brought together by the pairing of heavy and light chains form the antigen-binding site[2]. CDR3 is the most variable in both V_L and V_H. However, CDR3 of the V_H domain exhibits the highest variability of the six CDRs in the antigen-binding site (**Figure 1.1c**). Consequently, this CDR is often the most critical for high-affinity antigen binding.

Each domain of the heavy and light chain contains an intra-chain disulfide bond. Altogether, a full-length IgG requires 16 disulfide bonds to achieve its native structure (**Figure 1.2**).

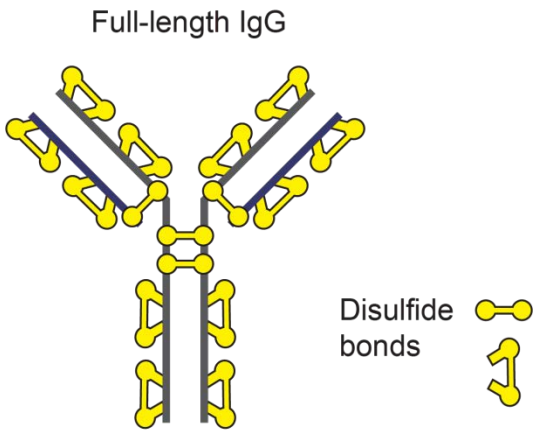

Figure 1.2 Disulfide bond connectivity of Full-length IgG antibodies. Schematic representation of the native disulfide bonds of a correctly folded IgG antibody. Light chain (blue) participates in an intermolecular bond with a heavy chain (gray). Each heavy chain makes two intermolecular disulfide bonds with the other heavy chain. Each domain has a stabilizing intramolecular disulfide bond. Redox state of cysteines (yellow balls) are indicated (oxidized = ball + stick). Figure adapted from Robinson et al[8].

Disulfide bonds in proteins

Disulfide bonds in proteins are post-translational modifications formed through the oxidation of two sulfhydryl or thiol groups (– **SH**) from individual cysteine residues. Biologically, formation of these covalent linkages is vital to the stability, structure, and activity of many proteins. Because of the increased stability disulfide

bonds provide, they are often found in proteins secreted out of the cell, such as antibodies[9]. Understanding the nature of disulfide bonds and their formation has long been a highly active area of research.

Disulfide bonds are most often formed and broken (reduced) i*n vivo* via the thiol-disulfide exchange mechanism. Thiol-disulfide exchange reactions are initiated by thiol oxidoreductases or small thiol containing molecules, such as glutathione[10]. These reactions proceed by an exchange of electrons between free thiol groups and an existing disulfide bond. Proteins belonging to the thiol disulfide oxidoreductase class often share a conserved Cys-X-X-Cys (where X is any amino acid) active site motif located in a domain structurally homologous to the ubiquitous protein thioredoxin[9].

Most organisms in each domain of life have evolved reducing pathways in the cytoplasm. Therefore, proteins do not normally acquire stable disulfide bonds within the cytosol. As a result, proteins needing disulfide bonds are transported to extra-cytoplasmic compartments where the machinery for catalysis of disulfide bond formation resides[11]. In eukaryotes, proteins are targeted to the endoplasmic reticulum to acquire stable disulfide bonds. Gram-negative bacteria, such as *E. coli*, transport proteins to the periplasm if they must be modified with disulfide bonds[10].

Disulfide bonding in the periplasm of E. coli

The periplasm of Gram-negative bacteria is a compartment located between the inner membrane which surrounds cytoplasm and the outer membrane which is exposed to the extracellular environment. In *E. coli*, stable disulfide bond formation is catalyzed in the periplasm in two stages: (1) oxidation and (2) isomerization. The Dsb (Disulfide bond formation) proteins are responsible for these two tasks [12, 13](**Figure 1.3)**.

Stage 1, the oxidation of disulfide bonds, is catalyzed by the DsbAB pathway. DsbA is a soluble periplasmic protein and is the primary catalyst of disulfide bond

formation in *E. coli* [14]. DsbA catalyzes the formation of disulfide bonds by donating its oxidized disulfide to a substrate protein (**Figure 1.3**). After donating its disulfide bond, DsbA is in its reduced form and must be reoxidized in order to catalyze another thiol-disulfide exchange[15]. DsbB, an integral membrane protein, performs the reoxidation of DsbA and transfers the electrons to a quinone [16-18](**Figure 1.3)**. The electrons are in turn transferred along the electron transport chain to a terminal election acceptor (e.g. molecular oxygen) [18, 19].

DsbA introduces disulfide bonds into proteins non-specifically, most often in a consecutive manner[20]. Therefore, DsbA often incorrectly oxidizes proteins that require non-consecutive disulfide bonds. Disulfide bonds that are misoxidized are corrected (isomerized), during stage (2) by the DsbCD pathway [21, 22](**Figure 1.3)**. Contrary to DsbA, the active site cysteines of DsbC must be in a reduced state to perform its function as an isomerase [23, 24]. To be regenerated after acting on a substrate, DsbD, a second Dsb integral membrane protein, reduces DsbC[23]. Ultimately, the reducing power of DsbD originates in the cytoplasm as it is reduced by thioredoxin[24](**Figure 1.3)**.

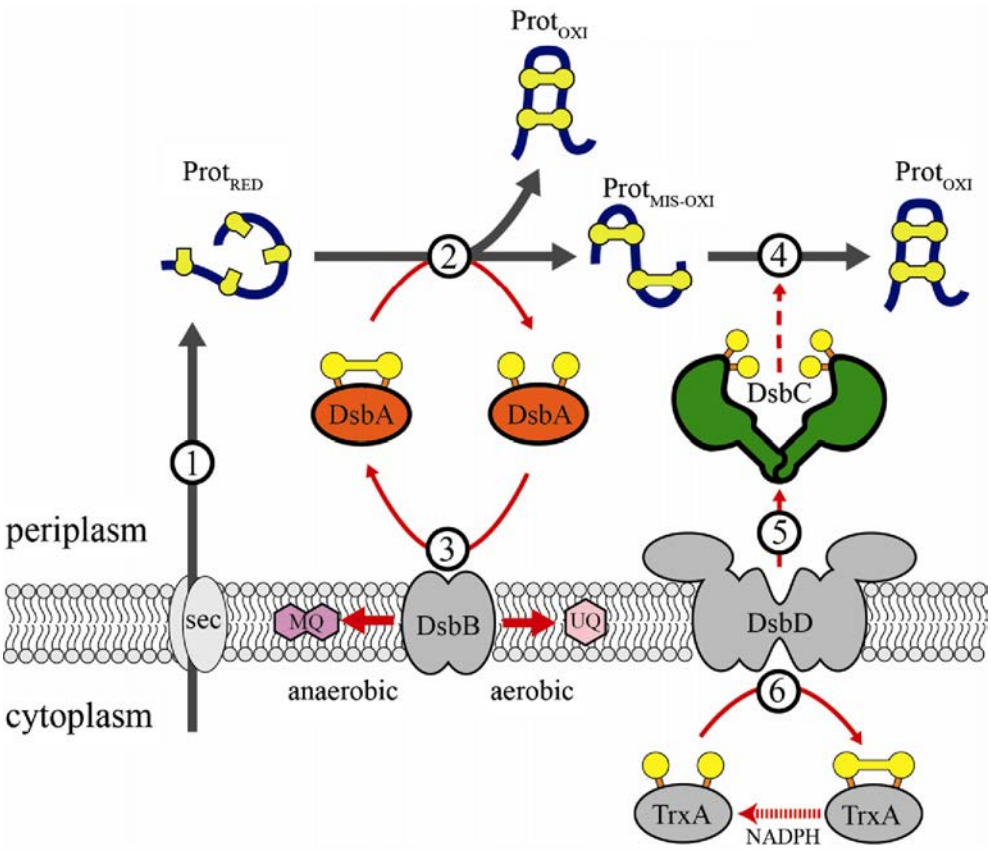

Figure 1.3 Disulfide bonding in the periplasm. (1) A substrate protein which requires disulfide bonds for its folding is exported to the periplasm in its reduced non-disulfide bonded state (ProtRED), usually via the sec pathway. (2) DsbA forms a disulfide-bonded complex with its reduced substrate resulting in the formation of a disulfide bond in the substrate protein (ProtOXI) and the reduction of DsbA's active site cysteines. (3) DsbA is reoxidized by the inner membrane protein DsbB, which donates the electrons it has received from DsbA either to ubiquinone (UQ) in aerobic conditions or to menaquinone (MQ) in anaerobic conditions. (4) If the substrate protein is misoxidized (ProtMIS-OXI) by DsbA, the misfolded protein is recognized by DsbC and is either isomerized to its native state or reduced, allowing DsbA to have another chance at correctly oxidizing the protein. (5) DsbC is maintained in its active reduced state by the inner membrane protein DsbD. (6) DsbD receives its electrons from the cytoplasmic thioredoxin (TrxA) which ultimately receives its electrons from the cytoplasmic pool of NADPH. Cysteines are represented as yellow balls in their reduced state or as sticks in their disulfide-bonded state. Grey arrows show products obtained after each step, whereas red arrows represent oxidation/reduction reactions. Figure taken from Berkmen[9].

Thiol reduction pathways in the cytoplasm of E. coli

In *E. coli,* cysteines in cytoplasmic proteins are maintained in a reduced state by the two main thiol reduction pathways, the thioredoxin and glutaredoxin pathways [25](**Figure 1.4)**. There are two thioredoxins natively expressed in the cytoplasm of *E. coli,* thioredoxin 1 (encoded by *trxA*), and thioredoxin 2 (encoded by *trxC*) [26]. Thioredoxins reduce disulfide bonds formed in a number of cytoplasmic enzymes during their catalytic cycles, thereby regenerating them for another round of catalysis [26, 27]. Ribonucleotide reductase is an essential substrate of the thioredoxin pathway as it is an enzyme that is involved in nucleotide synthesis. During the reduction of a substrate protein, thioredoxin is converted to its oxidized state with its active site cysteines paired in a disulfide bond[28]. The oxidized form of thioredoxin cannot perform its normal functions and must be reduced by a second oxidoreductase, thioredoxin reductase, encoded by *trxB*. Thioredoxin reductase ultimately derives its oxidizing power from the cofactor NADPH [27, 28](**Figure 1.4)**.

In the glutathione/glutaredoxin pathway, glutathione oxidoreductase (*gor*) reduces two enzymes, GshA and GshB, which are responsible for the synthesis of glutathione, a small sulfhydryl-containing tripeptide (Glu-Cys-Gly) (**Figure 1.4)**. Gor also uses a NADPH as a cofactor (**Figure 1.4)**. Glutathione reduces the four known glutaredoxins: glutaredoxin 1 (*grxA*), glutaredoxin 2 (*grxB*), glutaredoxin 3 (g*rxC*), and glutaredoxin 4(*grxD*) [27, 29]. The glutaredoxins in turn reduce their protein substrates in the cell[30]. Similar to the thioredoxins, the active site cysteines in glutaredoxins must be reduced in order to act on their native substrates[25].

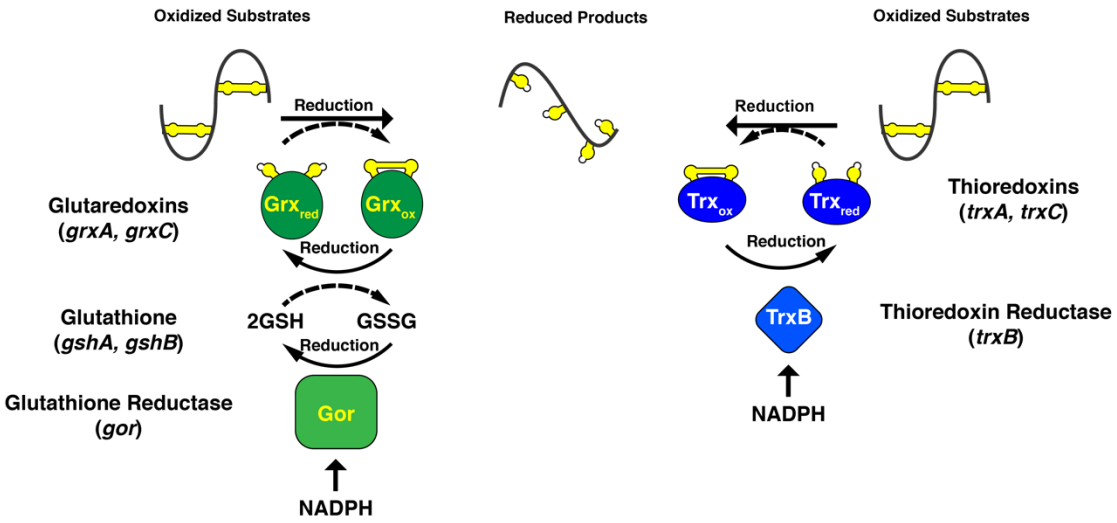

Figure 1.4 The Thioredoxin and Glutaredoxin pathways in the *E. coli* cytoplasm. The thioreductases glutathione oxidoreductase (Gor) and thioredoxin reductase (TrxB) reduce glutathione (GSH/GSSG) and thioredoxins, respectively. Glutaredoxins 2 and 4 are not shown. The solid arrows indicate reduction. The dashed arrows indicate oxidation. Redox state of cysteines (yellow balls) are indicated (oxidized = ball + stick; reduced = ball).

E. coli strains with an oxidizing cytoplasm

Through pioneering studies in the lab of Dr. Jon Beckwith at Harvard, mutations in the *E. coli* genome that permit stable formation of disulfide bonds in the cytoplasm were isolated. Derman et al., found that mutation of *trxB* allowed for cytoplasmic accumulation of active Alkaline Phosphatase, a native *E. coli* protein that requires two disulfide bonds for proper folding and activity[31]. The authors hypothesized that *trxB* mutants accumulate oxidized thioredoxin in their cytoplasm and that oxidized thioredoxins catalyze the formation of disulfide bonds. *E. coli* strains that allow for stable disulfide bond formation in their cytoplasm are often called oxidizing strains[31].

Mutating glutathione oxidoreductase (*gor*) was subsequently found to allow cytoplasmic accumulation of proteins that require disulfide bonds, indicating that disruption of either pathway results in the capacity to promote disulfide bonding in the cytoplasm[26]. In this case, oxidized glutaredoxins promote the formation of disulfide

bonds.

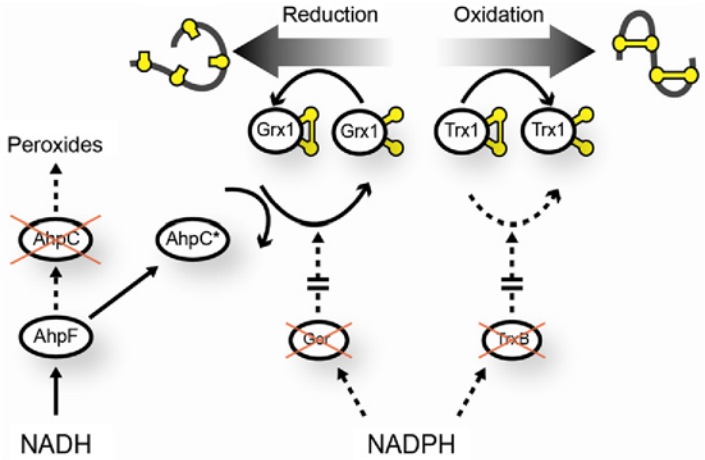

Figure 1.5 Disulfide bond formation in the cytoplasm of *trxB gor ahpC cells**
Schematic representation of the redox pathways involved in the formation of disulfide bonds in the cytoplasm of *trxB gor ahpC** cells. AhpC* gains the ability to reduce Grx1. Reduced Grx1 can catalyze the reduction of proteins. Accumulation of oxidized thioredoxins such as Trx1 catalyzes the formation of disulfide bonds. Disabled protein interactions are represented by dotted lines. For simplicity, other reductases (Grx2, Grx3 and Trx2) are omitted and only the redox state of cysteines (yellow balls) of Grx1 and Trx1 are indicated (oxidized = yellow balls are joined; reduced = ball). Figure adapted from Berkmen[9].

Double mutants (*trxB gor*), however, were found to grow very poorly in aerobic conditions as a result of their inability to reduce essential substrates (e.g. ribonucleotide reductase) [32]. Although these mutants grow poorly, unless in the presence of a reducing agent like dithiothreitol (DTT), they showed an increased capacity to promote the correct oxidative folding in the cytoplasm, when compared to the single mutant strain *trxB*[25]. Interestingly, the *trxB gor E. coli* mutants spontaneously acquired a growth suppressor mutation that allowed them to grow normally in the absence of a [25]reducing agent[25]. Later studies revealed that this mutation maps to the *ahpC* gene that codes for a peroxiredoxin. Strikingly, only a single codon is repeated, resulting in the insertion of a single amino acid, which converts AhpC from a peroxiredoxin that protects the cell from oxidative damage to a

disulfide reductase, AhpC*. The mutant enzyme is able to shuttle electrons through the glutathione/glutaredoxin pathway restoring its reducing power [33, 34](**Figure 1.5)**.

The triple mutant suppressor strain (*trxB gor ahpC*)*, FA113, has been demonstrated for the high level cytoplasmic production of proteins that require disulfide bonds for activity (**Figure 1.5)**[35]. It is now available commercially from Novagen under the trade name Origami[35].

A number of other systems have been developed for expression of proteins requiring disulfide bonds in the cytoplasm. Co-expression of the yeast sulfhydryl oxidase Erv1p was shown to promote the accumulation of disulfide bonded proteins in the *E. coli* cytoplasm without the disruption of the glutaredoxin and thioredoxin pathways [36, 37]. The same group also reported engineering the DsbAB pathway, specifically the membrane topology of DsbB, such that DsbA can catalyze disulfide bond formation in the cytoplasm[38]. Overall, these developments demonstrate that the cytoplasm still has untapped potential as a compartment for the production of disulfide bonded proteins.

History of antibody applications

For over a century, antibodies have been used as treatments for disease. In 1890, Emil von Behring and Kitasato Shibasaburō proved that diphtheria could be treated with antibody-containing serum harvested from animals immunized against the pathogen [39, 40]. Von Behring's and Kitasato's breakthrough was the first reported clinical success of the use of passive immunization. Serum therapies are examples of passive immunization, which is the administration of antibodies to prevent, treat, or cure a clinical indication. Passive immunization is currently used against several infections including tetanus, botulism, and diphtheria [40, 41]. Children with antibody deficiencies are treated with pooled human serum against common childhood diseases

to which they may be exposed [40, 41]. Human IgG are also administered as prophylaxis for serious viral pathogens, which include Hepatitis A, Hepatitis B, and Rabies [40, 41].

The first antibody-based immunotherapies developed to treat infectious disease were derived from serum containing polyclonal antibodies. More recently, medical scientists have shifted focus to developing monoclonal antibody therapeutics to cancer. In a landmark study, Levy and colleagues demonstrated that immunotherapy with anti-immunoglobulin idiotypic antibodies results in remission in B cell lymphoma patients[42]. This work showed for the first time that cancer could be effectively treated with a targeted monoclonal antibody. Of the five most successful monoclonal antibodies three are approved for cancer indications [43, 44]. Herceptin (trastuzumab) is used to treat certain types of breast cancer [3, 45]. Avastin (bevacizumab), which targets vascular endothelial growth factor (VEGF), can be used as a part of a treatment regimen for several types of cancer including colorectal and lung cancer[45]. Rituxan (rituximab), which targets the B cell antigen CD20, is a treatment for Non-Hodgkin's lymphoma and chronic lymphocytic leukemia [45, 46].

Another important class of monoclonal antibodies are those developed to relieve symptoms associated with autoimmune disorders including rheumatoid arthritis (RA), Crohn's disease, and plaque psoriasis[47]. For instance, Humira (adalimumab) and Remicade (infliximab) bind tissue necrosis factor alpha (TNFα) thereby blocking its interaction with its native receptors (TNFRs)[47, 48]. Blocking the TNFα and TNFR interaction disrupts the signaling cascade that leads to inflammation[48]. At least 47 monoclonal antibodies have been approved by the Food and Drug Administration (FDA) and in Europe for treatment of various disorders. With more than 50 monoclonal antibodies in late stage clinical trials and more than 300 candidates in development for several different indications, monoclonal antibody

immunotherapy is likely to remain important in the future[44, 49].

Researchers and clinicians have used antibodies to develop diagnostic and analytical technologies. Antibodies were used to develop the Coombs test, a test for Rhesus (Rh) factor in blood[50]. In 1960, Rosalyn Yalow and Solomon Berson pioneered a radioimmunoassay used to quantify insulin in plasma[51]. Eva Engvall and Peter Perlman described the Enzyme-linked immunosorbent assay (ELISA) in 1971[52]. The ELISA has since become one of the most widely used laboratory techniques having applications in disease diagnosis, binding studies, and molecular identification.

Antibodies have a rich history for use in diagnostic, analytical, and clinical applications that continues to this day. Many of the techniques described are still in use underscoring the continuing importance of developing antibody production and engineering technology. As the use of antibodies continues to expand and the number of antibody-based applications continues to grow, techniques for efficient and cost-effective development of new antibodies will be needed.

Hybridoma technology

The earliest breakthrough in monoclonal antibody technology came in 1975 when Milstein and Kohler described the production of large quantities of mAbs using hybridoma technology[53]. In hybridoma technology, healthy antibody-secreting murine plasma B cells are immortalized by fusing them with a myeloma cell line creating a hybrid cell line that can proliferate indefinitely in cell culture while continuing to secrete monoclonal antibodies (**Figure 1.6)**. In 1986, Muromonab-CD3 (Orthoclone OKT3) became the first monoclonal antibody therapeutic licensed by the FDA. The fully mouse antibody binds the CD3 T cell receptor and was approved to treat allograft rejection specifically after kidney transplantation.

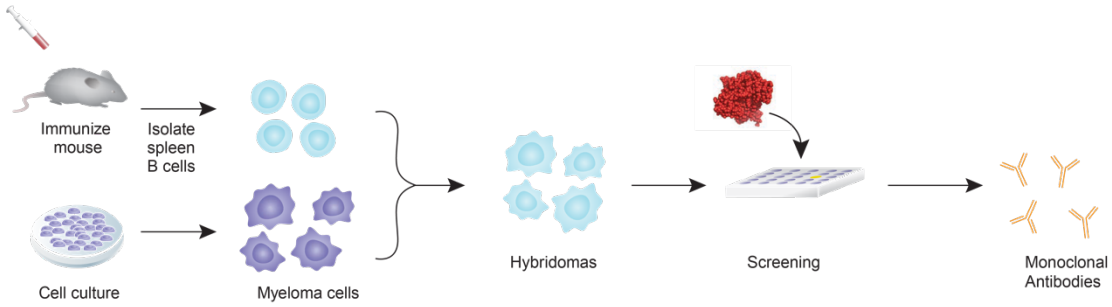

Figure 1.6 Antibody discovery via hybridoma technology. To generate hybridoma cells, an animal is immunized with the desired antigen (denoted in red). After spleen cell harvest and myeloma fusion, supernatants from hybridoma clones are screened and monoclonal antibodies of the desired specificity are identified with an appropriate functional assay. Figure adapted from Joyce et al[54].

However, mouse antibodies are often immunogenic when used in human therapy [55, 56] which often results in a reduction in therapeutic efficacy. Thus, it is a common practice to use DNA recombinant technology to replace potentially immunogenic mouse-derived Ig domains of an antibody with the human homologs of those domains in a process known as humanization. The chimeric antibody format, in which the constant domains of the mouse heavy (C_H1-C_H2-C_H3) and light chains (C_L) are replaced, and the humanized format, in which all but the CDR domains are replaced, are most prevalent formats used for therapeutic antibodies[57].

Researchers have also developed methods for generating hybridomas using human B cells[56]. However, isolating monoclonal antibodies using hybridoma systems is a technologically complex process and does not allow for engineering of desirable properties like antibody affinity, stability, or enhancement of effector function.

In an attempt to isolate fully human antibodies while still using mice as model hosts, transgenic strains were developed by replacing mouse antibody coding genes with human antibody coding gene loci resulting in mice that generate fully human antibodies upon immunization with an antigen[58-60]. However, it is often difficult to generate effective antibodies via immunization of transgenic mice when the antigen to

be administered is either toxic or highly conserved (immune tolerance) thereby limiting the applicability of the technology [57, 61].

To address these shortcomings, microbial systems have been developed to screen antibodies with enhanced functional properties from large combinatorial libraries. But first the challenge of expressing active antibodies in microbial systems had to be addressed.

Antibody fragments expressed in microbial systems

Expression of antibody fragments in *E. coli* was initially limited to the periplasm because of the requirement of stable disulfide bonds for folding. The Plückthun group reported the earliest use of recombinant DNA technology to express a soluble antibody fragment in *E. coli* [62]. Plückthun and associates expressed V_L and V_H domains as separate polypeptides that assemble via hydrophobic interactions into variable fragments (Fvs) (**Figure 1.7)**. These fragments retain the antigen binding specificity of a full-length antibody. Later, the single-chain Fv (scFv), where the V_L and V_H antibody sequences are genetically fused by the introduction of a short linker sequence, was introduced as a way to stabilize the Fv fragment[63] (**Figure 1.7)**. Eventually, expression of more complex antibody fragments in the *E. coli* periplasm like Fabs, dimeric antibody fragments composed of a full-length light chain (V_L-C_L) linked to the V_H and C_H1 domains of a heavy chain by a disulfide bond between the C_L and C_H1 domains**,** was also achieved [64, 65](**Figure 1.7)**. Successful production of scFvs and Fabs in *E. coli* was soon followed by technologies for isolating high affinity binders from combinatorial libraries.

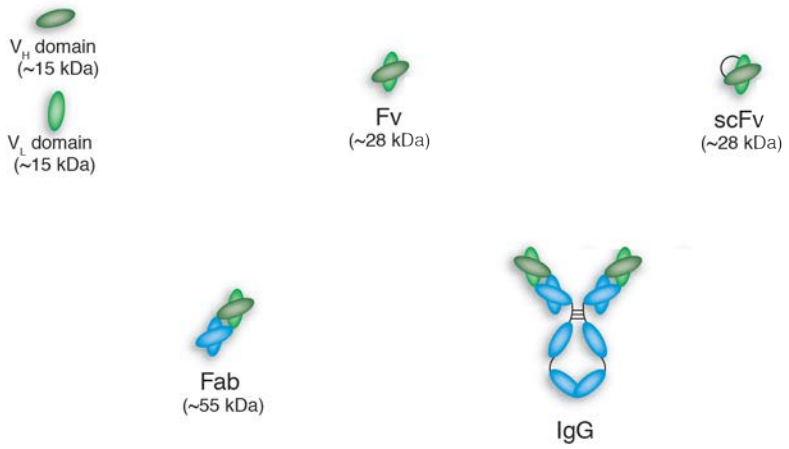

Figure 1.7 Common antibody fragments expressed in microbes. Schematic representation of different antibody formats, showing intact an IgG antibody along with Fab, Fv, and scFv fragments (sizes given in kilodaltons (kDa) are approximate). V_L and V_H domains are also depicted. Figure adapted from Holliger and Hudson[66].

Antibody engineering technology in microbial systems

The human immune system generates billions of antibodies, all with slightly different specificities, in response to a pathogen. As a result, an individual's immune repertoire contains antibodies that can be matured to bind virtually any substance[2]. To mimic this diversity, large libraries of DNA encoding V_H and V_L sequences are created to generate a rich pool of specificities to screen for antibodies against a target antigen. Libraries can either be immunized libraries that are biased for binders against a particular antigen, or naïve, which are unbiased[67]. The first libraries created for antibody isolation were amplified from mRNA harvested from animals immunized against a particular antigen[68]. Later, antibody engineers began to create de novo or synthetic antibody libraries. To create synthetic libraries, numerous strategies have been developed to introduce variation within V_H and V_L sequence DNA. Techniques that have been demonstrated for this purpose include CDR walking[69], random mutagenesis[70], DNA shuffling[71], or site specific recombination[72].

Phage display is one of the most widely used *in vitro* technologies for affinity

maturation and screening of antibody fragments from combinatorial libraries[73]. The Winter lab at the MRC Laboratory of Molecular Biology in Cambridge, England pioneered phage display as a tool for selecting specific antibodies from scFv libraries [74]. Concurrently, phage display was adapted for the selection of antigen-specific Fabs by the Lerner and Barbas labs at the Scripps Research Institute[75].

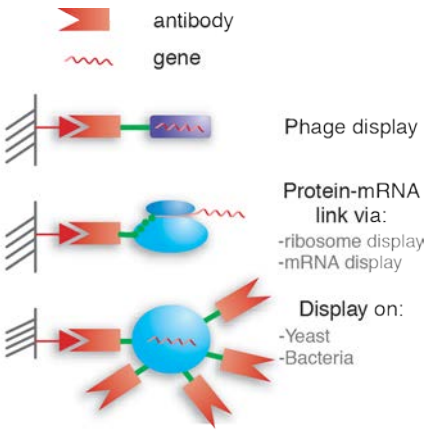

Figure 1.8 *In vitro* and microbial display technologies. Schematic representation of display technologies. Antibody phenotype (orange) is coupled to its genotype (wavy line) via a phenotype-genotype link (green) to a host (blue and purple). As a result, each host particle expresses (or displays) a unique antibody on its surface. Figure adapted from Hoogenboom[76].

The principle behind phage display is the coupling of a genotype with a selectable phenotype by fusing the antibody to the surface of bacteriophages harboring DNA encoding the antibody. Phage libraries can be selected for binding ("panning") against a target antigen and DNA from phages that bind can be recovered. Phage display has proved to be a powerful antibody engineering technology. The first fully human antibody approved by FDA for therapeutic use, Humira, was developed using this transformational technique. Since its approval in 2002, the anti-TNFα antibody has become one of the most commercially successful biologics. Alternative *in vitro* screening techniques, including ribosome[77-79] and nucleic acid display[80], operate

by similar principles(**Figure 1.8)**.

Microbial display technologies for screening antibody fragments have also been developed. These include yeast display [71, 81, 82] and bacterial display [70, 83, 84] . Also, *in vivo* selections have been reported using *E. coli* that allow isolation of antibody fragments by simple selection strategies such as growth on antimicrobial agents. These strategies include the protein complementation assay (PCA) [85-87], which depends upon reactivation of a reporter protein via antigen-antibody interactions, and bacterial hitchhiker selection [88-90].

Antibody fragments however, have proven to be of limited use in therapeutic applications due to their short circulating half-lives, rapid systemic clearance, and inability to activate the host's immune functions[91]. As a result, antibody fragments isolated using the described technologies are typically converted to full-length mAbs and expressed in mammalian systems. Unfortunately, this process is costly and labor intensive. The reformatting process also often results in a loss of binding activity [92, 93].

Full-length antibody expression and engineering in E. coli

The need to convert antibody fragments to full-length antibodies after they have been selected could be circumvented by a strategy to directly express and select full-length antibodies in *E. coli*. In an important technological advancement, Simmons and colleagues at Genentech reported the first instance of soluble full-length antibody expression in *E. coli*. In this study, heavy and light IgG chains were expressed in the periplasm where assembly into full-length IgG is favored via disulfide bonding[94].

The Georgiou group at the University of Texas-Austin adapted bacterial membrane display to screen specific IgG from an immunized library. Full-length IgG were captured on the *E. coli* inner membrane using a lipoprotein-Fc binding protein fusion (**Figure 1.9)**. The outer membrane was then removed creating "spheroplasts."

After incubating the spheroplasts with a fluorescently tagged antigen, the authors then screened the displayed IgG library by fluorescence-activated cell sorting (FACS) [93].

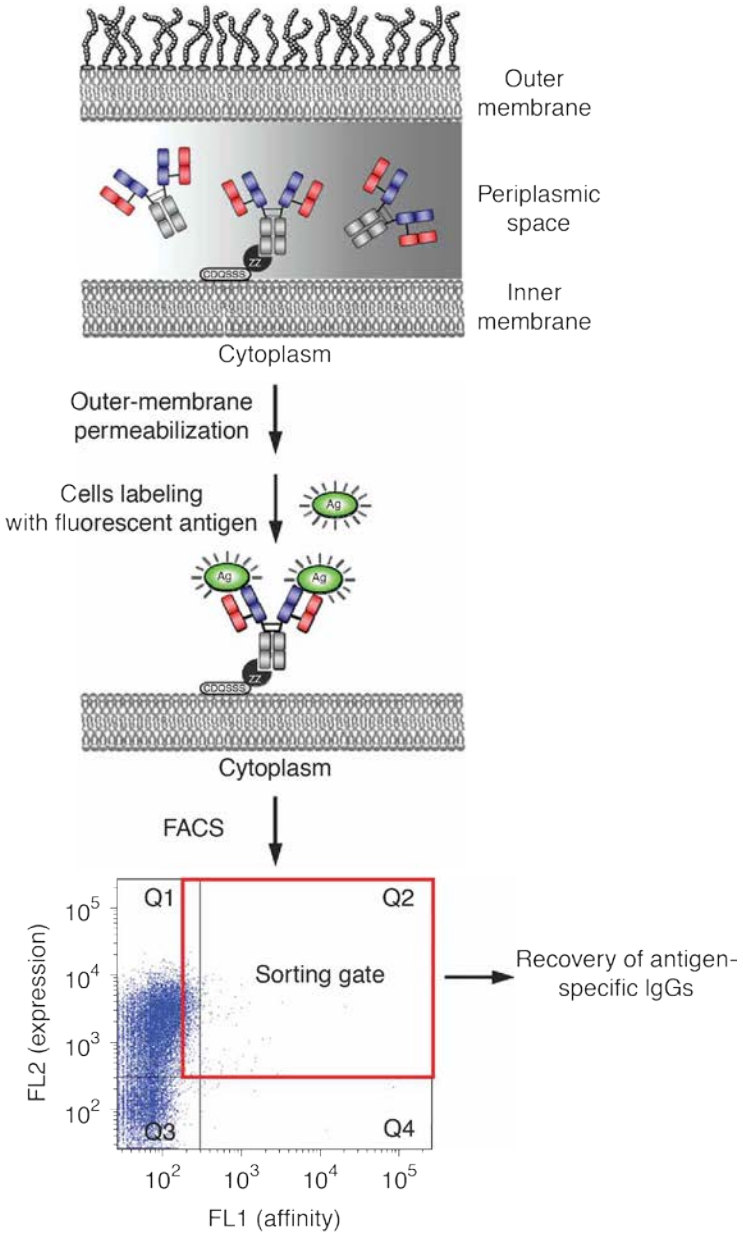

Figure 1.9 Isolation of full-length antibodies with E-clonal technology. Schematic representation of the E-clonal display technology. Libraries of full-length IgG antibodies expressed in the periplasm of *E. coli* are captured by an inner-membrane tethered NlpA-ZZ fusion protein. Following outer-membrane disruption, the inner-membrane-captured IgG antibodies specifically bind fluorescently labeled antigen and are enriched by FACS.

Spiess and colleagues at Genentech demonstrated isolation of full-length anti-VEGF framework variants with enhanced expression and thermostability using the bacterial antibody display (BAD) system[95]. The BAD method entails expressing full-length IgG in the periplasm followed by permeabilizing the outer membrane of the cells with EDTA. The permeabilized cells are then incubated with fluorescently labeled antigen. The antigen is able to penetrate the outer membrane of the cells and be captured by the expressed full-length antibodies. After antigen capture, the membrane integrity is restored though incubation with $MgCl_2$. Cells that capture the antigen can then be screened by fluorescence-activated cell sorting (FACS). To date, these are the only reports of isolation of full-length IgGs expressed in *E. coli*. However, these methods require specially designed antigens, expensive equipment (flow cytometer), and permeabilizing the cell membrane [93, 95] (**Figure 1.9)**. Additionally, the use of FACS limits the library size that can be realistically screened and thus would require pre-screening using a supplementary method to accommodate screening larger libraries[92].

A streamlined system for monoclonal antibody development

While the seminal work presented in this chapter addressed significant obstacles faced by the field in the past, there are still challenges that remain. These include the long process times associated with IgG production in mammalian cells, the dependence of antibody discovery on immunization, and limited control over antibody maturation or engineering. Though use of microbial systems offers much shorter antibody development timelines and more control over antibody diversity and optimization, these systems still depend on laborious multi-step processes.

In this thesis, I describe a simple prokaryotic system designed to streamline full-length IgG antibody production and discovery processes. By basing our system on the prokaryote *Escherichia coli*, we were able to take advantage of the relative ease and low cost of culture, the plethora of tools available for genetic manipulation and recombinant protein expression, and the high doubling rate associated with this model organism. We achieved full-length antibody production by expressing the immunoglobulin G subunits in an engineered strain of *E. coli* called SHuffle. SHuffle promotes the formation of stable disulfide bonds in the cytoplasm where the heavy and light immunoglobulin chains are assembled into an IgG. We call these cytoplasmic monoclonal antibodies "cyclonals". We demonstrated that a variety of cyclonals assembled efficiently and were functionally active. The binding kinetics, serum stability, and binding specificity of the cyclonals were extensively characterized and compared with IgG produced by mammalian cells. We also tested whether the binding specificity of a cyclonal can be readily engineered using standard DNA recombinant techniques. Several cyclonals with unique antigen specificities were generated by variable domain grafting using the framework of our model cyclonal and expressed in SHuffle. Furthermore, the Fc domain of aglycosylated cyclonals was remodeled to confer function that is essential in many cases for therapeutic efficacy. Overall yields of engineered cyclonals produced in shake flask cultures were measured.

After establishing that full-length, active IgGs could be produced at greater yields within the cytoplasm of *E. coli*, we implemented the cyclonal system for discovery of new IgGs. To do this, we applied our system to report intracellular antibody:antigen binding by implementing two distinct survival selections. In one approach antibody:antigen reactivity is linked to cell survival on chloramphenicol. In the other, a protein-fragment complementation assay (PCA) in which antibodies were isolated due to viability of cells on minimal media and resistance to glyphosate was

developed. We then examined the general applicability of both selections by testing whether each strategy correctly reported the binding of several known antibody:antigen pairs. Lastly, we isolated high affinity cyclonals from combinatorial libraries using one of our selection platforms. We show that the cyclonal platform represents a significant advancement in antibody engineering technology that could greatly simplify discovery, development, and production of monoclonal antibodies.

Recently, more than 100 of the preeminent experts in the field of antibody engineering technology called for an effort to establish consistent standards for antibodies used in research and the clinic [96]. Their recommendations include that: (1) the sequence of all antibodies should be defined and available and (2) that researchers should shift toward producing antibodies recombinantly. In addition, the co-authors Andrew Bradbury and Andreas Plückthun, suggest that antibody scientists turn to methods that directly yield recombinant binding reagents that can be readily sequenced [96]. Techniques like our cyclonal technology are well suited to meet these standards.

CHAPTER 2

EFFICIENT EXPRESSION OF FULL-LENGTH ANTIBODIES IN THE CYTOPLASM OF ENGINEERED BACTERIA[1]

Introduction

Over the past three decades, monoclonal antibodies (mAbs) have become one of the most useful protein tools with a myriad of diagnostic and therapeutic applications. For example, of the 151 unique recombinant therapeutics approved by the FDA, one-third of them are mAbs, with many more in research and development pipelines. At present, the majority of mAbs approved for therapeutic applications are produced in Chinese hamster ovary (CHO) cells (12 out of 28), followed by SP2/0 (7/28) and NS0 (5/28) mouse cell lines, and hybridomas (2/28)[97]. The remaining two are antigen-binding fragments (Fabs) that are produced periplasmically in *Escherichia coli*.

With this expansion in the use of mAbs has come an increased demand for systems that enable rapid, cost-effective production and customization using molecular engineering. Mammalian cell expression systems offer a number of potential advantages for generating mAbs including high-level expression and stability[98], and have recently been developed for the display of functional glycosylated IgGs on the cell surface[99, 100]. However, the selection of stable antibody-producing cell lines is very time-consuming. Additionally, despite the potential for high mAb yields in CHO cells (~10 g/L of culture), mammalian cell expression requires a long production cycle that results in higher cost of goods relative

[1] Adapted with permission from: Robinson, M.-P., N. Ke, J. Lobstein, C. Peterson, A. Szkodny, T. J. Mansell, C. Tuckey, P. D. Riggs, P. A. Colussi, C. J. Noren, C. H. Taron, M. P. DeLisa and M. Berkmen, Efficient expression of full-length antibodies in the cytoplasm of engineered bacteria. Nature Communications, 2015. 6: p. 8072.

to microbial expression systems that involve much faster growth rates and thus lower capital investment [101, 102].

Moreover, mammalian cell surface display has been hampered by the smaller library sizes that can be screened and the appearance of multiple copies of antibodies with different specificities on a single cell surface, making it difficult to directly identify and isolate antibodies with a desired property from naïve libraries. Additionally, with the increasing demand for animal-free products, alternative production platforms continue to be sought. Some possibilities include *in vitro* cell free expression systems[103], algae[104], baculoviral insect[105] or plant cells[106], and *Drosophila melanogaster*[107]; however, each of these presents many of the same challenges faced with mammalian systems while also being much less utilized.

E. coli on the other hand remains a system of choice, finding broad use in both industry and academia for bench- and large-scale production of recombinant proteins. A major challenge facing the use of *E. coli* as an antibody expression platform is the production of mAbs with the correct disulfide bonds. The formation of disulfide bonds in *E. coli* can be catalyzed in either the naturally oxidative periplasmic compartment [108] or in the cytoplasm of genetically engineered strains [35, 109]. Indeed, many fragments derived from mAbs such as Fab[110], single-chain Fv (scFv)[111], Fc[112], and an scFv-Fv fusion[113] have been expressed in the periplasm or in the cytoplasm of specially engineered *E. coli*[114, 115 , 116]. There have even been two reports describing expression and functional assembly of full-length IgGs in *E. coli*, both in the periplasm [93, 94]. However, periplasmic expression is thought to be limited by the smaller volume and the lack of ATP-dependent molecular chaperones in this compartment, as well as by the need for extensive optimization to efficiently secrete both the IgG heavy chain (HC) and light chain (LC) across the tightly sealed cytoplasmic membrane. To address these limitations, several groups have attempted to

produce soluble IgGs in the cytoplasm of *E. coli*; however, none have been successful [117-119]. At best, these efforts resulted in misfolded IgG chains within inclusion bodies, which required further *in vitro* refolding processes.

Here, we demonstrate that biologically active IgGs can be obtained by expression in the engineered oxidative cytoplasm of an *E. coli* strain called SHuffle[109]. In fact, significantly higher titers of cytoplasmic IgGs named "cyclonals" were obtained compared to periplasmic IgG expression, suggesting that membrane translocation is a limiting step in bacterial IgG production. Indeed, protein transport across biological membranes is energetically expensive and is often associated with negative pleiotropic effects [120, 121]. And unlike the periplasm, which lacks ATP, the cytoplasm of *E. coli* harbors several energy-dependent folding chaperones (e.g. GroEL, ClpXP, Hsp90) that may promote more efficient IgG folding and assembly. Further, we show that simple grafting of Fv domains from previously isolated IgGs permits on-demand production of entirely new cyclonals that bind specifically to diverse antigens. One concern, however, regarding the use of the cytoplasm is the absence of asparagine-linked (*N*-linked) glycosylation, which in the context of IgGs is necessary for *in vivo* effector function via binding to cognate Fcγ receptors (FcγRs)[122, 123] and for circulating half-life retention time[124]. We addressed this concern by modifying cyclonals with previously identified Fc mutations that endow IgGs with the ability to bind the receptors FcγRI, FcγRIIa, FcγRIIb and FcγRIIIa [5, 125, 126]. The end result is an entirely cytoplasmic system for efficient biosynthesis of immunologically and therapeutically relevant IgGs without the need for membrane translocation or glycosylation. This platform not only provides a powerful complement to the existing antibody expression toolkit, but should open the door to a range of applications such as the rapid conversion of phage-displayed scFvs into full-length IgGs or animal-derived IgGs into humanized clones.

Results

Cytoplasmic IgG production in SHuffle cells. To enable production of cyclonals in *E. coli*, the genes encoding HC (V_H-C_H1-C_H2-C_H3; C_H2-C_H3 is a murine γ1 constant region) and LC (V_L-C_L; C_L is a murine κ constant region) were assembled into a synthetic, bicistronic operon under the control of a strong T7/lac promoter in plasmid pET21b (**Figure 2.2a**). Our initial construct was generated using the V_H and V_L domains of an anti-maltose-binding protein (MBP) antibody. The resulting plasmid was transformed in either a wild-type (wt) *E. coli* B strain or the isogenic *trxB gor* suppressor strain MB1731, whose cytoplasmic reductive pathways have been diminished, allowing the formation of disulfide bonds in the cytoplasm[35, 109] (**Figure 2.1**).

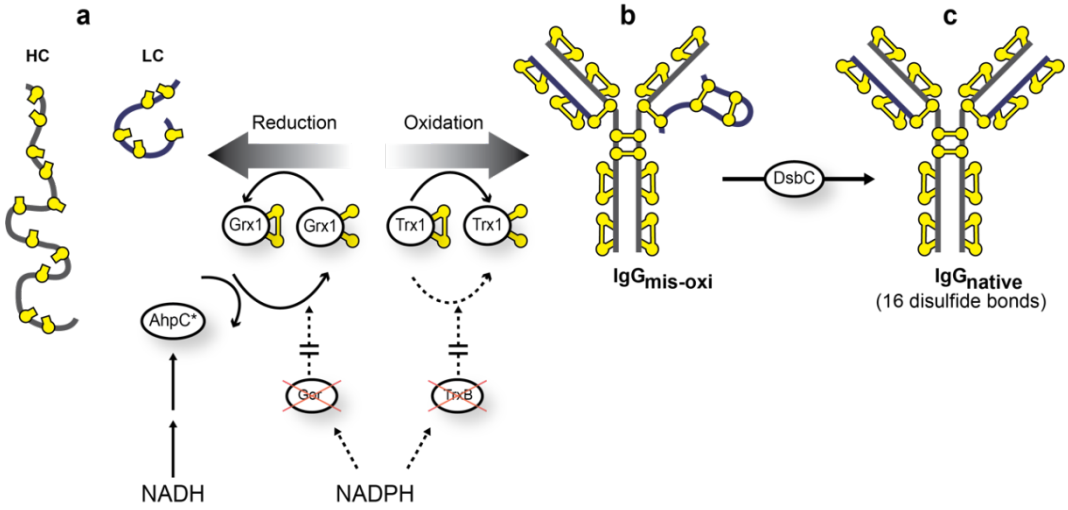

Figure 2.1 Disulfide bond formation in the cytoplasm of SHuffle. Schematic diagram of the redox pathways in the cytoplasm of SHuffle cells. Disabled protein interactions due to the deletion of trxB and gor are represented as dotted lines. Redox state of cysteines (yellow balls) are indicated (oxidized = ball + stick; reduced = ball). (a) Heavy chain (HC) with 11 cysteines and light chain (LC) with 5 cysteines are reduced by Grx1 or oxidized by Trx1. (b) Misoxidized IgG is isomerized to its (c) native correctly folded state by DsbC.

Both strains carry a genomic copy of T7 gene1, which encodes the T7 RNA

polymerase that permits expression of genes under the regulation of the T7 promoter. As expected, no IgG activity above background was observed in wt *E. coli* cells expressing the anti-MBP cyclonal (**Figure 2.2b**), consistent with the earlier observations that IgGs do not fold correctly in a normal reducing cytoplasm [117-119]. In contrast, expression of the anti-MBP cyclonal in MB1731 cells resulted in a marked increase in IgG activity (**Figure 2.2b**), indicating that an oxidizing cytoplasm is sufficient for the correct folding of full-length IgG.

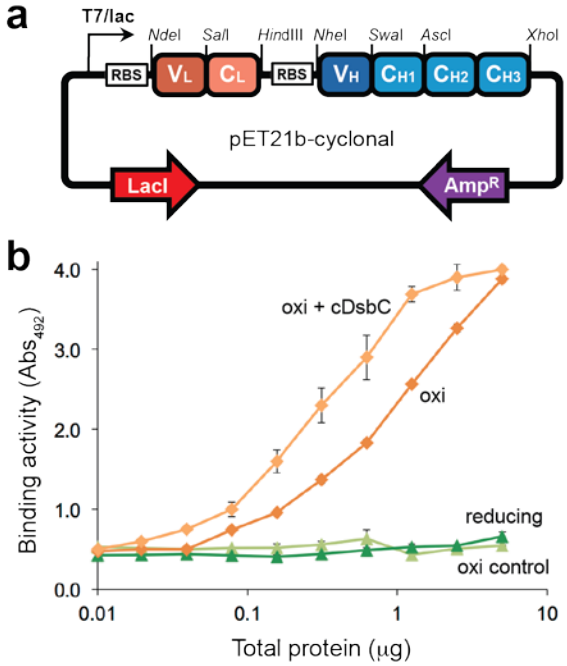

Figure 2.2 Cytoplasmic expression of mouse anti-MBP cyclonals in SHuffle. (a) Schematic of pET21b-based vector for expression of cyclonals in *E. coli*. V_H, variable heavy; V_L, variable light; C_H, constant heavy; C_L, constant light; RBS, ribosome binding site. (b) ELISA signals (Abs_{492}) for mouse anti-MBP cyclonals in lysates generated from the following: wt *E. coli* B strain with a reducing cytoplasm (reducing); isogenic *E. coli* strains MB1731 and SHuffle engineered with oxidizing cytoplasms (oxi); and, in the case of SHuffle, cytoplasmic DsbC (oxi + cDsbC). The activity measured in MB1731 cells carrying empty pET21b served as a negative control (oxi control). Data are expressed as the mean ± standard error of the mean (SEM) of biological triplicates.

IgG folding and assembly processes are dependent on multiple disulfide bonds[127]. Hence, we hypothesized that cyclonal production could be enhanced by expression of *E. coli* DsbC, an oxidoreductase chaperone capable of enhancing oxidative protein folding both in its native periplasmic compartment and when expressed cytoplasmically[35, 114, 128]. To test this notion, SHuffle T7 express cells (hereafter SHuffle), which are isogenic with MB1731 but carry a copy of *dsbC* that lacks its native signal sequence and is regulated by the *rrnB* promoter[109], were transformed with the anti-MBP cyclonal-encoding plasmid. In the presence of cytoplasmic DsbC, cyclonal activity was measurably increased (**Figure 2.2b**) without any significant difference in growth compared to MB1731 cells expressing the same cyclonal construct. In addition to mouse IgG, rabbit antibodies specific for two different human proteins, namely β2 microglobulin (B2M) and prostate-specific membrane antigen (PSMA), were actively expressed in the cytoplasm of SHuffle cells (**Figure 2.3a**).

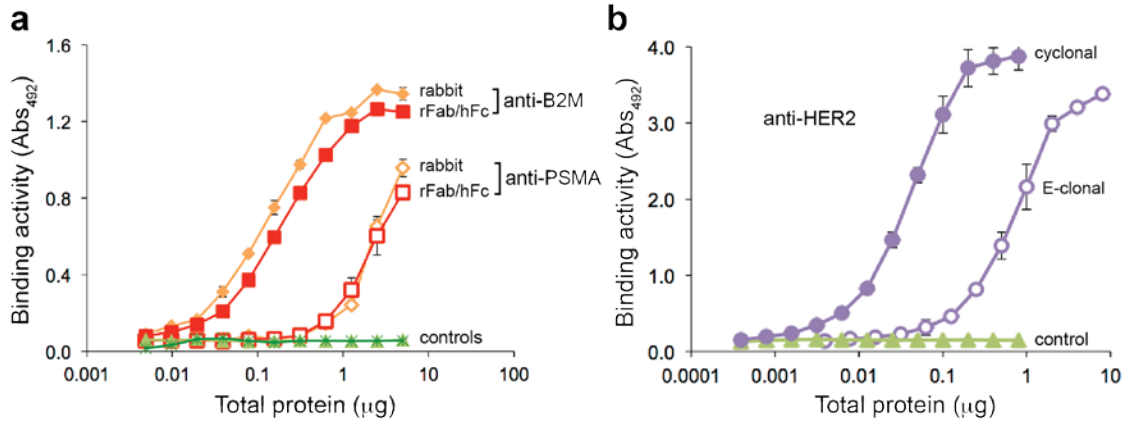

Figure 2.3 Antigen-binding activity of rabbit and humanized cyclonals. (a) Antigen-binding activity in SHuffle lysates for anti- β2 microglobulin (B2M) and anti-prostate-specific membrane antigen (PSMA) cyclonals as indicated. ELISA signals (Abs492) for rabbit cyclonals (diamonds) and empty plasmid control (triangles) were obtained using anti-rabbit antibodies; signals for rFab/hFc cyclonals (squares) and corresponding empty plasmid control (asterisks) were obtained with anti-human Fc antibodies. (b) HER2-binding activity in lysates for cyclonal (closed circles) and E-clonal (open circles) versions of Herceptin expressed from pMAZ360-Herceptin in SHuffle cells or from pSTJ4-AglycoT in the parental B strain, as well as for empty plasmid control (triangles). ELISA signals (Abs492) were obtained with anti-human HC+LC antibodies. All data are expressed as the mean ± standard error of the mean (SEM) of biological triplicates.

This is significant because rabbit monoclonal antibodies are much more difficult to develop compared to mouse antibodies due to the lack of a stable fusion partner cell line for hybridoma development. Taken together, these results confirm that (i) full-length IgGs can be produced as soluble proteins in the bacterial cytoplasm when the cytoplasmic reductive pathways have been diminished and (ii) the activity of antibodies produced in the cytoplasm is on par with those produced recombinantly in mammalian cells.

Humanizing cyclonals via domain swapping. Human, or human hybrid, antibodies are typically less immunogenic than those of mice[129]; therefore, it has become common practice to ‘humanize’ mouse antibodies. Humanizing involves combining the antigen-binding portions of a mouse antibody with the constant regions of a human

antibody using recombinant DNA techniques. To create humanized cyclonals, we re-engineered the mouse anti-MBP cyclonal in two ways. First, the mouse anti-MBP Fabs were spliced onto human Fc resulting in a mouse Fab/human Fc (mFab/hFc) hybrid. Second, the mouse anti-MBP variable domains were fused to human constant domains (mouse V_L to human C_L and mouse V_H to human C_H1-C_H2-C_H3 for LC and HC, respectively) resulting in a chimeric antibody that contained only ~30% mouse sequence as described previously[130, 131]. Both newly engineered cyclonals were expressed as functional IgGs in the cytoplasm of SHuffle cells at a level that was comparable to that of the mouse cyclonal (**Figure 2.4a**). Western blot analysis under non-reducing conditions revealed that nearly 70% of the HC was associated with the LC in fully assembled, heterotetrameric IgGs (**Figure 2.4b**), shown for the mFab/hFc hybrid. Size exclusion chromatography (SEC) further confirmed the high efficiency of heterotrimer formation for the SHuffle-derived anti-MBP cyclonal (**Figure 2.4c**). Similar domain swapping with rabbit cyclonals resulted in rabbit Fab/human Fc (rFab/hFc) hybrids that bound cognate antigens as effectively as their progenitors (**Figure 2.3a**).

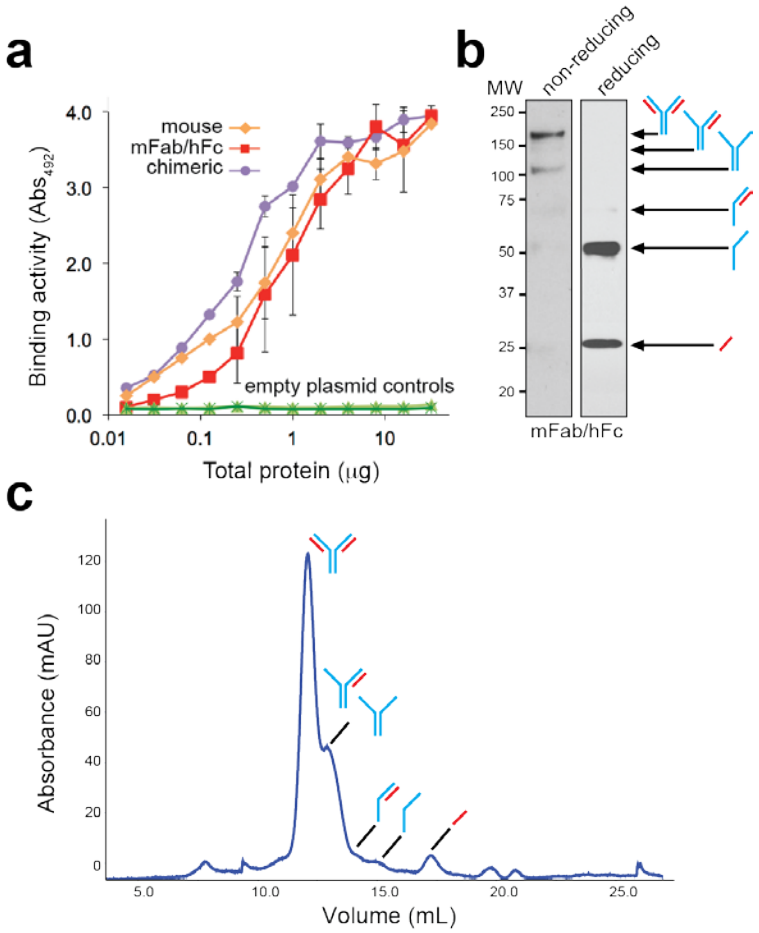

Figure 2.4 Expression of humanized cyclonals. (a) Antigen-binding activity for mouse, mFab/hFc hybrid, and chimeric anti-MBP cyclonals. ELISA signals (Abs_{492}) for mouse cyclonal and empty plasmid control (light green triangle) samples in cell lysates were obtained with anti-mouse antibodies; mFab/hFc cyclonal, chimeric cyclonal, and corresponding empty plasmid control (dark green star) were detected in cell lysates with anti-human Fc antibodies. Data are expressed as the mean ± SEM of biological triplicates. (b) Soluble anti-MBP cyclonal in the mFab/hFc format was purified from cell lysates prepared from SHuffle by protein-A affinity chromatography and analyzed by Western blot under non-reducing (left panel) and reducing (right panel) conditions. Arrows indicate fully assembled cyclonal as well as other intermediate species. The percentage of fully assembled heterotetrameric product among all product was 63 ± 5% (left panel) as determined by densitometry analysis. (c) Representative SEC analysis of protein A-purified anti-MBP cyclonal in the mFab/hFc format performed using a Superdex 200 10/300 GL gel filtration column. Heterotetramer and other intermediate products are labeled.

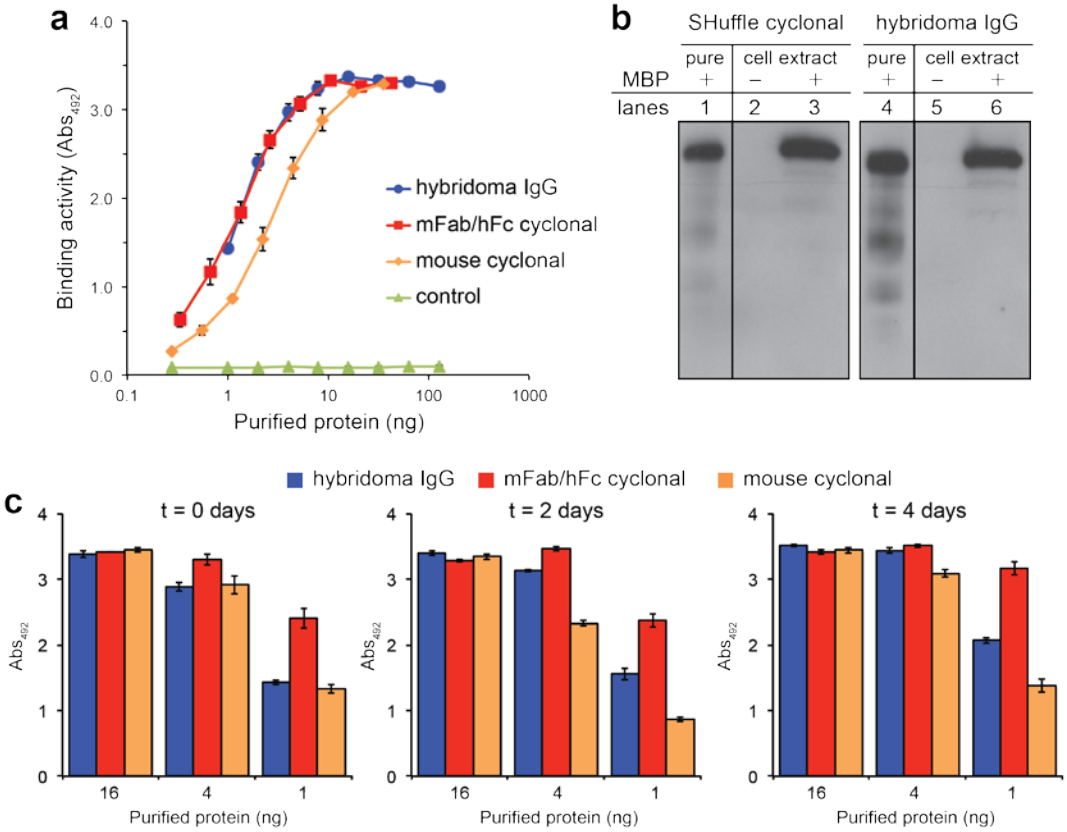

Figure 2.5 Comparison of SHuffle- versus hybridoma-derived IgGs. (a) Antigen-binding activity for protein A-purified hybridoma-produced anti-MBP monoclonal IgGs or anti-MBP cyclonals in the mFab/hFc hybrid or mouse formats. ELISA signals (Abs492) for all samples were obtained with anti-mouse IgG (Fab specific)-HRP antibodies. Data are expressed as the mean ± SEM of biological triplicates. (b) Western blots against purified MBP (lane 1 and 4) or MBP in crude cell lysates (lane 3 and 6) were probed with equal amounts of either SHuffle-produced anti-MBP cyclonals (lanes 1-3) or hybridoma-produced anti-MBP monoclonal IgGs (lanes 4-6). Cell lysates lacking cytoplasmic MBP served as controls and showed no unspecific cross-reaction for either of the IgGs (lanes 2 and 5). Each blot was incubated with 10-ml solution containing each antibody at a final concentration of 0.1 µg/ml. (c) Stability analysis for protein A-purified hybridoma-produced anti-MBP monoclonal IgGs or anti-MBP cyclonals in the mFab/hFc hybrid or mouse formats upon incubation in bovine serum. IgGs were diluted to a final concentration of 30 g/ml in 100% bovine serum and incubated at 37°C for the indicated time periods. Residual binding activity to MBP of each fraction was evaluated by ELISA.

Next, the bacterially produced cyclonals were compared to mammalian cell-derived IgG produced using conventional hybridoma cell culture. With respect to antigen binding, purified cyclonals in the mFab/hFc and mouse formats bound soluble MBP in ELISA with similar avidity to the corresponding hybridoma-derived IgG (**Figure 2.5a**). Cyclonals also performed comparably to the hybridoma IgG when each was used in a Western blot format (**Figure 2.5b**). With respect to stability, we compared the serum stability at 37°C of cyclonals in the mFab/hFc and mouse formats to that of hybridoma-derived IgG. Importantly, all IgGs were equally stable, losing little to no binding activity over the test period of four days (**Figure 2.5c**).

Variable region grafting yields new cyclonal specificities. Because of the ease with which new genes can be designed, cloned and expressed in *E. coli*, the cyclonal platform affords the unique opportunity for on-demand production of customized antibodies. To demonstrate this concept, we created a panel of new cyclonals in a process that required less than a week to complete. This involved first replacing the V_H and V_L genes of the anti-MBP cyclonal with the same genes from a variety of existing antibodies and antibody fragments including: YMF10, a humanized IgG specific for proteolytically processed and heptamerized *Bacillus anthracis* protective antigen (PA-63)[93]; 26.10-IgG, a murine IgG specific for digoxin (Dig)[93]; D10, an scFv specific for the capsid protein D (gpD) of bacteriophage lambda[132]; anti-Gcn4 scFv (Ω-graft variant) that binds the 47-residue bZIP domain of the yeast transcription factor Gcn4 (Gcn4-bZIP)[133]; and h6-4, an scFv that binds a 6-residue peptide derived from hemagglutinin (HAG) of influenza virus[134]. Following expression in SHuffle cells, cyclonals in the mFab/hFc format were observed to bind their cognate antigens with high affinity (**Figure 2.6a**).

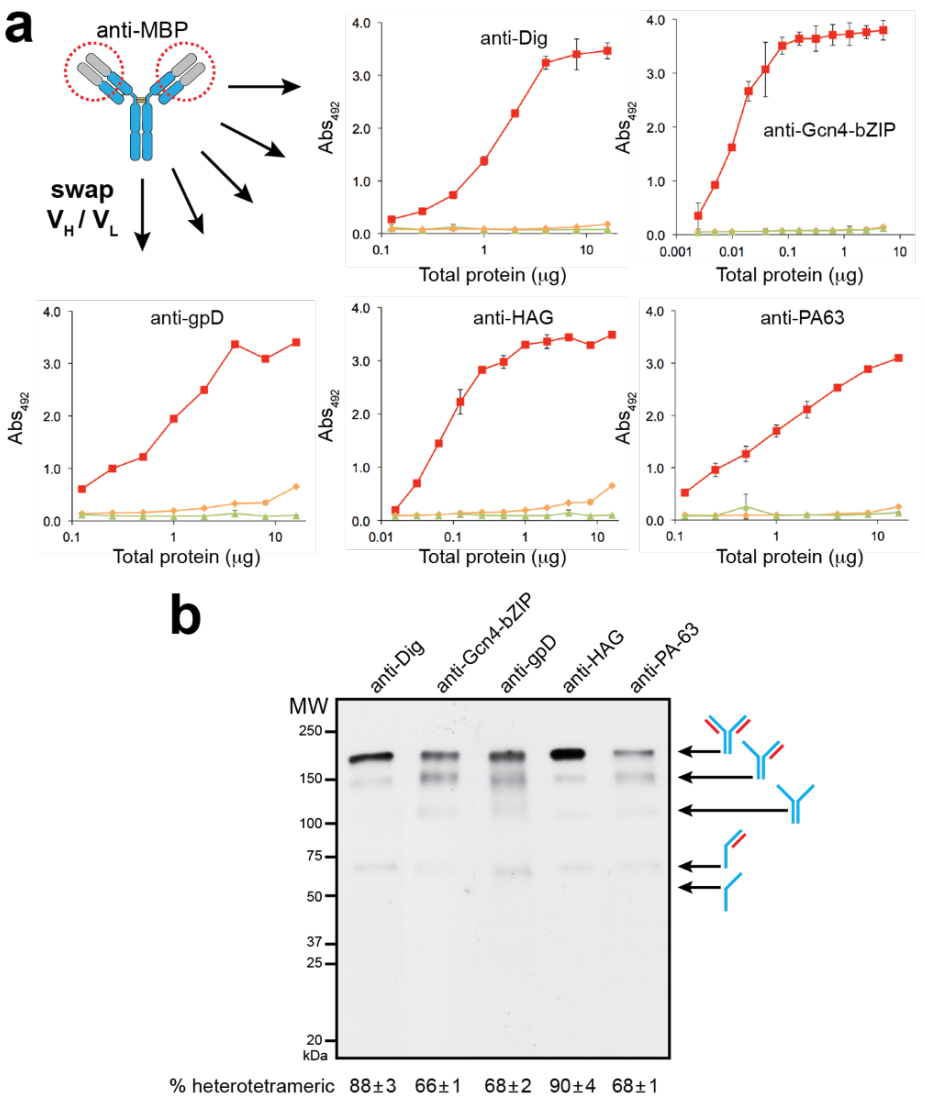

Figure 2.6 Redirecting cyclonals to new antigens with swapped variable regions. (a) Antigen-binding activity in SHuffle lysates for anti-MBP cyclonals with swapped V_H and V_L domains with specificity for antigens as indicated. ELISA signals (Abs_{492}) for mFab/hFc cyclonals (red), parental anti-MBP cyclonal (orange) and empty plasmid control (green) in cell lysates were obtained with anti-human Fc antibodies. Data are expressed as the mean ± SEM of biological triplicates. (b) Representative non-reducing Western blot of different cyclonals in the mouse Fab-human Fc format following protein-A affinity purification from cell lysates prepared from SHuffle cells. Arrows indicate fully assembled cyclonal and other HC intermediate species. The percentage of fully assembled product (% heterotetrameric) among all products was determined for each cyclonal using densitometry analysis. Percentages are expressed as the mean ± SEM of biological triplicates.

Importantly, the parental anti-MBP cyclonal showed no significant binding activity against the new antigens (**Figure 2.6a**) and none of the grafted cyclonals recognized MBP (**Figure 2.7**), confirming a complete change in specificity by simple swapping of the variable domains. Western blot analysis under non-reducing conditions revealed fully assembled, heterotetrameric IgGs in each case with the percentage of fully assembled heterotetrameric product among all products ranging from 66-90% under the conditions tested (**Figure 2.6b**).

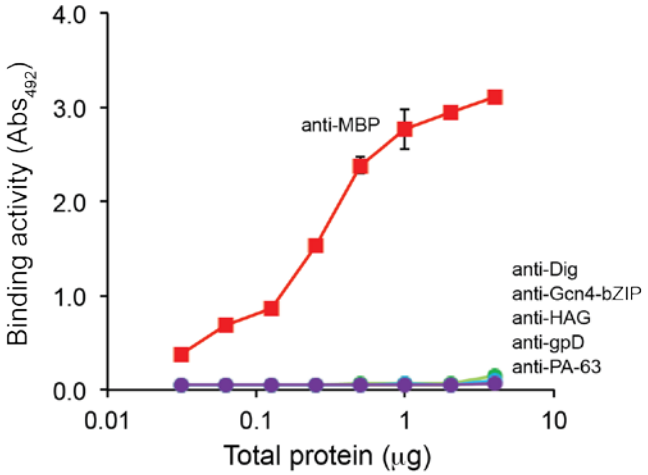

Figure 2.7 Recognition of MBP by anti-MBP cyclonal and grafted derivatives. MBP-binding activity in SHuffle lysates for anti-MBP cyclonal and derivatives containing swapped VH and VL domains with specificity for antigens as indicated. ELISA signals (Abs492) for the parental anti-MBP cyclonal in the mFab/hFc format (red) and all derivatives in the mFab/hFc format (various colors) were obtained with anti-human Fc antibodies. Data are the mean ± SEM of biological triplicates.

We routinely purified ~1-25 mg of highly active IgGs per liter of shake flask culture using affinity chromatography on a protein-A column (**Figure 2.8a and b**). It is also worth mentioning that one of the grafted cyclonals (anti-Gcn4-bZIP) and its progenitor scFv clone both exhibited nanomolar equilibrium dissociation constants as determined by Biacore analysis (**Figure 2.9**; K_d = 5.5 nM for cyclonal vs. 0.5 nM for scFv), confirming the feasibility of scFv-to-IgG reformatting in the cyclonal context.

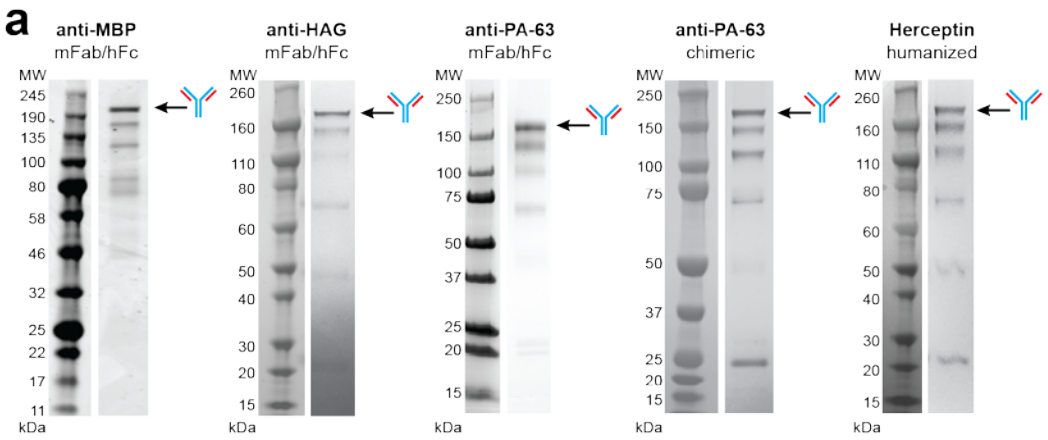

b

Cyclonal	Format	Plasmid	Titer (mg/L)
anti-MBP*	mFab/hFc	pET21b	1.0
anti-MBP	mFab/hFc	pMAZ360	3.6
anti-digoxin	mFab/hFc	pMAZ360	7.6
anti-HAG*	mFab/hFc	pMAZ360	8.4
anti-Gcn4-bZIP	mFab/hFc	pMAZ360	21.4
anti-gpD	mFab/hFc	pMAZ360	6.8
anti-PA-63*	mFab/hFc	pMAZ360	17.0
anti-PA-63*	chimeric	pMAZ360	1.1
Herceptin*	humanized	pMAZ360	3.7

*shown in SDS-PAGE above (Figure 2.8a)

Figure 2.8 Purification of cyclonals from the cytoplasm of SHuffle cells. (a) Representative non-reducing SDS-PAGE gels of cyclonals purified from SHuffle T7 cells. Expression of each cyclonal was induced with 1 mM IPTG for 16 h at 30°C. Cyclonals were purified from cell lysate by affinity chromatography involving protein A columns. Molecular weight (MW) markers are shown at left. Arrows indicate fully assembled cyclonal IgG antibodies. (b) Representative titers for different cyclonals following protein-A purification strategy described in (a).

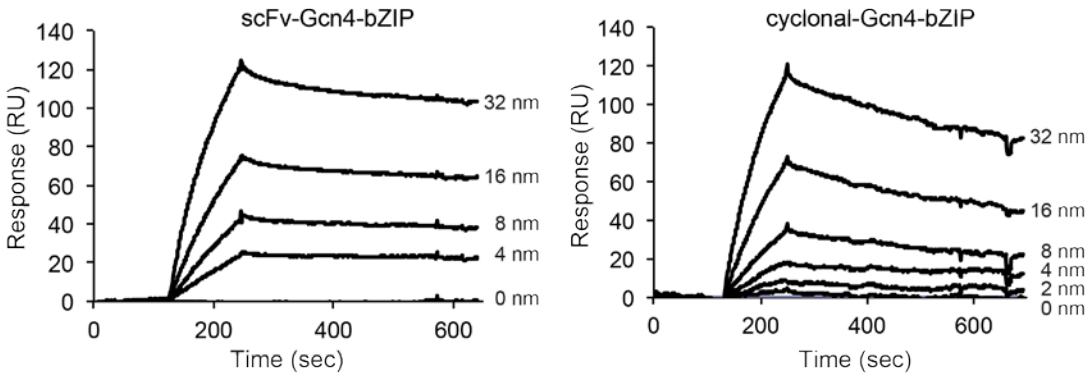

Clone	antigen	k_a (M^{-1} s^{-1})	k_d (s^{-1})	K_D (M)	Chi^2
scFv-Gcn4-bZIP	MBP-Gcn4	4.9×10^{5}	2.6×10^{-4}	$5.3 \pm 0.1 \times 10^{-10}$	1.1
cyclonal-Gcn4-bZIP	MBP-Gcn4	1.4×10^{5}	7.9×10^{-4}	$5.5 \pm 0.1 \times 10^{-9}$	2.8

Figure 2.9 Binding kinetics of cyclonal versus scFv antibodies. Biacore sensorgrams generated for purified scFv-Gcn4-bZIP (left) and cyclonal-Gcn4-bZIP (right) measured by surface plasmon resonance. Binding kinetics were monitored using Biacore 3000. Purified scFv-Gcn4-bZIP or cyclonal-Gcn4-bZIP was immobilized on CM5 chips and the response of varied concentrations of purified MBP-Gcn4, given in each curve, was compared with an empty flow cell. Purity of all recombinant proteins was assessed by SDS-PAGE. Affinity values were obtained by fitting the equilibrium binding responses with a 1:1 Langmuir binding model using a simultaneous non-linear program. Representative results are depicted.

Remodeling Fc domain of cyclonals for binding to FcγRs. IgGs lacking glycosylation in their Fc domain, such as those produced in *E. coli*, are completely unable to bind to Fcγ receptors (FcγRs), and therefore do not induce FcγR-mediated effector functions[94, 135]. However, aglycosylated Fc variants that productively engage the receptors FcγRI (CD64), FcγRIIa (CD32a), FcγRIIb (CD32b) and FcγRIIIa (CD16a) with moderate to high affinity have recently been isolated[5, 125, 126]. In the case of FcγRI, binding was critically dependent on the amino acid substitution E382V, and to a lesser extent M428I, within the C_H3 domain. To engineer cyclonals that bind FcγRs, we introduced the E382V and M428I mutations to the human Fc domain of the chimeric anti-PA-63 cyclonal. The wt and E382V/M428I variant cyclonals were each expressed in the cytoplasm of SHuffle cells and purified by protein A affinity chromatography. As expected, only the E382V/M428I variant

exhibited binding of FcγRI that was significantly above background and on par with the binding obtained with glycosylated IgGs produced by hybridoma cells (**Figure 2.10**). These results confirm that the activity conferred by Fc remodeling is maintained following expression in the bacterial cytoplasm and that *in vitro* FcγRI binding by cyclonals rivals that of antibodies produced by mammalian cell culture.

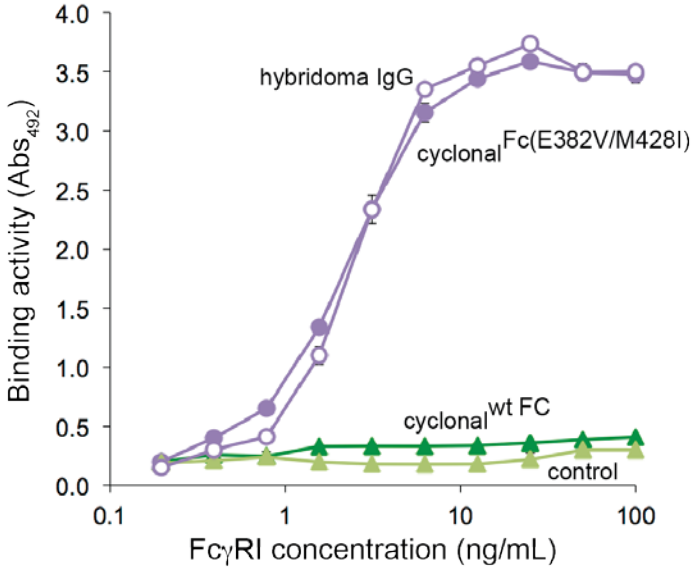

Figure 2.10 Binding of FcγRI by cyclonals with remodeled Fc domains. Antigen-binding activity of chimeric anti-PA-63 cyclonal with either wt or mutated Fc domain (cyclonal$^{Fc(E382V/M428I)}$). Glycosylated IgGs with wt Fc were purified from hybridoma cultures and included as positive control. Equivalent amounts of purified *E. coli* cyclonals or hybridoma IgGs were used to coat ELISA plates and purified FcγRI was applied at various concentrations as indicated. Blank buffer was used as a control. Data are expressed as the mean ± SEM of biological triplicates.

Comparison of cytoplasmic versus periplasmic IgG expression. It has been reported that secretory production of functional IgGs in the periplasm is inefficient and could only be achieved by lowering protein translation rates[94]. This observation combined with the large energetic cost associated with moving polypeptides across biological membranes [120] led us to hypothesize that the exceptional expression levels achieved in the cytoplasm of SHuffle cells might be due to the elimination of the membrane translocation step and/or access to ATP-dependent chaperone systems.

To test this hypothesis, we directly compared the accumulation of the anti-MBP IgG in the mFab/hFc format following expression in the cytoplasm and periplasm. For periplasmic expression, we generated a bicistronic construct in pET21b where the HC and LC of the anti-MBP IgG were both fused to the *pelB* signal peptide, yielding a so-called "E-clonal"[93] specific for MBP. Unlike the periplasm of wild type cells, SHuffle cells overexpress a cytoplasmic version of DsbC that could unfairly bias the cytoplasmic versus periplasmic analysis. Therefore, for this comparison we used the SHuffle progenitor strain MB1731 to express all cyclonal constructs because it has an oxidizing cytoplasm but lacks a cytoplasmic copy of *dsbC*. When over-expressed from a T7 promoter, the antigen-binding activity for the anti-MBP E-clonal was barely above that measured for cells carrying an empty plasmid, regardless of whether we used MB1731 cells or the wt B strain that was isogenic with MB1731 but with a reducing cytoplasm[109] (**Figure 2.11**; shown for wt B strain). In stark contrast, expression of the anti-MBP cyclonal in isogenic MB1731cells resulted in a marked increase in antigen-binding activity, reaching a level that was ~10-fold greater than its E-clonal counterpart (**Figure 2.11a**). Western blot analysis indicated that the HC and LC of the anti-MBP cyclonal accumulated almost exclusively in the soluble fraction, whereas periplasmic targeting of the E-clonal HC and LC resulted in significant accumulation in the insoluble fraction with only slight accumulation in the soluble fraction (**Figure 2.11b**). Since expression from T7-based plasmids can often lead to this type of severe insoluble accumulation, we decided to test an alternative expression plasmid, pMAZ360, that was previously shown to be optimized for E-clonal production[93]. When the anti-MBP E-clonal construct was expressed from pMAZ360, where expression was driven from a *lac* promoter, a modest increase in activity was observed (**Figure 2.11a**). In line with this increased activity, we observed greater accumulation of the E-clonal HC and LC in the soluble fraction; however, a

significant amount still partitioned to the insoluble fraction (**Figure 2.11b**). As above, expression of the anti-MBP cyclonal from pMAZ360 was significantly greater than expression of the E-clonal from the same plasmid (**Figure 2.11a**). In fact, cyclonal expression from pMAZ360 was indistinguishable from pET-based expression.

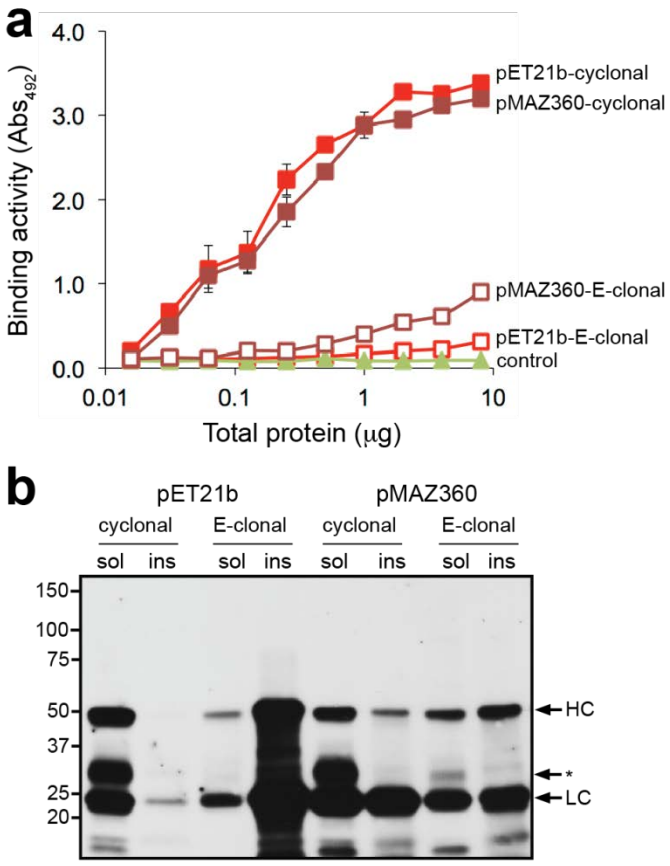

Figure 2.11 Comparison of cytoplasmic versus periplasmic IgG expression. (a) Antigen-binding activity of mFab/hFc anti-MBP cyclonals derived from the cytoplasm of MB1731 cells (closed squares) or E-clonals derived from the periplasm of parental B strain (open squares). Expression was either from plasmid pET21b (red) or pMAZ360 (dark red); signal from cells carrying empty plasmid was used as negative control (green). Data are expressed as the mean ± SEM of biological triplicates. (b) Western blot analysis of soluble (sol) and insoluble (ins) fractions derived from the same cells as in (a). HC, heavy chain; LC, light chain; asterisk, degraded HC. Mass spectrometry analysis of the degraded HC revealed that the cleavage site is in the CH1 domain of HC, known to fold inefficiently and be the major limiting factor in the assembly of IgG in eukaryotic cells. This bottleneck seems to carry over to SHuffle cells and is likely due to site-specific cleavage of misassembled HC by cytoplasmic protease(s).

Despite this high activity, the cyclonal HC and LC accumulated in the insoluble fraction following pMAZ360 expression at a level that was similar to the E-clonal chains (**Figure 2.11b**). Nonetheless, soluble accumulation of the cyclonal HC and LC was significantly higher compared to that of the E-clonal, especially in the case of the HC.

Nearly identical results were obtained when comparing cytoplasmic and periplasmic expression of the anti-HAG and anti-PA-63 IgGs from pET21b and pMAZ360 (**Figure 2.12**) and Herceptin from pMAZ360 (**Figure 2.3b**), indicating that the advantage of cytoplasmic expression was not confined to the anti-MBP IgG construct.

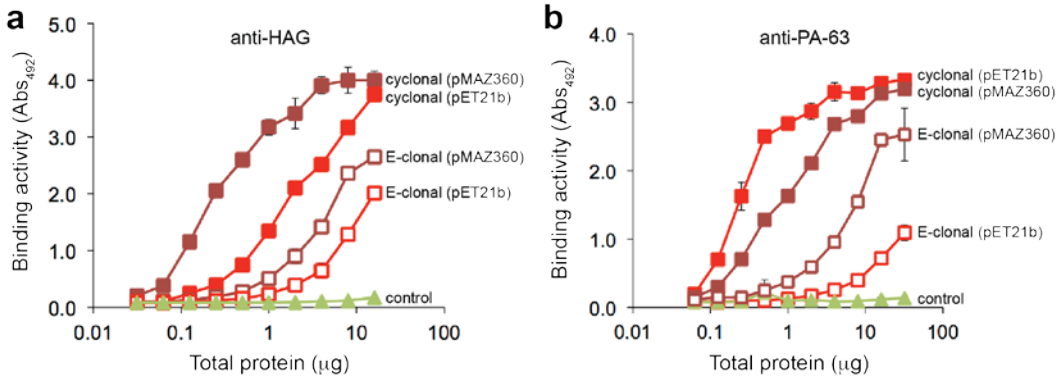

Figure 2.12 Cytoplasmic versus periplasmic IgG expression. Antigen-binding activity of mFab/hFc IgGs specific for (a) HAG or (b) PA-63. Cyclonals (filled squares) were produced in the cytoplasm of K12 strain SMG96; E-clonals (open squares) were produced in the periplasm of the parental K12 strain. Expression was either from plasmid pET21b (red squares) or pMAZ360 (dark red squares); signal from cells carrying empty plasmid was used as negative control (green). Data are expressed as the mean ± SEM of biological triplicates.

Discussion

We report the first soluble expression of active, full-length IgGs in the cytoplasm of SHuffle *E. coli* cells, a feat that was previously unattainable using wt *E. coli* cells whose cytoplasmic compartments were not engineered for disulfide bond formation [117-119]. This advance taps the wealth of knowledge and comprehensive tools (e.g., tightly regulated promoters, chaperone co-expression systems) available for this host, making it possible to produce large quantities of recombinant antibodies for *in vitro* diagnostic techniques as well as *in vivo* therapeutic applications. Moreover, we show that expression in the SHuffle cytoplasm can be combined with standard molecular engineering strategies such as grafting alternative epitope recognition domains, humanizing[129-131] and Fc engineering[94, 135] to rapidly (~1 week or less) create custom mouse, rabbit or humanized antibodies exhibiting clinically relevant properties. These results are in direct agreement with the recent observation that engineered biophysical properties can be readily transferred between different antibody formats and expression systems[136]. Hence, we anticipate that the cyclonal expression technology described here will find use in several applications such as rapidly converting phage-displayed scFvs into full-size IgGs or molecular reformatting mouse- or rabbit-derived IgGs into humanized analogs.

A significant limitation in the therapeutic use of IgGs expressed from prokaryotes is the lack of post-translational glycosylation of the Fc domain. Specifically, *N*-linked glycosylation at the conserved N297 residue is necessary for efficient binding of the Fc domain with its cognate Fcγ receptors. Upon binding, effector function is activated resulting in antibody-dependent cell-mediated cytotoxicity (ADCC) or antibody-dependent cell-mediated phagocytosis (ADCP) or complement dependent cytotoxicity (CDC)[123]. We have bypassed this limitation by remodeling cyclonal Fc domains with previously discovered mutations (e.g.,

E382V/M428I) that permit efficient binding of aglycosylated IgG to Fcγ receptors [5]. The result is a synthetic pathway, entirely in the *E. coli* cytoplasm, for producing IgGs that bind specific antigens and also engage FcγRs with the potential to activate immune cells. In fact, bacterially produced cyclonals equaled the performance of the same IgGs produced using conventional mammalian cell culture (i.e., hybridomas) in both antigen- and FcγR-binding properties.

A major advantage of cytoplasmic expression is the elimination of the membrane translocation step, which is a prerequisite for soluble antibody production in all other cell-based systems. By circumventing the physical membrane barrier, we observed much greater soluble accumulation and activity for two different cyclonals, independent of the plasmid backbone choice, compared to their periplasmic counterparts. In particular, the expression of cyclonals but not periplasmic IgGs was harmonious with pET-based plasmids, which are well known for their high levels of protein expression. It should be noted that this high level of expression was achieved following direct cloning into the multi-cloning site of standard plasmids and did not require any additional gene-level optimization, even in the face of major changes to variable and framework regions. In contrast, to achieve soluble IgG expression in the *E. coli* periplasm required screening of a panel of translation initiation regions (TIRs) to balance expression of each polypeptide chain and lower the protein translation rate[94]. The lower translation rate is thought to decrease protein load on the Sec pathway and also ensure that protein substrates remain unfolded for efficient secretion. Indeed, although not reported for IgGs specifically, when large amounts of complex hybrid proteins (e.g., the signal sequence of outer membrane protein LamB fused to LacZ) are made, rapid folding of the hybrid in the cytoplasm can cause a lethal jamming of the Sec translocase [137]. Importantly, all of these secretion-related problems are avoided with cytoplasmic expression.

Another major advantage to expressing proteins in the cytoplasm is the presence of the many energy-dependent chaperones that facilitate correct folding of proteins, which are absent in the periplasm (e.g., GroEL/S, ClpXP, DnaKJ systems). Such chaperone systems may be responsible for the significant cyclonal titers (~1-24 mg/L) observed here. By way of comparison, yields of periplasmically-expressed IgGs produced in shake flasks rarely exceed 1 mg of assembled full-length antibodies per liter of culture with literature values of 0.004-0.008 mg/L[138], 0.1-1.3 mg/L[93], and 1-4 mg/L[139]. In fact, cyclonal titers were typically greater than other less complex immunoglobulin formats regardless of the whether they were expressed in the periplasm (e.g., 0.2 mg/L Fv[62]; 2 mg/L Fab[140]) or the cytoplasm of redox-engineered *E. coli* (e.g., 1-2 mg/L scFv[114]; 3-4 mg/L Fab[115]). This may be due to the cytoplasmic copy of DsbC in SHuffle cells that was absent in earlier cytoplasmic expression systems. Indeed, levels of active cyclonal increased by ~70% when expressed in the presence of cytoplasmic DsbC compared to an isogenic strain that lacked cytoplasmic DsbC (see **Figure 2.2**). Taken together, our findings confirm the capacity of the cytoplasm as a compartment for high-titer IgG production.

Looking forward, many remaining factors known to be important for IgG expression and folding in other systems remain to be optimized for cyclonals. For example, we co-expressed a set of helper proteins that were previously shown to improve the production of disulfide bonded proteins in SHuffle cells[109]. Several of these helpers including the yeast PDI homolog (MPD1) and a mutant thioredoxin with an altered active site (CPHC) enhanced the levels of active cyclonal (**Table 2.1**). In light of these preliminary results, we suspect that co-expression of other ER folding factors could further augment the accumulation of full-length cyclonals. Another strategy for improving cyclonal production titers is to toggle the ratio of light and heavy chains in the cytoplasm in a manner that favors the formation of fully

assembled IgGs. Such toggling could be achieved by either modifying the sequences that control heavy and light chain expression (e.g., translation initiation regions (TIRs), promoters) or altering the primary sequence of the IgG directly through the use of alternative frameworks and/or constant region sequences (i.e., IgG isotypes). In one notable example, Yansura and colleagues showed that heavy and light chain levels in the *E. coli* periplasm could be more efficiently assembled using different strength TIRs for light and heavy chains[94]. It is therefore conceivable that even higher titers of cyclonals can be reached in the future following further host and process optimization.

Materials and Methods

Bacterial strains and growth conditions. The bacterial strains used in this study are listed in Table 2.2. A single colony of SHuffle T7 Express transformed with one of the pMAZ360-cIgG expression vectors was used to inoculate 5 mL Luria-Bertani (LB; 10 g/L tryptone, 5 g/L yeast extract, 5 g/L NaCl, NaOH to pH 7.2) supplemented with 100 μg/mL carbenicillin (Carb) and 25 μg/mL spectinomycin (Spec), and grown overnight at 30ºC. The next day, 300 mL of fresh LB supplemented with 100 μg/ml carbenicillin was inoculated 1/100 with the overnight culture and cells were grown at 30ºC until reaching an absorbance at 600 nm (A_{600}) of 0.7. At this point, cyclonal expression from the pMAZ360-cIgG vector was induced by addition of 1.0 mM isopropyl β-D-thiogalactopyranoside (IPTG), after which cells were incubated an additional 16 h at 30ºC. Cells were harvested by centrifugation prior to preparation of lysates or purification of IgGs.

Immunization, cell fusion and selection of hybridoma. A protein fusion consisting of bacteriophage M13 pIII (residues 259-406) and MBP was constructed in the pMAL expression system, expressed and purified according to manufacturer's protocols (New England Biolabs). Two female BALB/c mice (Jackson Laboratories) were

immunized intraperitoneally over a period of 4 months with a primary injection containing 50 μg antigen emulsified in Freund's complete adjuvant, followed by three subsequent boosts in Freund's incomplete adjuvant. A final tail vein injection containing 25 μg of antigen in 50 μL of sterile saline was administered three days prior to removing the spleen and fusion of splenocytes with X63Ag8.653 parental myeloma cells[141]. Splenocytes were fused with X63Ag8.653 myelomas using the ClonaCell™-HY hybridoma cloning kit (StemCell Technologies Inc.). Hybridoma tissue culture supernatants (TCS) were screened initially by ELISA with MBP as antigen. The isotype of monoclonal antibodies was determined using an antigen-capture ELISA. Wells were coated with anti-mouse immunoglobulin antibody (American Qualex International). Undiluted hybridoma TCS was used for isotyping. The isotype of each captured mAb was then determined using goat anti-isotype-specific alkaline phosphatase conjugated antibodies (Caltag).

Plasmid construction. A list of plasmids used in this study is given in Table 2.2. To generate the initial anti-MBP IgG construct, total RNA was isolated from $4x10^7$ hybridoma cells using Qiagen RNeasy kit with the following modifications: $4x10^7$ cells were resuspended in 600 μL RLT buffer, homogenized with hand-held homogenizer for 2 min followed by the addition of 1800 μL RLT buffer (2400 total, 600 μL per $1x10^7$ cells), mixed, separated into 4x600 μL aliquots and homogenized for another 30 s. Total RNA for each sample was purified separately according to protocol, eluted 2x30 μL for each sample and pooled (240 μL total). A mixture of degenerate forward primers (Deg1 to Deg7, **Table 2.3**) was designed from κ chain sequences in the Kabat database[142] and used with 3' reverse primer LC-9 (**Table 2.3**) to amplify the cDNA sequence of the IgG κ LC gene. 50-μL PCR mixtures for κ LC cDNA amplification with Deep Vent DNA polymerase (New England Biolabs) contained buffer supplied by the manufacturer supplemented with 200 μM dNTPs, 0.8

μM forward primer mixture, 4 μM reverse primer, and ~300 ng cDNA. Thermocycling consisted of incubation at 94°C for 5 min followed by 30 cycles of successive incubations at 94°C for 30 s, 55°C for 30 s and 72°C for 60 s. After thermocycling, a final extension was performed at 72°C for 10 min. The amplified product was digested with *Eco*RI and cloned between the *Eco*RI-*Sma*I sites of pNEB193, resulting in plasmid pNEB-LC-MBP. To amplify the cDNA sequence of the IγG HC, a degenerate primer pair (Kabat-F and Kabat-R, **Table 2.3**) were designed from IgG_{2A}-chain sequences from the Kabat database[142]. PCR mixtures for IγG HC cDNA amplification with Taq DNA Polymerase (New England Biolabs) contained buffer supplied by the manufacturer supplemented with 200 μM dNTPs, 4 μM each of forward and reverse primers, and ~300 ng cDNA. Thermocycling consisted of incubation at 94°C for 5 min, 80°C for 60 s, followed by 30 cycles of successive incubations at 94°C for 30 s, 52°C for 30 s and 72°C for 2 min. After thermocycling, a final extension was performed at 72°C for 10 min. The amplified product was digested with *Eco*RI and *Not*I and cloned between the *Eco*RI-*Not*I sites of pNEB193, resulting in plasmid pNEB-HC-MBP. Sequencing of this plasmid was used to design a synthetic HC gene in pUC57 (GenScript; pUC57-HC-MBPsyn) that was modified with unique internal restriction sites for future cloning.

The construction of all bacterial IgG expression plasmids and the reagents used in their construction (e.g., DNA templates, primers, restriction enzymes) are described in Tables 2.3 and 2.4. Briefly, the anti-MBP HC and LC lacking native export signals were PCR-amplified from pNEB-LC-MBP and pUC57-HC-MBPsyn, respectively, and subsequently assembled as a bicistronic operon using overlap extension PCR. This operon was initially cloned in plasmid pMAZ360-IgG[93] and then subcloned into pET21b. The resulting plasmid, pET21b-cyclonal-MBP, placed expression of the HC and LC under the control of the strong T7/lac promoter (**Figure 2.2a**). Construction of

pET21b-cyclonal-MBP(mFab/hFc) involved double digestion of pET21b-cyclonal-MBP with *Asc*I/*Xho*I to remove the mouse C_H2 and C_H3 domains followed by ligation of DNA encoding human C_H2 and C_H3 domains between the same sites. Construction of pET21b-cyclonal-MBP (chimeric) involved double digestion of pET21b-cyclonal-MBP (mFab/hFc) with *Sal*I/*Hin*dIII to remove the mouse C_L followed by ligation of DNA encoding human C_L between the same sites. To generate mFab/hFc cyclonals with new antigen specificity, V_L domain sequences from existing antibodies and antibody fragments [93, 132-134] were amplified by PCR, while in parallel, mouse C_L region DNA was also amplified by PCR. During PCR, engineered sequence overlaps were introduced into both the V_L and C_L sequences. The two PCR products were combined by overlap extension PCR and the resulting product was cloned between *Nde*I/*Hin*dIII of pET21b-cyclonal(mFab/hFc). Corresponding V_H domain sequences from the same existing antibodies and antibody fragments were amplified by PCR, while in parallel, mouse C_H1 region DNA was also amplified by PCR. During PCR, engineered sequence overlaps were introduced into both the V_H and C_H1 sequences. The two PCR products were combined by overlap extension PCR and the resulting product was cloned between *Nhe*I/*Asc*I of pET21b-cyclonal(mFab/hFc). For chimeric constructs with new antigen specificity, PCR amplified V_L domain sequences from existing antibodies and antibody fragments were cloned directly between *Nde*I/*Sal*I of pET21b-cyclonal(chimeric). Corresponding V_H domain sequences were assembled with human C_H1 region DNA by overlap extension PCR and the resulting products were cloned between *Nhe*I/*Asc*I of pET21b-cyclonal(chimeric). The E382V Fc mutation[28] was introduced into the C_H3 sequence of the chimeric anti-PA-63 HC by overlap extension PCR followed by a nested PCR using a mutagenic reverse primer to generate the M428I Fc substitution[28]. The resulting mutant HC was ligated between *Nhe*I/*Xho*I of pET21b-cyclonal-PA-63(chimeric). To construct E-clonal expression

plasmids, DNA encoding the *E. carotovora* pectate lyase signal peptide (spPelB) was fused to the 5' end of the HC and LC genes from anti-MBP (mFab/hFc) using nested PCR. An RBS was introduced upstream of the spPelB-HC fusion in the same manner. The resulting spPelB-HC and spPelB-LC sequences were cloned between the *Nde*I/*Hin*dIII and *Hin*dIII/*Xho*I sites, respectively, of pET21b-cyclonal-MBP, yielding pET21b-E-clonal-MBP(mFab/hFc). All subsequent periplasmic constructs were synthesized by inserting the appropriate LC and HC pairs into pET21b-E-clonal-MBP(mFab/hFc) using the *Nco*I/*Hin*dIII and *Nhe*I/*Xho*I sites, respectively. To generate additional pMAZ360 expression constructs, a synthetic multi-cloning site was cloned between *Nde*I/*Asc*I of pMAZ360[93] such that the same restriction sites used in synthesizing the bicistronic pET21-cyclonal and pET21-E-clonal plasmids could also be used to generate pMAZ360-cyclonal and pMAZ360-E-clonal expression vectors coding for any of the different IgGs. For construction of rabbit antibodies, HC and LC genes from rabbit anti-PSMA and anti-B2M clones (kindly provided by Cell Signaling Technologies) were PCR amplified and cloned between *Nco*I/*Bam*HI of pETDuet-1 (Novagen). Construction of rFab/hFc hybrids in pETDuet-1 was performed using overlap extension PCR as described above for mFab/hFc cyclonals. Construction of Herceptin in the cyclonal format was performed by first PCR amplifying the gene encoding the LC from pSTJ4-AglycoT [5] and cloning the PCR product between the *Nde*I/*Hin*dIII sites of pMAZ360-cIgG-aMBP. Next, DNA encoding the HC was amplified from pSTJ4-AglycoT and cloned between the *Nhe*I/*Xho*I sites of pMAZ360-cIgG resulting in the vector pMAZ360-cIgG-Herceptin. Genes encoding the target antigens bacteriophage lambda gpD[132], the 47-residue bZIP domain of the yeast transcription factor Gcn4[133]; and 6-residue peptide derived from hemagglutinin (HAG) of influenza virus[134] were each cloned into pET28a(+), which introduced a 6x-His tag to the N terminus of each antigen. Due to

their relatively small sizes, Gcn4-bZIP and HAG were fused to the C terminus of glutathione *S*-transferase (GST). All plasmids constructed in this study were confirmed by sequencing.

Preparation of soluble and insoluble fractions. SHuffle cells expressing cyclonals were harvested by centrifugation at 13,000xg and 4°C for 30 min. Harvested cells were resuspended in a volume of PBS, 1x SigmaFAST™ protease inhibitor cocktail (EDTA free), and 5 mM EDTA equal to one tenth of the original culture volume. Cells were ruptured by passage through an Emulsiflex-C5 High Pressure Homogenizer at 16,000-18,000 psi. The cell lysate was then clarified by centrifugation at 30,000xg and 4°C. The supernatant containing soluble cytoplasmic proteins was recovered as the soluble fraction and then passed through a 0.2-μm sterile membrane filter. Insoluble pellets were washed 3 times in 50 mM Tris-HCl, 1 mM EDTA (pH 8.0) and then resuspended in PBS supplemented with 2% SDS. Inclusion bodies were solubilized by heating at 100^{o}C for 10 min. The solubilized mixture was centrifuged at 16,000xg for 10 min and the supernatant was collected as the insoluble fraction.

Protein purification. For cyclonal purification, protein A-agarose resin was equilibrated with 10 mL PBS and then mixed with the filtered soluble lysate fraction. The resin-soluble lysate fraction mixture was incubated at room temperature with end-over-end mixing for 2 h. The mixture was then applied to a polypropylene gravity column and the soluble lysate was allowed to completely pass through the column. After settling in the column, the protein A-agarose was washed with 25 mL PBS. Cyclonals were eluted from the column with 0.1 M glycine-HCl (pH 3.0) in 1-mL fractions and neutralized with 100 μL 1 M Tris (pH 9.0). Purified fractions were resolved by SDS-PAGE under non-reducing conditions and either visualized by staining with Coomassie Blue G-250 or further processed for Western blot as described below.

Western blot analysis. For SDS-PAGE analysis under non-reducing conditions, samples were diluted 1:1 in 2x Laemmli sample buffer. For reducing conditions, samples were diluted 1:1 in 2x Laemmli sample buffer supplemented with 2.5% 2-mercaptethanol. In both cases, samples were heated at 100^{o}C for 10 min and then loaded on 4-20% Tris-Glycine gels (Bio-Rad). All samples were normalized by total protein, as determined by Bradford assay. Following electrophoresis, resolved proteins were transferred to polyvinylidene fluoride membranes (Millipore). Membranes were rinsed with PBS and then blocked with 5% milk (w/v) in PBS containing 0.05% Tween-20 (PBST) for 1 h. After 3 washes with PBST, membranes containing mFab/hFc or chimeric IgGs were probed with 1:7,500-diluted anti-human Fc-HRP conjugate antibodies (Thermo scientific) plus 1:10,000-diluted anti-mouse Igκ chain-HRP conjugate antibodies (Jackson ImmunoResearch) in 2% milk (w/v)-PBST for 1 hr. After washing 6 more times with PBST, membranes were incubated with Immun-star HRP substrate (Bio-Rad) and then visualized using a Bio-Rad Chemidoc XRS+ or by exposing membranes to X-ray film.

ELISA. Costar 96-well ELISA plates (Corning) were coated overnight at 4°C with 50 μL of 4-10 μg/mL antigen in 0.05 M sodium carbonate buffer (pH 9.6). Antigens used were MBP5 (New England Biolabs), digoxin-BSA (Fitzgerald Industries), PA-63 (Calbiochem), as well as gpD, GST-Gcn4, and GST-HAG that were each expressed in *E. coli* T7 express cells and purified by standard Ni-NTA purification. After blocking with 3% (w/v) milk in PBST for 1-3 h at room temperature, the plates were washed 4 times with PBS buffer and incubated with serially diluted purified IgG samples or soluble fractions of crude cell lysates for 1 h at room temperature. IgG-containing samples were quantified by Bradford assay and an equivalent amount of total protein (typically 8-64 μg) was applied to the plate. After washing 4 times with the same buffer, 50 μL of the following antibodies in 3% PBST was added to each well for 1 hr:

1:4,000-diluted goat anti-mouse IgG (H+L)-HRP conjugate (Promega) or anti-mouse IgG (Fab specific)-HRP conjugate (Sigma) for mouse IgGs; 1:5,000-diluted rabbit anti-human IgG (Fc) antibody-HRP conjugate (Pierce) for chimeric and mFab/hFc IgGs; 1:5000-diluted goat anti-rabbit IgG (H+L)-HRP conjugate (Pierce) for rabbit IgGs; and 1:5000 anti-human IgG (H+L)-HRP conjugate (Abcam) for Herceptin. Plates were washed and developed using standard protocols. FcγR-binding assays were performed as described elsewhere [5] except that 50 μL of 5 μg/mL of cyclonals with wt and mutant Fc domain (cyclonal$^{Fc(E382V/M428I)}$) both purified from SHuffle cells and wt IgG purified from hybridoma cells were diluted in 0.05 M Na_2CO_3 (pH 9.6) buffer and used to coat 96 well polystyrene ELISA plates overnight at 4°C. Following blocking, the plate was incubated with serially diluted recombinant human FcγRI/CD64 (R&D Systems) at room temperature for 1 h. After washing, 1:20,000-diluted rabbit anti-6x-His tag antibody-HRP conjugate (Abcam) was added and plates were washed and developed using standard protocols

Gel filtration. Protein A-purified cyclonals were analyzed by SEC using a Superdex 200 10/300 GL gel filtration column and the ÄKTA Purifier FPLC system. The Superdex 200 was equilibrated with 60 mL (~2 CV) of PBS gel filtration buffer (50 mM phosphate buffer, 150 mM NaCl, pH 7.0) at 0.5 ml/min. 300 μL of protein A-purified sample concentrated to 1 mg/mL was loaded onto and passed through the column at 0.25 ml/min with gel filtration buffer. Absorbance at 280 nm (Abs_{280}) was measured and recorded using UNICORN 5.1 software. Apparent molecular weights (MW) were calculated by interpolation using the elution volume at the maxima of each major absorption peak and a calibration curve generated using gel filtration high MW standards (GE healthcare).

Serum stability. Protein A-purified IgGs from SHuffle or hybridoma cell culture were diluted to a final concentration of 30 μg/ml in 100% fetal bovine serum (FBS; Sigma)

and incubated at 37°C for 4 days. Residual binding activity to MBP was evaluated by ELISA as described above.

Surface plasmon resonance (SPR). Equilibrium binding affinity measurements were made using a Biacore 3000 system. Cyclonal IgG or scFv antibodies were covalently linked to the surface of a CM5 sensor chip through amine coupling chemistry. First, the surface of the CM5 sensor chip was activated using *N*-hydroxysuccinimide (NHS) and *N*-ethyl-*N*-(3-dimethylaminopropyl)carbodiimide hydrochloride (EDC) (GE Healthcare). Purified anti-Gcn4 cyclonals or scFvs diluted to 50 μg/mL in 10 mM sodium acetate pH 4.0 were immobilized to the surface of the CM5 chip with a target level of 900 response units (RU). Unreacted sites on the chip surface were subsequently blocked with 1 M ethanolamine hydrochloride. Serial dilutions of the antigen, MBP-TEV-Gcn4, prepared in 10 mM HEPES, pH 7.4, 150 mM NaCl, 3mM EDTA, 0.005% polysorbate-20 (HBS-EP buffer, GE Healthcare) at concentrations ranging from 0.5-32 nM were injected over the chip using the same buffer at a flow rate of 30 μl/min (2 min injection time, 5 min dissociation). The surface of the chip was regenerated between the injections of each serial dilution with 10 mM glycine, pH 2.0 (2 min injection time, 2 min stabilization time). Kinetic parameters (k_a, k_d, and K_D) were determined by fitting the response curves with a Langmuir 1:1 binding model within the BIAevaluation software.

Acknowledgements

We would like to thank Constantine Chrysostomou for kindly sharing the pMAZ360-IgG plasmid; George Georgiou for pMAZ360-26.10-IgG and pMAZ360-YMF10-IgG; Andreas Plückthun for pHK19 (anti-Gcn4 scFv), pHK38 (anti-HAG) and pHK49 (anti-gpD); W.C. Cheung, Khanh Huynh and Jason G. Beaudet from Cell Signaling Technology for sharing rabbit IgG DNA; and Richard Roberts and William Jack for helpful comments on the manuscript. This work was supported by the

National Institutes of Health grant # AI092969-01A1 (to M.P.D. and M.B.), a Ford Foundation Predoctoral Fellowship (to M.-P.R.), and a National Science Foundation Graduate Research Fellowship (to M.-P.R.).

Tables

Table 2.1. Effects of helper protein co-expression on cyclonal production

Description	Helper	Normalized activity[1]
	pBAD33	1.0
Redox active helpers	AaDsbC	**1.4**
	DsbC	1.2
	$TrxA_{CGPC}$	1.1
	$TrxA_{CPYC}$	**1.3**
	$TrxA_{CPHC}$	**1.5**
	AaPDO	1.2
	QSOX	1.2
	PDI	1.2
	EUG1	1.1
	MPD1	**1.7**
	MPD2	1.2
Chaperone helpers	MalE	1.2
	Skp	0.9
Oxidative stress helpers	KatG	**1.4**
	AhpC, AhpF	1.1
	AhpC*, AhpF	0.9

[1]Activity of anti-MBP cyclonal in crude cell lysates derived from SHuffle cells was quantified by ELISA. All samples were normalized according to total protein as determined by Bradford assay and the activity data was normalized to the activity for cells expressing empty vector alone (pBAD33). Bold font indicates the five best helpers in terms of fold improvement.

Table 2.2. List of *E. coli* strains and plasmids used in this study

Strain or plasmid	Relevant genotype or features	Source
Strain		
NEB express T7	BL21 fhuA2 lacZ::T7 gene1 [lon] ompT gal sulA11 R(mcr-73::miniTn10--Tet^S)2 [dcm] R(zgb-210::Tn10--Tet^S) endA1 Δ(mcrC-mrr)114::IS10	NEB
MB1731	NEB express T7 ΔtrxB Δgor ahpC*	Ref.[109]
SHuffle T7 express	MB1731 λatt::pNEB3-r1-cDsbC ($Spec^R$, $lacI^q$)	NEB
Plasmid		
pBAD33-cAaPDO	Gene encoding Aquifex aeolicus oxido-reductase (PDO) in plasmid pBAD33	Ref.[109]
pBAD34-cAaDsbC	Gene encoding A. aeolicus DsbC homolog devoid of signal peptide in plasmid pBAD34	Ref.[109]
pBAD33-cDsbC	Gene encoding *E. coli* DsbC devoid of signal peptide in plasmid pBAD33	Ref.[109]
pBAD33-$TrxA_{CGPC}$	Gene encoding *E. coli* thioredoxin A (TrxA) with wt active site (CGPC) in plasmid pBAD33	Ref.[109]
pBAD33-$TrxA_{CPYC}$	Gene encoding *E. coli* TrxA with grx active site (CPYC) in plasmid pBAD33	Ref.[109]
pBAD33-$TrxA_{CPHC}$	Gene encoding *E. coli* TrxA with dsbA active site (CPHC) in plasmid pBAD33	Ref.[109]
pBAD33-QSOX	Gene encoding human quiescin sulphydryl oxidase in plasmid pBAD33	Ref.[109]
pBAD34-MalE	Gene encoding *E. coli* maltose binding protein (MBP) devoid of signal peptide in plasmid pBAD34	Ref.[109]
pBAD34-PDI	Gene encoding yeast protein disulfide isomerase (PDI) in plasmid pBAD34	Ref.[109]
pBAD34-EUG1	Gene encoding yeast PDI homolog (EUG1) in plasmid pBAD34	Ref.[109]
pBAD34-MPD1	Gene encoding yeast PDI homolog (MPD1) in plasmid pBAD34	Ref.[109]
pBAD34-MPD2	Gene encoding yeast PDI homolog (MPD2) in plasmid pBAD34	Ref.[109]
pBAD34-KatG	Gene encoding *E. coli* catalase (KatG) in plasmid pBAD34	Ref.[109]
pBAD33-AhpCF	Genes encoding *E. coli* wt peroxidase pair (AhpC and AhpF) in plasmid pBAD33	Ref.[109]
pBAD33-AhpC*F	Genes encoding *E. coli* mutant peroxidase pair (AhpC* and AhpF) in plasmid pBAD33	Ref.[109]

pBAD34-Skp	Gene encoding *E. coli* periplasmic chaperone Skp devoid of signal peptide in plasmid pBAD34	Ref.[109]
pMAZ360-IgG	Bicistronic expression of IgGs in the *E. coli* periplasm; HC and LC each carries N terminal PelB signal peptide	Ref.[93]
pMAZ360-26.10-IgG	Bicistronic expression of 26.10-IgG in the *E. coli* periplasm	Ref.[93]
pMAZ360-YMF10-IgG	Bicistronic expression of YMF10-IgG in the *E. coli* periplasm	Ref.[93]
pHK19	Gene encoding Gcn4-specific scFv antibody	Ref.[133]
pHK38	Gene encoding HAG-specific scFv antibody	Ref.[134]
pHK49	Gene encoding gpD-specific scFv antibody	Ref.[132]
pET21b-cyclonal-MBP	Mouse anti-MBP HC and LC genes lacking export signals in pET21b; bicistronic expression	This study*
pET21b-cyclonal-MBP(mFab/hFc)	Mouse anti-MBP Fab spliced onto human Fc in pET21b; bicistronic expression	This study*
pET21b-cyclonal-MBP(chimeric)	Mouse anti-MBP variable domains fused to human constant domains (mouse V_L to human C_L and mouse V_H to human C_H1-C_H2-C_H3 for light and heavy chains, respectively) in pET21b; bicistronic expression	This study*
pET21b-cyclonal-Dig(mFab/hFc)	pET21b-cyclonal-MBP(mFab/hFc) but with V_H and V_L from murine 26-10-IgG that binds digoxin[143]	This study*
pET21b-cyclonal-Dig(chimeric)	pET21b-cyclonal-MBP(chimeric) but with V_H and V_L from murine 26-10-IgG that binds digoxin[143]	This study*
pET21b-cyclonal-Gcn4(mFab/hFc)	pET21b-cyclonal-MBP(mFab/hFc) but with V_H and V_L from anti-GCN4 scFv that binds Gcn4-bZIP domain[133]	This study*
pET21b-cyclonal-Gcn4(chimeric)	pET21b-cyclonal-MBP(chimeric) but with V_H and V_L from anti-GCN4 scFv that binds Gcn4-bZIP domain[133]	This study*
pET21b-cyclonal-gpD(mFab/hFc)	pET21b-cyclonal-MBP(mFab/hFc) but with V_H and V_L from D10 scFv that binds bacteriophage lambda gpD[132]	This study*
pET21b-cyclonal-gpD(chimeric)	pET21b-cyclonal-MBP(chimeric) but with V_H and V_L from D10 scFv that binds bacteriophage lambda gpD[132]	This study*
pET21b-cyclonal-HAG(mFab/hFc)	pET21b-cyclonal-MBP(mFab/hFc) but with V_H and V_L from the h6-4 scFv that binds 6-residue HAG peptide[134]	This study*

pET21b-cyclonal-HAG(chimeric)	pET21b-cyclonal-MBP(chimeric) but with V_H and V_L from the h6-4 scFv that binds 6-residue HAG peptide[134]	This study*
pET21b-cyclonal-PA-63(mFab/hFc)	pET21b-cyclonal-MBP(mFab/hFc) but with V_H and V_L from M18.1 Hum-IgG that binds B. anthracis PA-63[93]	This study*
pET21b-cyclonal-PA-63(chimeric)	pET21b-cyclonal-MBP(chimeric) but with V_H and V_L from M18.1 Hum-IgG that binds B. anthracis PA-63[93]	This study*
pET21b-cyclonal-PA63($Fc^{E382V/M428I}$)	pET21b-cyclonal-PA-63(chimeric) but with E382V and M482I mutations in Fc domain	This study*
pET21b-E-clonal-MBP(mFab/hFc)	Mouse Fab/human Fc anti-MBP IgG in pET21b; PelB signal peptides on heavy and light chains	This study*
pMAZ360-cyclonal-MBP(mFab/hFc)	Mouse Fab/human Fc anti-MBP cyclonal in pMAZ360-IgG	This study*
pMAZ360-E-clonal-MBP(mFab/hFc)	Mouse Fab/human Fc anti-MBP IgG in pMAZ360-IgG; PelB signal peptides on heavy and light chains	This study*
pET21b-E-clonal-HAG(mFab/hFc)	Mouse Fab/human Fc anti-HAG IgG in pET21b; PelB signal peptides on heavy and light chains	This study*
pMAZ360-cyclonal-HAG(mFab/hFc)	Mouse Fab/human Fc anti-HAG cyclonal in pMAZ360-IgG	This study*
pMAZ360-E-clonal-HAG(mFab/hFc)	Mouse Fab/human Fc anti-HAG IgG in pMAZ360-IgG; PelB signal peptides on heavy and light chains	This study*
pET21b-E-clonal-PA-63(mFab/hFc)	Mouse Fab/human Fc anti-PA-63 IgG in pET21b; PelB signal peptides on heavy and light chains	This study*
pMAZ360-cyclonal-PA-63(mFab/hFc)	Mouse Fab/human Fc anti-PA-63 cyclonal in pMAZ360-IgG	This study*
pMAZ360-E-clonal-PA-63(mFab/hFc)	Mouse Fab/human Fc anti-PA-63 IgG in pMAZ360-IgG; PelB signal peptides on heavy and light chains	This study*
pET28a-gpD	gpD cloned in pET pET28a(+), which introduced a 6x-His tag to the N terminus	This study
pET28a-GST-Gcn4	Gcn4-bZIP domain cloned as GST fusion in pET pET28a(+), which introduced N terminal 6x-His tag	This study
pET28a-GST-HAG	6-residue HAG peptide cloned as GST fusion in pET pET28a(+), which introduced N terminal 6x-His tag	This study

*Construction of plasmids described in Table 2.3

Table 2.3. Construction of plasmids used in this study.

Plasmid	Template	Primer pair	Restriction Enzymes
pMAZ-cyclonal-MBP	pNEB-LC-MBP pUC57-HC-MBPsyn* PCR (cLC + cHC)	52-53 (= PCR cLC) 50-51 (= PCR cHC) 52-51 (= PCR cLH)	 PCR cLH *Nde*I/*Asc*I
pET21b-cyclonal-MBP	pMAZ-cyclonal-MBP	123-124	*Nde*I/*Xho*I
pET21b-cyclonal-MBP(mFab/hFc)	pUC57-mFab/hFcsyn*	*Asc*I/*Xho*I fragment	*Asc*I/*Xho*I
pET21b-cyclonal-MBP(chimeric)	pET21b-cyclonal-MBP(mFab/hFc) pUC57-hLCsyn* pET21b-cyclonal-MBP(mFab/hFc) pUC57-hHCsyn* PCR (A + B + C + D)	 160-161 (= PCR A) 162-163 (= PCR B) 164-165 (= PCR C) 166-167 (= PCR D) 160-167 (= PCR E)	 PCR E *Nde*I/*Asc*I
pET21b-cyclonal-Dig(mFab/hFc)	pMAZ360-26.10-IgG pET21b-cyclonal-MBP(mFab/hFc) pMAZ360-26.10-IgG pET21b-cyclonal-MBP(mFab/hFc) PCR (A+B) PCR (C+D)	201-202 (= PCR A) 203-216 (= PCR B) 204-205 (= PCR C) 206-220 (= PCR D) 201-216 (= PCR E) 204-220 (= PCR F)	 PCR E *Nde*I/*Hin*dIII PCR F *Nhe*I/*Asc*I
pET21b-cyclonal-Gcn4(mFab/hFc)	pHK19 (anti-GCN4 scFv) pET21b-cyclonal-MBP(mFab/hFc) pHK19 (anti-GCN4 scFv) pET21b-cyclonal-MBP(mFab/hFc) PCR (A+B) PCR (C+D)	207-208 (= PCR A) 209-216 (= PCR B) 210-211 (= PCR C) 212-220 (= PCR D) 207-216(= PCR E) 210-220 (= PCR F)	 PCR E *Nde*I/*Hin*dIII PCR F *Nhe*I/*Asc*I
pET21b-cyclonal-gpD(mFab/hFc)	pHK49 (anti-gpD scFv, D10) pET21b-cyclonal-MBP(mFab/hFc) pHK49 (anti-gpD scFv, D10) pET21b-cyclonal-MBP(mFab/hFc) PCR (A+B)	213-214 (= PCR A) 215-216 (= PCR B) 217-218 (= PCR C) 219-220 (= PCR D) 213-216 (= PCR E) 217-220 (= PCR F)	 PCR E *Nde*I/*Hin*dIII PCR F *Nhe*I/*Asc*I

	PCR (C+D)		
pET21b-cyclonal-HAG(mFab/hFc)	pHK38 (anti-Hag scFv) pET21b-cyclonal-MBP(mFab/hFc) pHK38 (anti-Hag scFv) pET21b-cyclonal-MBP(mFab/hFc) PCR (A+B) PCR (C+D)	221-222 (= PCR A) 223-216 (= PCR B) 224-225 (= PCR C) 226-220 (= PCR D) 221-216 (= PCR E) 224-220 (= PCR F)	 PCR E *Nde*I/*Hin*dIII PCR F *Nhe*I/*Asc*I
pET21b-cyclonal-PA63(mFab/hFc)	pMAZ360-YMF10-IgG pET21b-cyclonal-MBP(mFab/hFc) pMAZ360-YMF10-IgG pET21b-cyclonal-MBP(mFab/hFc) PCR (A+B) PCR (C+D)	227-228 (= PCR A) 229-216 (= PCR B) 230-231 (= PCR C) 232-220 (= PCR D) 227-216 (= PCR E) 230-220 (= PCR F)	 PCR E *Nde*I/*Hin*dIII PCR F *Nhe*I/*Asc*I
pET21b-cyclonal-Dig(chimeric)	pMAZ360-26.10-MBP pMAZ360-26.10-MBP pET21b-cyclonal-MBP(chimeric) PCR (B+C)	201-233 (= PCR A) 204-234 (= PCR B) 235-245 (= PCR C) 204-245 (= PCR D)	PCR A *Nde*I/*Sal*I PCR D *Nhe*I/*Asc*I
pET21b-cyclonal-Gcn4(chimeric)	pHK19 (anti-GCN4 scFv) pHK19 (anti-GCN4 scFv) pET21b-cyclonal-MBP(chimeric) PCR (B+C)	207-236 (= PCR A) 210-237 (= PCR B) 238-245 (= PCR C) 210-245 (= PCR D)	PCR A *Nde*I/*Sal*I PCR D *Nhe*I/*Asc*I
pET21b-cyclonal-gpD(chimeric)	pHK49 (anti-gpD scFv, D10) pHK49 (anti-gpD scFv, D10) pET21b-cyclonal-MBP(chimeric) PCR (B+C)	213-239 (= PCR A) 217-240 (= PCR B) 241-245 (= PCR C) 217-245 (= PCR D)	PCR A *Nde*I/*Sal*I PCR D *Nhe*I/*Asc*I
pET21b-cyclonal-HAG(chimeric)	pHK38 (anti-Hag scFv) pHK38 (anti-Hag scFv) pET21b-cyclonal-MBP(chimeric) PCR (B+C)	221-242 (= PCR A) 224-243 (= PCR B) 244-245 (= PCR C) 224-245 (= PCR D)	PCR A *Nde*I/*Sal*I PCR D *Nhe*I/*Asc*I

pET21b-cyclonal-PA63(chimeric)	pMAZ360-YMF10-IgG pMAZ360-YMF10-IgG pET21b-cyclonal-MBP(chimeric) PCR (B+C)	227-267 (= PCR A) 230-265 (= PCR B) 266-245 (= PCR C) 230-245 (= PCR D)	PCR A *Nde*I/*Sal*I PCR D *Nhe*I/*Asc*I
pET21b-cyclonal-PA63($Fc^{E382V/M428I}$)	pET21b-cyclonal-PA63(chimeric) pET21b-cyclonal-PA63(chimeric) PCR B PCR C PCR (A+D)	230-246 (= PCR A) 247-248 (= PCR B) 247-249 (= PCR C) 247-250 (= PCR D) 230-250 (= PCR E)	 PCR E *Nhe*I/*Xho*I
pMAZ360-cyclonal-MBP(mFab/hFc)	pET21b-cyclonal-MBP(mFab/hFc)	264-263	*Nde*I/*Mlu*I
pMAZ360-cyclonal-HAG(mFab/hFc)	pET21b-cyclonal-HAG(mFab/hFc)	221-263	*Nde*I/*Xho*I
pMAZ360-cyclonal-PA63(mFab/hFc)	pET21b-cyclonal-PA63(mFab/hFc)	227-263	*Nde*I/*Xho*I
pET21b-E-clonal-HAG(mFab/hFc)	pET21b-cyclonal-HAG(mFab/hFc) PCR A	257-216 (= PCR A) 258-256 (= PCR B) 259-256 (= PCR C)	PCR A *Nco*I/*Hin*dIII PCR C *Nhe*I/*Xho*I
pET21b-E-clonal-MBP(mFab/hFc)	pET21b-cyclonal-MBP(mFab/hFc) PCR A pET21b-cyclonal-MBP(mFab/hFc) PCR C PCR D	251-261 (= PCR A) 252-261 (= PCR B) 253-256 (= PCR C) 254-256 (= PCR D) 255-256 (= PCR E)	 PCR B *Nde*I/*Hin*dIII PCR E HindIII/Xho I
pET21b-E-clonal-PA63(mFab/hFc)	pET21b-cyclonal-PA63(mFab/hFc) pMAZ360-YMF10-IgG pET21b-cyclonal-MBP(mFab/hFc) PCR (B+C)	260-216 (= PCR A) 262-231 (= PCR B) 232-220 (= PCR C) 262-220 (= PCR D)	PCR A *Nco*I/*Hin*dIII PCR D *Nhe*I/*Asc*I
pMAZ360-E-	pET21b-E-clonal-	262-263	*Nde*I/*Xho*I

clonal-HAG(mFab/hFc)	HAG(mFab/hFc)		
pMAZ360-E-clonal-MBP(mFab/hFc)	pET21b-E-clonal-MBP(mFab/hFc)	263-263	*Nde*I/*Xho*I
pMAZ360-E-clonal-PA63(mFab/hFc)	pET21b-E-clonal-PA63(mFab/hFc)	262-263	*Nde*I/*Xho*I
pETDuet-cyclonal-PSMA	CST-rLC-PSMA CST-rHC-PSMA	NK438-NK397 NK440-NK399	*Nco*I/*Bam*HI
pETDuet-cyclonal-B2M	CST-rLC-B2M CST-rHC-B2M	NK438-NK397 NK440-NK399	*Nco*I/*Bam*HI
pETDuet-cyclonal-PSMA(rFab/hFc)	CST-rLC-PSMA CST-rHC-PSMA pUC57-mFab/hFcsyn* PCR A + B	NK438-NK397 NK440-NK400 (= PCR-A) NK401-NK402 (= PCR-B) Gibson Assembly	*Nde*I/*Eco*RV
pETDuet-cyclonal-B2M(rFab/hFc)	CST-rLC-B2M CST-rHC-B2M pUC57-mFab/hFcsyn* PCR A + B	NK438-NK397 NK439-NK400 (= PCR-A) NK401-NK402 (= PCR-B) Gibson Assembly	*Nde*I/*Eco*RV

*****Gene synthesis, GenScript

Table 2.4. List of primers and the sequences used in construction of plasmids.

Name	Sequence (5' to 3')
50	TATATATATATATATATTCTAGAGAAGGAGATATACACATGCA GGTCCAACTGCAGCAACCTGGG
51	TATGCGGCGCGCCTTATTATTTACCCGGAGTCCGGGAGAAGC
52	ATATACATATGGACATTGTGATGACACAGTCTCC
53	GTGTATATCTCCTTCTCTAGAATATATATATATATATATTAACA CTCATTCCTGTTGAAGC
123	ATATACATATGGACATTGTGATGAC
124	ATGCCTCGAGTTATTTACCCGGAGTCCGGGAGAAGCTC
160	ATATACATATGGACATTGTGATGAC
161	CCGTACGTTTCATGTCGACTTTGGTCCCCCCCCCGAACGTGTA CGGAG
162	CTCCGTACACGTTCGGGGGGGGGACCAAAGTCGACATGAAAC GTACGG
163	GGTTGCTGCAGTTGGACCTGCATGGCTAGCTCTCCTTCTCTAG AATA
164	TATTCTAGAGAAGGAGAGCTAGCCATGCAGGTCCAACTGCAG CAACC
165	GGTACCCTGGCCCCAGTATTTAAATAACCCTCTTGTACAGTAA TAGACCGCAGA
166	TCTGCGGTCTATTACTGTACAAGAGGGTTATTTAAATACTGGG GCCAGGGTACC
167	ACGGTGGGCATGTGTGAGTTTTGTCGGCGCGCCCTTTCGGTTC AACTTTT
NK397	GCCGAGCTCGAATTCGTTAACAGTCACCCCTATTGAAGC
NK399	CGCGTGGCCGGCCGATTTATTTACCCGGAGAGCG
NK400	GTTTTGTCGGCGCGCCCGCATGTCGAGGGCG
NK401	TGCGCCCTCGACATGCGGGCGCGCCGA
NK402	CGCGTGGCCGGCCGATTTATTTACCCGGAGACAGGG
NK438	CTTTAAGAAGGAGATATACATGGCCGTGCTGACCC
NK439	GTATAAGAAGGAGATATACAATGCAGTCGGTGGAGGAGTCC
NK440	GTATAAGAAGGAGATATACAATGCAGTCGCTGGAGGAGTCC
Deg1	GGGAATTCCACCATGGASACAGACACACTCCTGCTATGG
Deg2	GGGAATTCCACCATGGATTTTCWRGTGCAGATYTTCAG
Deg3	GGGAATTCCACCATGRAKTCACAKRCYCAGGTYYTYAT
Deg4	GGGAATTCCACCATGAKKNHYTCWSCTCAGYTYYTKGG
Deg5	GGGAATTCCACCATGAAGTTGCCTGTTAGGCTGTTG
Deg6	GGGAATTCCACCATGGACATRAGKRCYCYYGCTCAG
Deg7	GGGAATTCCACCATGCATCAGAYCAGCATGGGCWTCAAG
LC-9	GCGCCGGTCGACATTAACACTCATTCCTGTTGAAGC
Kabat-F	GGGAATTCCACCATGGRATGSAGCTGKGTMATSCTC

Kabat-R	GTGGGGCGGCCGCTCATTTACCCGGAGTCCGGGAGAAGC
201	TTTTTTCATATGGCGGACATAGTACTGACCCAGTC
202	GATGGATACAGTTGGTGCAGCATCAGTGGCCGATTTGATCTCG AGCTTG
203	CAAGCTCGAGATCAAATCGGCCACTGATGCTGCACCAACTGT ATCCATC
204	TTTTTTGCTAGCCATGGCGGAGCTGCAGCAGTC
205	CCGATGGGGCTGTTGTTTTGGCAGAGCTCACAGTAACACTAGC ACCATG
206	CATGGTGCTAGTGTTACTGTGAGCTCTGCCAAAACAACAGCCC CATCGG
207	TTTTTTCATATGCGAGATATCGTTATGACCCAATCTC
208	GATACAGTTGGTGCAGCATCAGCGCGCTTAAGCTCCACTTTGG TTC
209	GAACCAAAGTGGAGCTTAAGCGCGCTGATGCTGCACCAACTG TATC
210	TTTTTTGCTAGCCATGGAAGTCAAACTTCTTGAGTCAGGTG
211	GTTGTTTTGGCTGCAGAGACAGTAACCAGCGTGCCCTGC
212	GCAGGGCACGCTGGTTACTGTCTCTGCAGCCAAAACAAC
213	TTAAATCATATGGATATCGAACTGACCCAGCCG
214	CCCGTTTTATTTCCAGCTTGGTGCCGCCGCCAAACACAG
215	CTGTGTTTGGCGGCGGCACCAAGCTGGAAATAAAACGGG
216	TTTTTTAAGCTTTTAACACTCATTCCTGTTGAAGCTC
217	ATTAATGCTAGCCATGGAAGTGCAATTGGTGGAAAGCG
218	GATGGGGCTGTTGTTTTGGCTGCGCTAACCGTCACCAGGGTGC
219	GCACCCTGGTGACGGTTAGCGCAGCCAAAACAACAGCCCCAT C
220	GTGGGCATGTGTGAGTTTTGTC
221	AAAAAACATATGGATATCGTTATGACCCAGTCACCG
222	GATGGATACAGTTGGTGCAGCATCAGCGCGCTTAAGTTCCAGT TTG
223	CAAACTGGAACTTAAGCGCGCTGATGCTGCACCAACTGTATCC ATC
224	ATTAATGCTAGCCATGGAAGTTCAACTAGTTGAATCCGGTGGT G
225	CGATGGGGCTGTTGTTTTGGCAGCTGAAACGGTAACCAGGGT AC
226	GTACCCTGGTTACCGTTTCAGCTGCCAAAACAACAGCCCCATC G
227	TTTTTTCATATGGCGGATATTGTGATGACCCAGTC
228	GATGGATACAGTTGGTGCAGCATCAGTACGATTCAGCTCCAGC TTGG
229	CCAAGCTGGAGCTGAATCGTACTGATGCTGCACCAACTGTATC

	CATC
230	TTTTTTGCTAGCCATGGCGGAGGTCCAGCTTC
231	CCGATGGGGCTGTTGTTTTGGCTGAGGAGACTGTGAGAGTGGTG
232	CACCACTCTCACAGTCTCCTCAGCCAAAACAACAGCCCCATCGG
233	TTTTTTGTCGACCTTGGTCCCCGAGCCGAAC
234	CACCAGGGTACCCTGGCCCCAATAATCCATGGCCCATTTGTTACCAG
235	CTGGTAACAAATGGGCCATGGATTATTGGGGCCAGGGTACCCTGGTG
236	TTTTTTGTCGACTTTGGTTCCTTGACCAAATACCCAGTG
237	CAGGGTACCCTGGCCCCAGTAGTCGAAAAGTCCTGTCACGCAG
238	CTGCGTGACAGGACTTTTCGACTACTGGGGCCAGGGTACCCTG
239	TTTTTTGTCGACCTTCGTGCCGCCGCCAAACAC
240	CACCAGGGTACCCTGGCCCCAATAATCCATACCAGAAACATAAGAAAAACGC
241	GCGTTTTTCTTATGTTTCTGGTATGGATTATTGGGGCCAGGGTACCCTGGTG
242	TTTTTTGTCGACTTTGGTGCCACCACCGAAGGTC
243	CAGGGTACCCTGGCCCCAGTAGGCGAAACCGTTTTCGTCATAAC
244	GTTATGACGAAAACGGTTTCGCCTACTGGGGCCAGGGTACCCTG
245	TATATAGGCGCGCCCGCAGCTTTTCGGTTCAACTTTTTTATCCACTTTCG
246	CTGCCCATTGCTCACCCACTCCACGGC
247	GCCGTGGAGTGGGTGAGCAATGGGCAG
248	GAGCCTCGTGGATCACGGAGC
249	GAGAGGCTCTTCTGCGTGTAGTGGTTGTGCAGAGCCTCGTGGATCACGGAGCATGAGAAG
250	CTCAGC CTCGAG TCATTTACCCGGAGACAGGGAGAGGCTCTTCTGCGTGTAGTGG
251	TGGATTGTTATTACTCGCGGCCCAGCCGGCCATGGCGGACATTGTGATGACACAGTCTCC
252	CTCAGT CATATG AAATACCTATTGCCTACGGCAGCCGCTGGATTGTTATTACTCGCGGC
253	CCGCTGGATTGTTATTGCTAGCGGCTCAGCCGGCAATGGCGCAGGTCCAACTGCAGCAAC
254	AGGAGAGAATTCCATGAAATACCTATTGCCTACGGCAGCCGCTGGATTGTTATTGCTAGC
255	CTCATG AAGCTT TATATATATATATATATTCTAGAGAAGGAGAGAATTCCATGAA

	ATACCTATTG
256	CTCAGT CTCGAG TCATTTACCCGGAGAC
257	TTTTTTCCATGGCGGATATCGTTATGACCCAGTCACCGTC
258	GCAATGGCGGAAGTTCAACTAGTTGAATCCGGTGGTG
259	TATAATGCTAGCGGCTCAGCCGGCAATGGCGGAAGTTCAACT AGTTG
260	GATTCA CCATGG CGGATATTGTGATGACC
261	GAACTT AAGCTT TTAACACTCATTCCTGTTGAAGCTCTTGAC
262	CTCAGTTCTAGAATGAAATCCCTATTGCCTACGGC
263	AATATTACGCGTGTACTCGAGTTATCATTTACCCGGAGACAGG GAG
264	TATATT CATATGGACATTGTGATGACACAGTC
265	GACGGGCCTTTGGTGCTGGCTGAGGAGACTGTGAGAGTGGTG
266	CACCACTCTCACAGTCTCCTCAGCCAGCACCAAAGGCCCGTC
267	TTAATTGTCGACCTTGGTCCCAGCACCGAAC

*Engineered restriction sites are underlined.

CHAPTER 3

A FUNCTIONAL SELECTION FOR FULL-LENGTH ANTIBODIES IN THE CYTOPLASM OF ENGINEERED BACTERIA

Introduction

Monoclonal antibodies have become ubiquitous tools in biological and medical research. Many protein detection methods, e.g. imaging techniques and binding assays, depend on the existence and availability of reliable antibodies. In medicine, monoclonal antibodies are both the largest and fastest growing class of protein therapeutics[44]. Despite the number of advancements in antibody engineering technology, development of antibodies for research and therapeutic applications remains challenging and expensive.

Currently, most antibodies are developed using methods that require immunization including hybridoma technology[53] and immunization of wild-type and transgenic animals[58-60]. These technologies offer several advantages including harnessing the natural immune repertoire, using natural mechanisms of clonal selection, and selection of full-length antibodies with important post-translational modifications. However, immunization-based discovery methods are both time-consuming and labor intensive making them technically challenging to perform and poorly suited for developing antibodies against multiple antigens in parallel. In addition, the applicability of hybridoma technology and transgenic animals is limited by a poor immune response against proteins that are well conserved (immune tolerance) and the inability to directly control antibody sequence diversity. These limitations make it difficult to enhance desired properties like affinity, stability, solubility, and expression level.

Display technologies including phage[74, 75], ribosome[77], bacterial[84], and yeast display[71, 81], have become increasingly popular for the isolation and

engineering of antibodies. The genetic tractability of display systems allows near complete control of the antibody sequence diversity [144]. Furthermore, the ease of propagation of model microbes allows for the screening of large combinatorial libraries in a relatively short period of time[76]. In the past, these systems were limited to isolation of antibodies in single-chain Fv (scFv) or Fab formats, which lack the effector functions and long circulating serum persistence of full-length antibodies. However, full-length antibodies have recently been engineered using creative adaptations of bacterial [93], yeast [145, 146], and phage display[92]. Although microbial based display systems have been used to address the drawbacks of hybridoma technology and animal immunization, there are also several disadvantages to microbial based display including the requirement for multiple labor-intensive steps, and specialized equipment. Moreover, display technologies typically require several rounds of screening before a suitable lead antibody is isolated. Furthermore, display technologies like immunization based methods usually require purification, immobilization, special preparation, and/or modification of the target antigen.

Genetic selections have been employed for decades to elucidate biological phenomena as well as to evolve and engineer proteins, cells, and pathways [31, 147, 148]. Genetic selections are attractive as they are designed to link a desired property to the fitness of the host organism; requiring minimal interference in the isolation process. Selections are high-throughput strategies for isolating desirable traits as large libraries can be subjected to explicit selection conditions, and most cells that survive should exhibit the desired property. On the other hand, screens require every member of a library be analyzed making the process of identifying beneficial mutations much more labor intensive. *E. coli* is often the host of choice for engineering recombinant proteins due to its fast doubling time and ease of genetic manipulation. *E. coli* based survival selections for isolating antibody fragments have been reported in several

cases. One strategy based on reconstitution of split antibiotic resistance enzymes facilitated by antibody:antigen binding, has been used to report known antibody:antigen interactions and to select antibody fragments from combinatorial libraries [85-87, 149, 150]. This strategy, however, has been limited to selecting antibody fragments and has not been demonstrated for full-length antibodies.

The use of antibiotics in genetic selections is widespread especially given the vast range of targets whether aimed at transcription, translation, or cell wall synthesis. One well studied antibiotic is chloramphenicol (Cm), which inhibits cell growth by arresting protein synthesis in the cytoplasm by interacting with the 23s rRNA of the 50 S subunit of the ribosome. A natural countermeasure towards chloramphenicol is the production of an enzyme called chloramphenicol acetyltransferase (CAT). CAT inhibits the action of chloramphenicol by covalently adding an acetyl group to chloramphenicol preventing it from binding to ribosomes and allowing protein synthesis to continue in the cell. Since translation is catalyzed by ribosomes in the cytoplasm, CAT must also be present the cytoplasm in order to deactivate chloramphenicol [151, 152]. We formulated a strategy to link cell survival to the subcellular localization of CAT using the twin-arginine translocation (Tat) pathway. There are two distinct pathways in *E. coli* for the translocation of proteins to the periplasm: the general secretory pathway or Sec pathway and the Tat pathway. The *E. coli* twin arginine translocation (Tat) pathway consists of a complex of proteins, TatABC, which preferentially export folded proteins carrying an N terminal Tat signal peptide across the inner membrane to the periplasmic space.

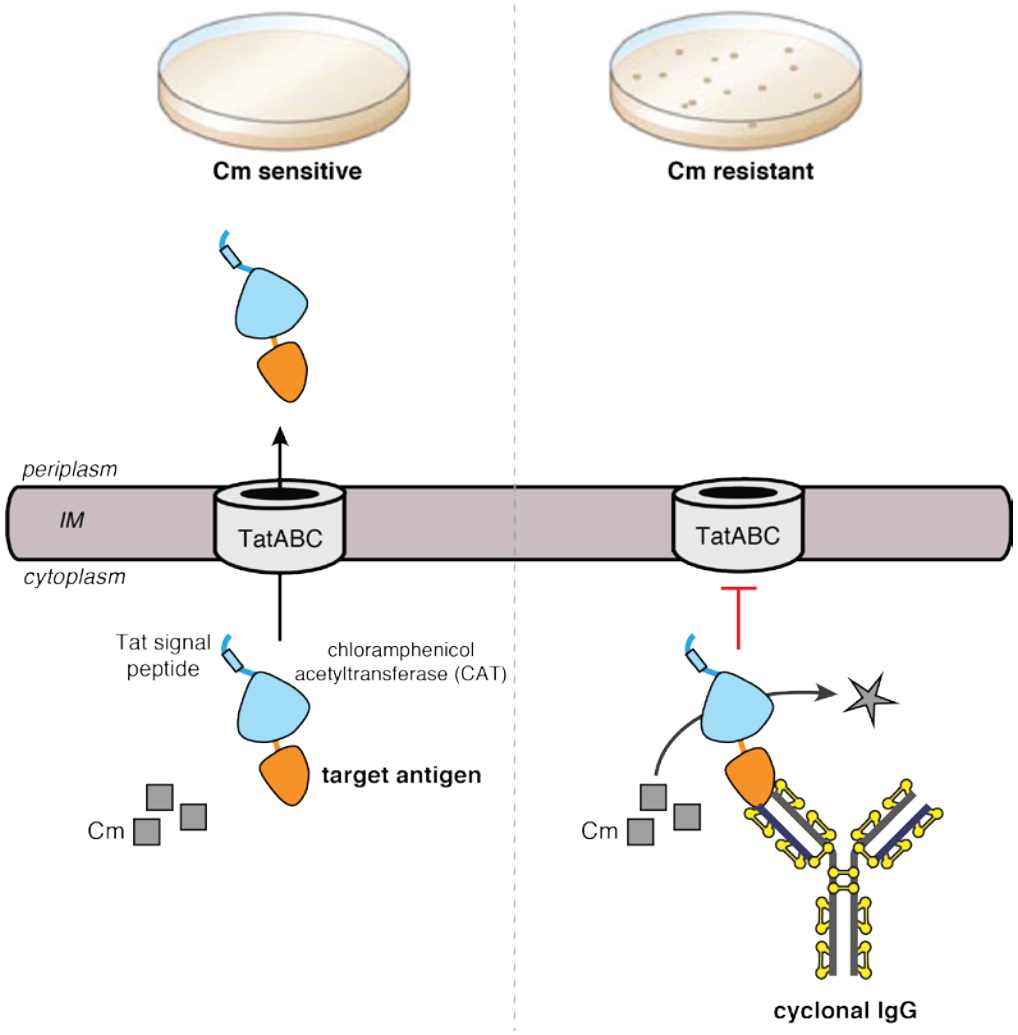

Figure 3.1. CAT selection for engineering antigen specific cytoplasmic IgG antibodies. Schematic representation of the Tat-CAT assay for identifying intracellular binding between specific cyclonal antigen pairs. A fusion protein consisting of CAT and a target antigen modified with a Tat signal peptide at its N terminus. In the absence of a binding partner the fusion protein is freely exported to the periplasmic space where it cannot deactivate chloramphenicol resulting in Cm sensitive cells. When a cyclonal that binds the target antigen is present, the interaction retains the CAT fusion protein in the cytoplasm where it can deactivate chloramphenicol thereby conferring resistance (Cm resistant).

Recently we reported the expression of active full-length IgG antibodies within the cytoplasm (cyclonals) of *E. coli* cells[8]. We achieved this by co-expressing heavy and light chains in *trxB gor aphC* E. coli* cells that promote stable disulfide bond formation in the cytoplasm. Building upon this work, we developed a genetic selection

strategy to isolate functional full-length antibodies against an antigen fused to CAT (CAT-Ag) and relying on the Tat pathway to select for higher affinity binders that keep CAT-Ag in the cytoplasm conferring resistance to chloramphenicol, while weak or non-binders allow CAT-Ag to be exported to the periplasm. When a full-length antibody is coexpressed in the cytoplasm with its antigen fused to CAT carrying an N terminal Tat signal peptide (spTorA-CAT), antibody:antigen binding impedes export thereby retaining CAT in the cytoplasm where it can confer resistance to chloramphenicol (**Figure 3.1**). We hypothesize that by this blocking mechanism specific antigen binding in the cytoplasm will be linked to a simple growth phenotype. Using this strategy, we demonstrate for the first-time isolation of antigen-specific full-length antibodies by genetic selection.

Results

Cytoplasmic retention of CAT is a selectable phenotype. We hypothesized that the cytoplasmic reporter CAT fused to an antigen of interest (CAT-Ag) exported to the periplasm via the Tat pathway would render cells sensitive to chloramphenicol. This would allow a selection based upon Tat mediated translocation of the CAT-Ag substrate. To determine whether we could select for Tat export of CAT-Ag, we constructed a vector encoding a Tat-specific signal peptide (spTorA) genetically fused to the N terminus of CAT followed by a target antigen fused to the CAT with a 7 amino acid (Gly- Thr-Ser-Ala-Ala-Ala-Gly) flexible linker (spTorA-CAT-Ag). CAT exists as a trimer *in vivo* composed of identical monomers all approximately 25 kDa in size [153]. As such, we hypothesized that antigens that are relatively small in size would reduce the probability that inefficient CAT-Ag transport would be a complicating factor in developing the selection. Therefore, HAG peptide[134], c-Myc epitope tag[154], and the basic-region leucine zipper domain of *S. cerevisiae* Gcn4[155], all relatively small polypeptides, were each cloned into the target antigen

position of the reporter construct to generate spTorA-CAT-HAG, spTorA-CAT-c-Myc, and spTorA-CAT-Gcn4, respectively. SHuffle cells expressing the spTorA-CAT-Ag hybrid proteins were evaluated for resistance to chloramphenicol. Regardless of the antigen fused to CAT, cells expressing spTorA-CAT-Ag fusions grew poorly on media supplemented with chloramphenicol (**Figure 3.2**). Having observed that translocation of the CAT fusions resulted in chloramphenicol sensitivity; we predicted that blocking the export of the CAT reporter would result in the restoration of chloramphenicol resistance. If so, we would have the ability to select for attenuated Tat export of the CAT-Ag reporter. In order to determine whether blocking Tat translocation of spTorA-CAT-Ag could restore chloramphenicol resistance, we replaced the wild-type spTorA signal sequence with one in which the twin-arginine motif RR had been mutated to KK (spTorA(KK)). The RR to KK mutation has been shown to abolish Tat export [156, 157]. Without exception, cells carrying plasmids for spTorA(KK)-CAT-Ag were more resistant to chloramphenicol than those expressing CAT-Ag hybrids with functional Tat signal peptides (RR) (**Figure 3.2**).

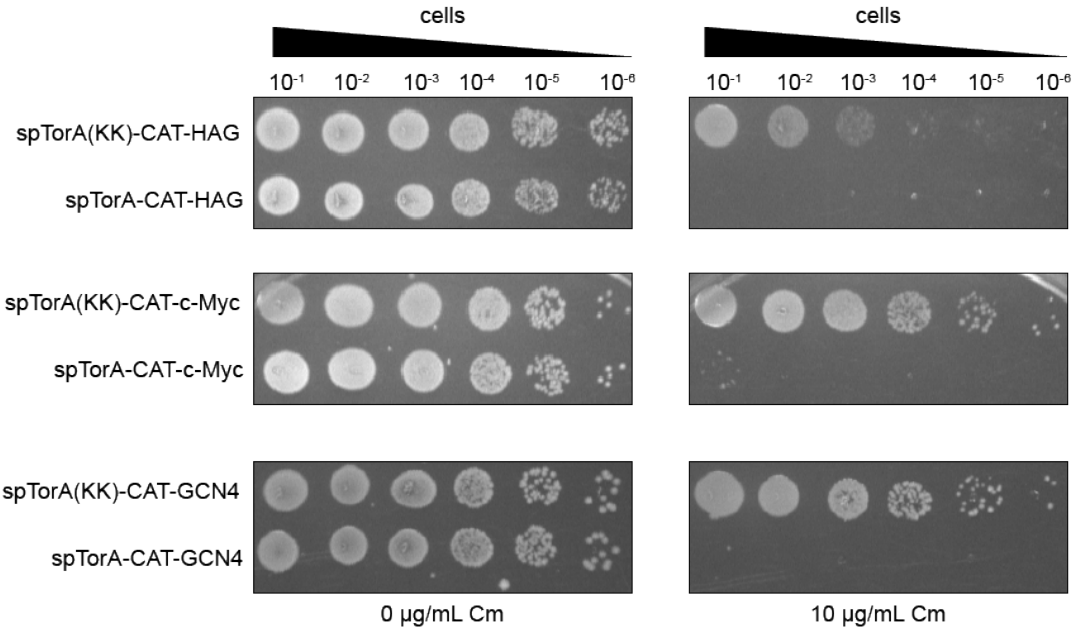

Figure 3.2 CAT selection for Tat export. Selective spot plating of SHuffle cells with plasmids for CAT-antigen fusions (spTorA-CAT-Ag) and CAT-antigen fusions with a defective Tat signal peptide that impedes translocation (spTorA(KK)-CAT-Ag) are indicated. SHuffle cells were serially diluted in LB media and 5 µl was plated on LB-agar supplemented with 0 or 10 µg/ml chloramphenicol, 0.4 % arabinose, and 1mM IPTG.

These results suggest that when grown in the presence of Cm, blocking CAT-Ag translocation to the periplasm and thereby retaining the putative cytoplasmic reporter within the cytosol, is a selectable phenotype. Therefore, we built a selection strategy based upon disrupting the export of spTorA-CAT-Ag reporter hybrids.

Antibody:Antigen reactivity promotes cell viability in CAT assay. Rodrigue et al described the "hitchhiker" transport mechanism by which proteins lacking a N terminal Tat signal peptide can be cotransported provided it is part of a complex in which at least one of the proteins possesses a functional signal peptide[158]. We speculated that increasing the size of the spTorA-CAT-Ag reporter by coexpressing an antibody (Ab) specific for spTorA-CAT-Ag would impede efficient export. The export of the spTorA-CAT-Ag:Ab complex would be poor relative to that of the smaller unbound spTorA-CAT-Ag reporter (or blocked all together) resulting in higher

concentration of CAT in cytoplasm. This should allow selection for complex formation in the cytoplasm on Cm. To test this theory, we cloned plasmids for cytoplasmic expression of two scFvs, namely scFv-HAG, specific for the 18 amino acid HAG peptide, and scFv-gpD (D10)[149], specific for the phage coat glycoprotein D. We chose the scFv format as it provides the simplest case of Ab:Ag interaction. SHuffle cells expressing scFv-HAG and spTorA-CAT-HAG showed resistance to chloramphenicol while cells expressing scFv-gpD (D10) with spTorA-CAT-HAG showed no detectable growth (**Figure 3.3**). These observations suggest that the binding interaction between CAT-HAG and scFv-HAG impedes Tat export.

Single-chain Fvs are one of the simplest models for antibody binding as the V_L and V_H binding domains are expressed as a single polypeptide linked covalently through a flexible linker. Furthermore, scFv-HAG and scFv-gpD are “intrabodies”, which are antibody fragments evolved to retain their function in the absence of structural disulfide bonds so as to be functional in intracellular (reducing) environments. Next, we tested whether a more complex antibody fragment could provide a similar selective advantage to cells cultured on Cm. Fab antibody fragments have similar binding specificity to scFvs but are expressed as two chains each linked to an antibody constant domain. Importantly, Fab fragments require five structural disulfide bonds for correct assembly and activity (i.e. must be assembled via bonding).

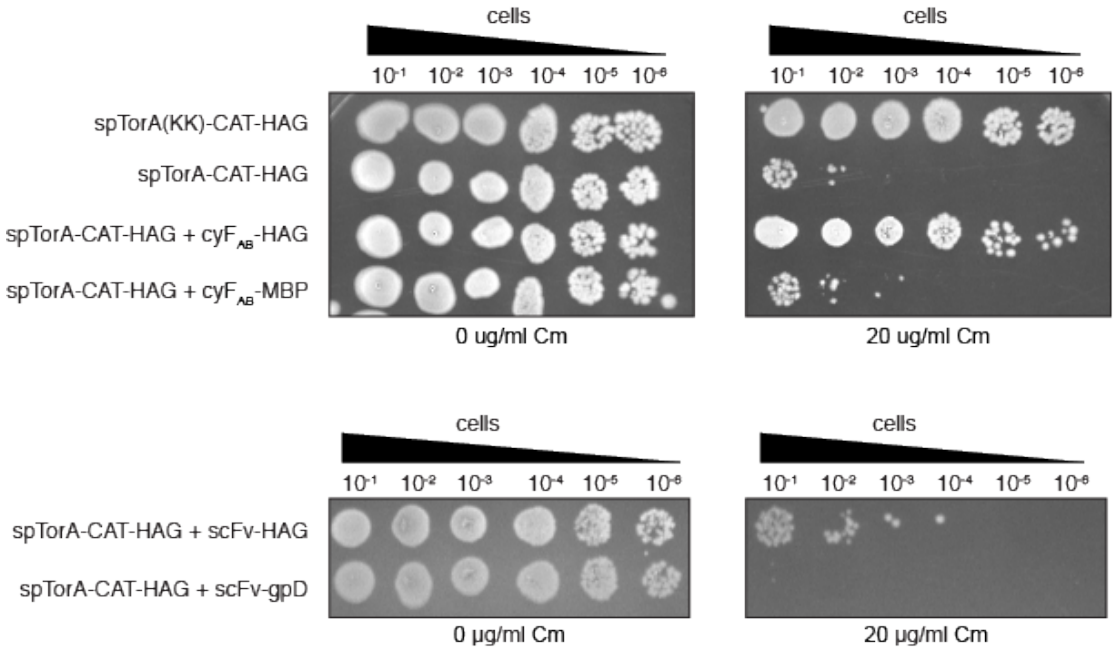

Figure 3.3 CAT selection for antibody fragments that bind antigens. Selective spot plating of SHuffle cells with plasmids for expressing scFv, Fab (cyF_{AB}), and CAT-antigen fusions as indicated. SHuffle cells carrying plasmids for the CAT-antigen fusions with a defective Tat signal peptide (spTorA(KK)-CAT-Ag) that impedes translocation were plated as negative controls. SHuffle cells were serially diluted in LB media and 5 µl was plated on LB-agar supplemented with 0 or 20 µg/ml chloramphenicol, 0.4 % arabinose, and 1mM IPTG.

To create a vector for the anti-HAG Fab antibody the V_L domain of scFv-HAG was fused to the $C_L\kappa$ domain of mouse IgG2a (V_L- $mC_L\kappa$), while the V_H domain was fused to C_H1 domain of mouse IgG2a (V_H-mC_H1), and cloned into a two-promoter vector for coexpression of the two chains in the cytoplasm. Expression of the anti-HAG Fab in the cytoplasm with spTorA-CAT-HAG conferred resistance to chloramphenicol on SHuffle cells (**Figure 3.3**). Cells coexpressing the Fab and its specific antigen grew nearly as well as the positive control in which CAT-HAG export is blocked (**Figure 3.3**). On the contrary, SHuffle cells expressing an anti-MBP Fab and spTorA-CAT-HAG showed much lower tolerance for Cm compared with cells that express the binding pair. We observed similar phenomena when we challenged cells expressing another Fab:Ag pair, anti-Gcn4 and Gcn4, with chloramphenicol

(**Figure 3.3**). This suggests that the selective advantage conferred by antibody binding is a general phenomenon and not specific to the Ag in the fusion provided that it is sufficiently exported by Tat. Our results indicate that specific binding of the spTorA-CAT-Ag hybrid within the cytoplasm offers a similar selective advantage to cells as blocking export of the reporter via Tat.

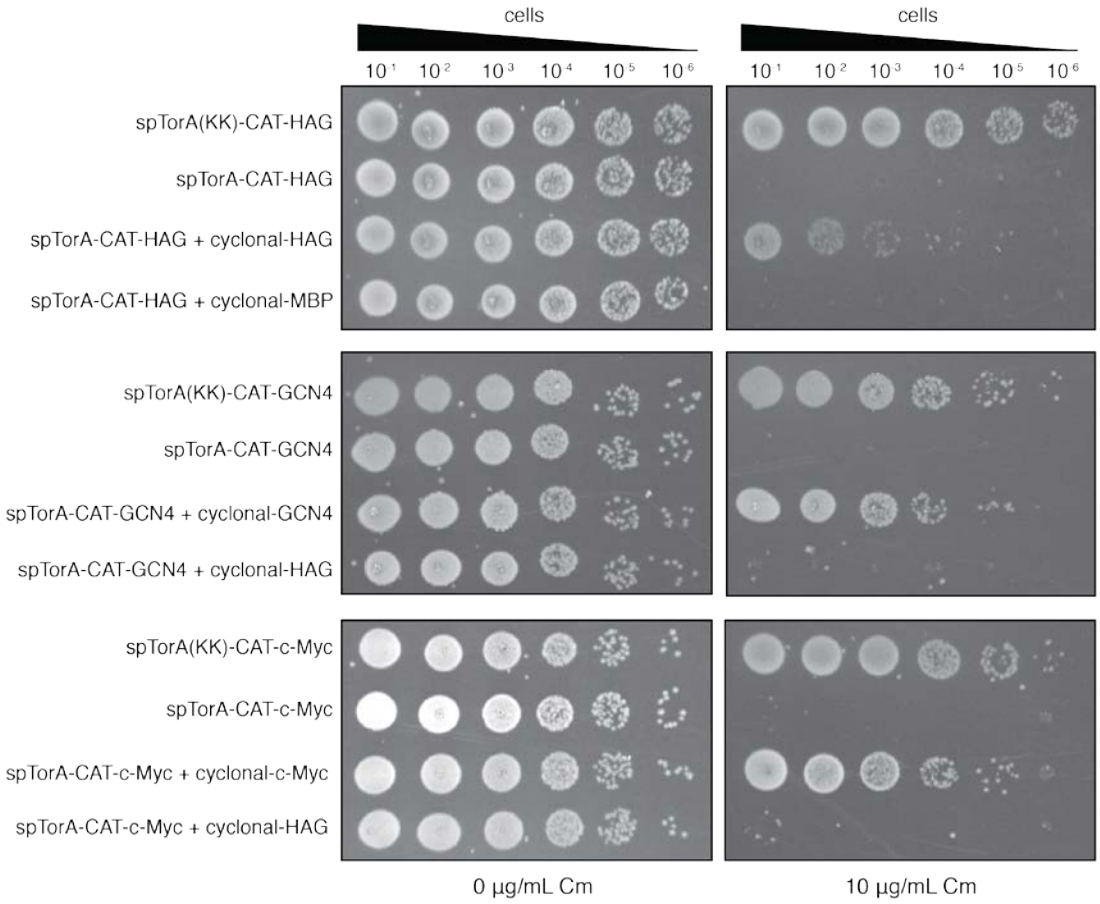

Figure 3.4. CAT selection for cyclonals that bind antigens. Selective spot plating of SHuffle cells with plasmids for expressing cyclonals and CAT-antigen fusions as indicated. SHuffle cells carrying plasmids for the CAT-antigen fusion alone and the CAT-antigen fusion with a defective Tat signal peptide that impedes translocation were plated as negative controls. Shuffle cells were serially diluted in LB media and 5 μl was plated on LB-agar supplemented with 0 or 10 μg/ml chloramphenicol, 0.4 % arabinose, and 1mM IPTG.

Cyclonal:Antigen reactivity promotes cell viability in CAT assay. Having determined that binding of the spTorA-CAT-Ag reporter by specific antibody fragments results in a selectable phenotype, we hypothesized that the selection could be extended to isolating binding interactions with full-length IgG. To adapt the selection to full-length IgGs we cloned the anti-HAG mFab/hFc cyclonal created in previous work into the two-promoter vector constructed for Fab expression. We also chose the cyclonal against *E. coli* maltose binding protein (MBP)[8], a cyclonal against Gcn4[8], and a mFab/hFc cyclonal we generated against the c-Myc epitope tag by grafting the V_L and V_H sequences from a previously reported scFv, scFv-3DX, onto the mFab/hFc framework as additional test cases [154]. SHuffle T7 Express cells were transformed with plasmids expressing specific antigen:antibody pairs and plated on varying concentrations of chloramphenicol. In each case, cells carrying plasmids for cognate antigen:antibody pairs possessed an observable fitness advantage over cells co-producing non -specific pairs (**Figure 3.4**).

We also tested whether the binding specificity of CDR-H3 variants of the anti-Gcn4 scFv (scFv-Gcn4(GLF)) would be faithfully reported in the context of our assay. These scFv variants differ within the third hypervariable region of the variable heavy chain domain (V_H) and were chosen from two previous studies. In one study conducted by the Plückthun group [155]and the other from our group[88], scFvs with randomized CDR-H3 were selected from synthetic libraries for both intracellular binding activity and stability in yeast and *E. coli*, respectively. We selected a panel of 4 scFvs, isolated between the two reports, scFv-Gcn4(ALF) and scFv-Gcn4(GLQ), scFv-Gcn4(GLH), and scFv-Gcn4(GLM) and grafted them into our two-promoter cyclonal expression plasmid. A fifth scFv, scFv-Gcn4(GFA), was grafted as a negative control as it was shown to be non-specific for Gcn4. SHuffle cells expressing each specific variant with the spTorA-CAT-Gcn4 hybrid showed higher resistance to Cm

than cells expressing the non-reactive variant GFA (**Figure 3.5**).

Each variant confers similar levels of resistance to Cm when compared with cells expressing the anti-Gcn4 cyclonal. As expected, the non-binding cyclonal variant anti-Gcn4(GFA) did not grow well under the selective conditions of assay. These results corroborate findings of both Plückthun and coworkers and Waraho and DeLisa, providing further evidence that our assay is functioning successfully as an intracellular antigen:antibody binding reporter.

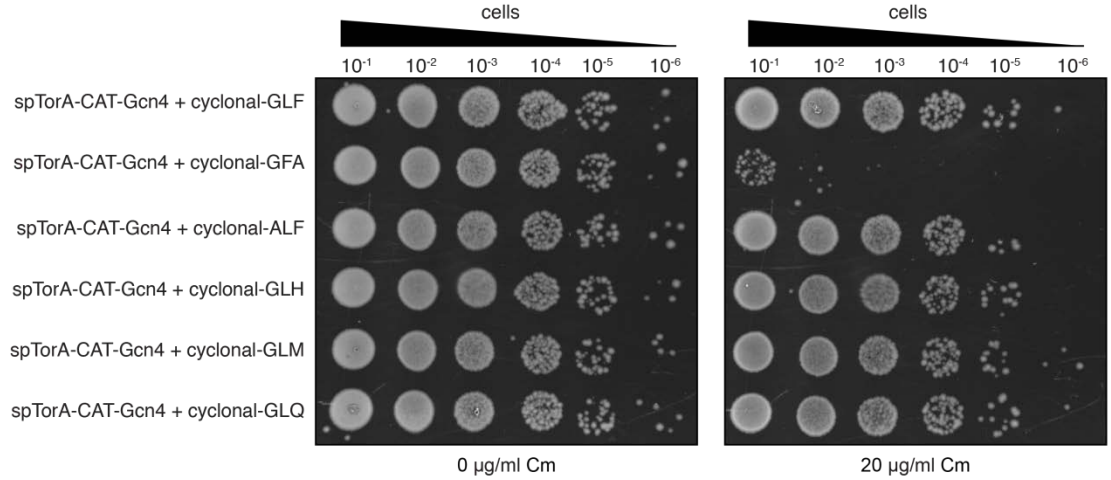

Figure 3.5 Performance of anti-Gcn4 variant cyclonals in CAT selection. Selective spot plating of SHuffle cells with plasmids for expressing anti-Gcn4 variant cyclonals and CAT-antigen fusions as indicated. Selected CDR-H3 residues are indicated in parenthesis cyclonal(XXX). SHuffle cells carrying plasmids for the non-specific cyclonal [cyclonal(GFA)] and parent cyclonal [cyclonal(GLF)] were plated as negative and positive controls, respectively. SHuffle cells were serially diluted in LB media and 5 µl was plated on LB-agar supplemented with 0 or 20 µg/ml chloramphenicol, 0.4 % arabinose, and 1mM IPTG.

CAT selection of specific antibodies from synthetic cyclonal library. Next, we examined whether our strategy could be employed to select antigen specific binders from a library composed of cyclonals with randomized CDR-H3 sequences. Structural studies indicate that the third complementarity determining region of the IgG heavy chain typically forms crucial interactions with the bound antigen [159-162]. We chose the basic leucine zipper domain of Gcn4 as it has been used as a model antigen to test

other antibody selection strategies [133]. The CDR-H3 of the published anti-Gcn4 cyclonal variants consists of 5 residues (e.g. GLFDY, ALFDY). We elected to construct an IgG library similar to the scFv libraries selected against Gcn4 in Waraho and DeLisa. In order to generate an IgG library, we randomized the first three residues of the heavy chain CDR3 of the non-binding anti-Gcn4 cyclonal, anti-Gcn4(GFA) leaving the last two residues (DY) constant. Two libraries were constructed: one in which the NDT codon was used to randomize the CDR-H3, and a second where the NNK degenerate codon was used for random mutagenesis of CDR-H3. SHuffle cells carrying the spTorA-CAT-Gcn4 reporter were cotransformed with each library. To isolate Gcn4 binders, a total of ~2.8×10^7 clones from each library were selected on LB agar supplemented with 10 µg/ml Cm. SHuffle cells coexpressing spTorA-CAT-Gcn4 and anti-Gcn4(GFA) were plated similarly as a negative control. After 72 h, 20 clones were selected at random from each library plate (NDT and NNK). The growth phenotype was confirmed by retransforming SHuffle cells carrying the Gcn4 reporter with plasmids isolated from the 20 clones and plating under selective conditions. A total of 20 positive clones, 10 from the NDT and 10 from the NNK library, were then sequenced. Of those clones, 19 were unique. To verify Gcn4 specificity, the 19 unique cyclonal clones were expressed in SHuffle cells and soluble extract from these clones was measured for Gcn4 binding activity. Four of the clones, anti-Gcn4(GLF), anti-Gcn4(SLF), anti-Gcn4(GIN), anti-Gcn4(GTK) exhibited Gcn4 binding activity (**Figure 3.6**).

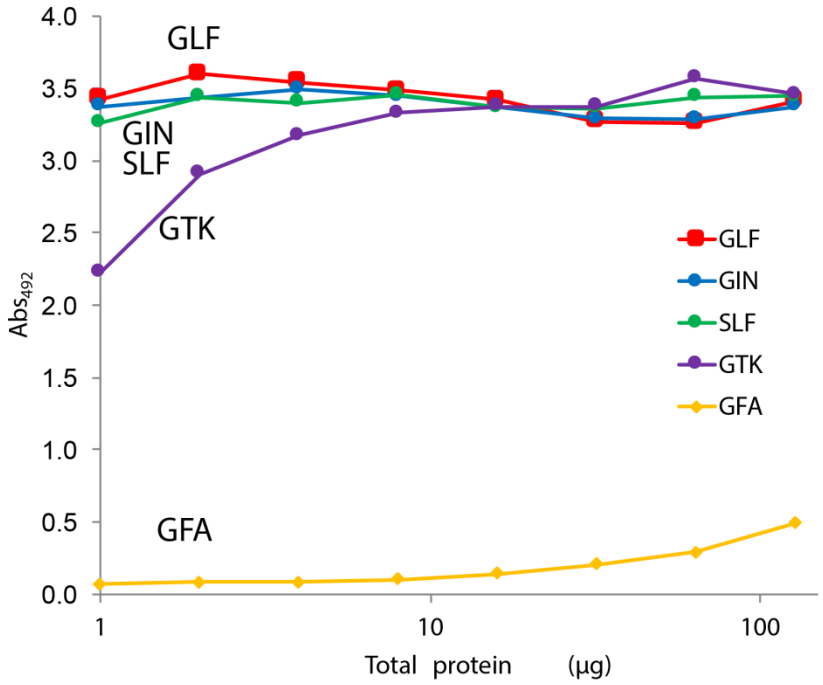

Figure 3.6. Confirmation of Gcn4 binding activity of selected clones from randomized 3-residue libraries. Soluble extracts prepared from SHuffle T7 express cells expressing clones selected from the 3-residue NNK and NDT libraries were assayed for binding activity against Gcn4 by ELISA. Extracts containing GLF and GFA cyclonals were used as positive and negative controls, respectively. Extracts were serially diluted 2-fold in PBS buffer. Absorbance was measured at 492 nm. Binding was detected with a peroxidase-conjugated anti-human Fc IgG.

The observed binding activity confirmed the authenticity of the selected sequences. Of those clones, three (GLF, SLF, and GIN) were selected from the NDT library and the other (GTK) from the NNK library. It is noteworthy that the only sequence we isolated that is identical to one selected in the previous studies is GLF. However, this is not surprising as GLF is the original anti-Gcn4 sequence isolated by ribosome display in an earlier work by the Plückthun group[78]. The other three sequences are unique to our study. However, an equally interesting observation is that the hits still adhere to a similar pattern to those selected in previous studies. For instance, GIN and GTK both contain glycine in the first position, which is consistent with all hits selected by Waraho and DeLisa and with a majority of those selected by

de Maur et al [88, 155]. The GIN clone in particular shares not only glycine in the first position with the hits selected by Waraho and DeLisa, but, also a similar amino acid isoleucine (I) in the second position. Each hit isolated by Waraho and DeLisa contained leucine (L) in the second position within the three-amino acid CDR-H3 in addition to glycine in the first position. Similarly, SLF shares the identity of the amino acids in the second and third position with the wild-type sequence GLF. Clones GIN and SLF support the findings of both studies that there is a strong preference for a straight chain hydrophobic amino acid (Isoleucine or Leucine) at the second position.

Noting that *in vivo*, CDR-H3 sequences frequently vary in length, we tested whether cyclonals could be directly selected from a library with a longer randomized CDR-H3. We chose to insert an additional randomized position into CDR-H3 again leaving the final two residues constant. The result was a library with four total randomized positions within the CDR (NDT4). To construct the NDT4 library, four residues within the expanded CDR-H3 of anti-Gcn4(GFA) were randomized with the NDT codon. The NDT4 library was screened using the SHuffle reporter strain on LB agar supplemented with 10-20 μg/ml Cm. A total of ~$2.8x10^7$ clones were plated and cultured for 72 hrs. Twenty positive clones were verified by retransforming the SHuffle reporter strain and confirming antibiotic resistance. Ten clones were tested for binding activity against Gcn4 and one clone (GLLD) specifically bound the antigen with high affinity (**Figure 3.7**).

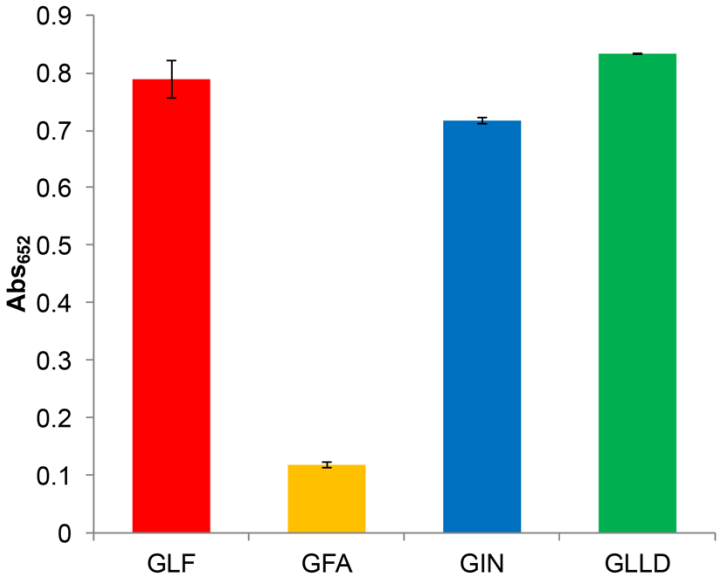

Figure 3.7. Confirmation of Gcn4 binding activity of selected clones from randomized 4-residue libraries. Soluble extracts prepared from SHuffle T7 express cells expressing selected positive cyclonal clones were assayed for binding activity against Gcn4 by ELISA. Extracts containing GLF and GFA cyclonals were used as positive and negative controls, respectively. GIN cyclonal was previously selected from the NDT3 library. Extracts were serially diluted 5-fold in PBS buffer. Data shown are the anti-Gcn4 binding activity for 2 µg total protein extract (0.04 µg/ml). Absorbance was measured at 652 nm. Binding was detected with a peroxidase-conjugated anti-human Fc IgG.

Interestingly, the identities of the selected CDR-H3 residues of this clone strictly follow the pattern observed in the two previous works [88, 133]. In fact, the GLLD clone is nearly identical to the 3-residue CDR-H3 clone GLL selected in both studies. In summary, we have demonstrated the potential of our CAT reporter assay as a tool for isolating functional antigen-specific full-length IgG antibodies.

Discussion

In this chapter, we report a novel strategy for direct selection of functional full-length IgGs in bacteria cells. Our simple genetic selection is based upon inhibiting Tat mediated secretion of a hybrid cytoplasmic reporter to the periplasm. It is made possible by building upon previous work in which we achieved soluble expression of full-length antibodies within the cytoplasm of engineered *E. coli* cells, which is not possible using wild-type *E. coli* cells. The CAT reporter selection bypasses the need

for the costly and time-consuming step of immunization.

We first showed that we could select for attenuated export via the Tat pathway of three-part fusions, consisting of Tat signal peptide, followed by the CAT enzyme and an antigen of interest (spTorA-CAT-Ag). The selective advantage, resistance to Cm, was observed for several antigens. Blocked export due to a deficient Tat signal peptide presumably leads to a higher concentration of the spTorA(KK)-CAT-Ag reporter within the cytoplasm; however, further experiments must be performed to confirm this. We also showed that the effect of blocked reporter export could be observed by coexpressing antibody fragments that specifically bind the CAT reporter. Exploiting this phenomenon, we demonstrated that by simply observing a growth phenotype under appropriate selective conditions cognate antigen:antibody could be identified from non-cognate ones. Conferral of chloramphenicol resistance was observed using both scFv and Fab antibody fragments, the latter proving that the assay is compatible with formats that require disulfide bonds for proper assembly. Additionally, we proved that the specificity of a scFv could be reported with the spTorA-CAT-Ag reporter strategy suggests that the assay might be used as a general protein-protein interaction reporter for proteins as small as ~28 kDa.

The spTorA-CAT-Ag selection method was further extended to report specific binding between a full-length IgG and its target. As with the antibody fragments, this method proved to be applicable across a number of different antigen:antibody interactions. Furthermore, we demonstrated that the CAT reporter assay could be used for selection of functional antibodies from a synthetic antibody library. Five specific clones that bind Gcn4 were selected from 3 different libraries demonstrating the potential for using CAT hybrid selection as a tool for antibody engineering (**Table 3.1**). Clone GTK is a notable case, as it does not have a leucine or isoleucine in the second position of its CDR-H3. Although GTK was found to have measurable binding

activity against Gcn4, it is less active than the other selected clones, GIN and SLF. The GTK clone differs the most from the hits selected in the two previous works, and therefore warrants further characterization and study. The selection of the GTK clone over expected clones is intriguing, and further characterization of this clone could provide some insight into the mechanism of selection.

	CDRH3	92	93	94	95	96	97	98	99	100
Reference	Library	C	V	T	X	X	X	X	D	Y
WT	-	.	.	.	G	L	F	-	.	.
This study	NNK3	.	.	.	G	T	K		.	.
This study	NDT3	.	.	.	G	I	N		.	.
This study	NDT3	.	.	.	S	L	F	-	.	.
This study	NDT3	.	.	.	G	L	F	-	.	.
This study	NDT4	.	.	.	G	L	L	D	.	.
Waraho	NNK3	.	.	.	G	I	M		.	.
der Maur	NNK3	.	.	.	G	L	M		.	.
der Maur	NNK3	.	.	.	G	L	Q		.	.

Table 3.1. Comparison of CDR-H3 sequences of confirmed anti-Gcn4 hits to previous studies. CDR-H3 sequences of confirmed anti-Gcn4 hits are aligned with hits from previous studies. The study and the strategy used to diversify the library from which the hit was isolated are indicated in the first two columns. Conserved residues before and after CDR-H3 are shown in the second row. Amino acid positions are numbered according to the system devised by Kabat [163].

It is noteworthy that we do not completely understand the mechanism by which our selection works as the Tat translocation mechanism itself is not well-understood. For instance, we observed that the size of the antigen component of the reporter is important. Each antigen that worked well within the context of the assay was very small in size with the largest compatible antigen being the Gcn4 leucine zipper. This is not surprising given that CAT has a molecular weight of ~25 kDa and is a known trimer[153]. Thus, even when expressed as a fusion to a small 10 kDa protein, this results in a ~105 kDa CAT-Ag complex. As a result, the CAT-Ag hybrid may be poorly exported due to its size. At this juncture care must be taken when choosing an appropriate antigen for use in the assay. The effect of export efficiency of the reporter on the efficacy of the selection is worth investigating so as to better

understand the parameters of the method.

While there are a handful of genetic selections that have been reported for isolating functional antibodies, none has been adapted for full-length IgG antibodies. All currently reported genetic selections have only been demonstrated for scFvs and similar antibody fragment formats [85, 88, 89, 132, 164]. Furthermore, these strategies require the modification of the antibody, with either a signal peptide or reporter fragment, to be compatible with the selection. On the other hand, our CAT reporter selection requires no modification of the IgG and therefore the selected plasmid can be used directly for functional IgG expression without sub cloning. Therefore, the process is streamlined from selection to expression for end use or further characterization.

Our strategy also offers several advantages over microbial display methods that have been developed in the past decade. First, it does not require purification or immobilization of the target antigen. Furthermore, to use the CAT-Ag selection there is no need for labeling of the antigen (e.g. fluorophore) as is required for the fluorescence-activated cell sorting (FACS) based screening technologies developed for isolating full-length IgG including the BAD and E-clonal systems [93, 95]. In addition, successful performance of the CAT reporter selection does not require the use of expensive or specialized equipment. Our selection system alleviates the need for laborious washing steps and time-consuming panning steps associated with plate and bead based screens. Another advantage is that selection is conducted with viable cells that can be recovered and amplified after selection. This is in contrast to most bacterial display screens in which the cells are non-viable after permeabilization of the outer membrane.

Though further development is needed, the CAT reporter assay is possibly the simplest method for engineering full-length antibodies reported to date.

Materials and Methods

Bacterial Strains and Plasmids. SHuffle T7 Express (New England Biolabs) was used for all library selections, and cyclonal expression experiments. DH5alpha was used for all cloning experiments, plasmid construction, and library construction. Protein antigens for immunoassays were expressed in T7 Express (New England Biolabs) and BL21 (DE3) (Novagen) strains. The vector pCOLA-Duet cIgG (Novagen) was purchased from EMD Millipore and this vector was used to express all antibody fragments and cyclonals. The vector pBAD24[165] was used for expression of spTorA-CAT-Ag reporter fusions. The GST-Gcn4 antigen was expressed from the plasmid pET28a-GST-Gcn4 in *E. coli* T7 express cells (NEB).

Plasmid construction. The gene encoding scFv-HAG was amplified using primers that added a 5' NcoI site and 3' SalI site by PCR using the plasmid pHK38[134]as a template. FLAG epitope DNA sequence was constructed by annealing complementary phosphorylated oligonucleotides that added a SalI overhang to the 5' end and an XhoI overhang at the 3' end. The scFv-HAG PCR product and pCOLA-Duet were digested using NcoI and SalI. The FLAG oligonucleotide dimer and scFv-HAG gene was inserted by double ligation into the NcoI/XhoI site of pCOLA-Duet generating pCOLA-Duet-scFv-HAG-FLAG. DNA for scFv-gpD was PCR amplified from pHK49 adding an NcoI and SalI to the 5' and 3' ends, respectively. The resulting product and pCOLA-Duet-scFv-HAG-FLAG were double digested by NcoI and SalI and ligated to produce pCOLA-Duet -scFv-gpD-FLAG. To construct plasmids for Fab expression, the light chain genes (V_L-m$C_L\kappa$) for anti-HAG and anti-Gcn4 Fab were PCR-amplified from the pMAZ360-cIgG-aHAG-mFab/hFc and pMAZ360-cIgG-aHAG-mFab/hFc vectors, respectively using primers that added an NcoI site upstream and a downstream NotI. After digesting pCOLA-Duet and the light chain genes with NcoI and NotI, the digestion products were ligated resulting in pCOLA-Duet –cIgL-

aHAG and pCOLA-cIgL-aGcn4. The genes coding for heavy chain Fab fragment (V_H-mC_H1) were also amplified by PCR using pMAZ360-cIgG-aHAG-mFab/hFc and pMAZ360-cIgG-aHAG-mFab/hFc as templates during which NdeI and AscI restriction sites were introduced at the 5' and 3' ends of the product. DNA coding for the FLAG epitope tag was assembled by annealing complementary phosphorylated oligonucleotides that added a 5' AscI and a 3' XhoI overhang to the gene fragment. Separately, the intermediate vector products pCOLA-Duet –cIgL-aHAG and pCOLA-cIgL-aGcn4 were digested with NdeI and XhoI. The PCR amplified anti-HAG heavy chain Fab fragment was digested using NdeI and AscI, and double ligated with FLAG and pCOLA-Duet –cIgL-aHAG to create pCOLA-Duet –cF_{AB}-aHAG-Mus-FLAG. Similarly, the PCR amplified anti-Gcn4 heavy chain Fab fragment was digested using NdeI and AscI, and double ligated with FLAG and pCOLA-cIgL-aGcn4 to generate the final product pCOLA-Duet –cF_{AB}-aGcn4-Mus-FLAG. The anti-MBP Fab expression vector was cloned by first inserting the murine light chain, into the NcoI/ NotI site pCOLA-Duet –cF_{AB}-aHAG-Mus-FLAG and subsequently ligating V_H-mC_H1 genes from pMAZ360-cIgG-aMBP-mFab/hFc into the NdeI/AscI site of the get the final product pCOLA-Duet –cF_{AB}-aMBP-Mus-FLAG.

For the expression of cyclonals, the mFab/hFc heavy chain genes (V_H-mC_H1-hFc) for anti-HAG, anti-Gcn4, and were PCR-amplified from vectors pMAZ360-cIgG-aHAG-mFab/hFc, pMAZ360-cIgG-aGcn4-mFab/hFc, and pMAZ360-cIgG-aMBP-mFab/hFc, respectively. 5' NdeI and 3'XhoI restriction sites were introduced during the amplification of each heavy chain product. The heavy chain PCR products and associated pCOLA-Duet –cF_{AB} vectors were digested with NdeI and XhoI and the digestion products were ligated to produce pCOLA-Duet –cIgG-aHAG-mFab/hFc, pCOLA-Duet –cIgG-aGcn4-mFab/hFc, pCOLA-Duet –cIgG-aMBP-mFab/hFc.

Anti-Gcn4 CDR-H3 cyclonal variants (ALF, GFA, GLH, GLM, and GLQ)

were generated by site-directed mutagenesis of the original anti-Gcn4 cyclonal heavy chain (GLF) [133] by overlap extension PCR. For each anti-Gcn4 variant, the V_H sequence was amplified with a common forward primer that introduced a 5' NdeI site and a unique reverse primer that encoded the 9-nucleotide CDR-H3 sequence of the specific variant. In parallel, the DNA sequence for the constant domains of the mFab/hFc heavy chain, mC_H1-hFc, was amplified using a forward primer that introduced a sequence that overlaps with the end of the V_H gene. Full-length heavy chains (V_H-mC_H1-hFc) were produced by fusing each V_H PCR product encoding a CDR-H3 variant with the mC_H1-Fc product by overlap extension PCR. The full-length CDR-H3 variants were digested with NdeI and XhoI and ligated into the NdeI/XhoI site of pCOLA-Duet-cIgG-aGcn4 yielding pCOLA-Duet-cIgG-aGcn4(ALF), pCOLA-Duet-cIgG-aGcn4(GFA), pCOLA-Duet-cIgG-aGcn4(GLH), pCOLA-Duet-cIgG-aGcn4(GLM), and pCOLA-Duet-cIgG-aGcn4(GLQ).

For cytoplasmic expression of the anti-c-Myc IgG, V_L domain sequence was amplified from scFv-3DX[154] while using primers that added a 5' NcoI site and a sequence overlapping with the mouse constant light chain kappa domain ($mC_L\kappa$). In a parallel PCR, the mCLκ sequence was amplified with primers that introduced a 5' sequence overlap with the V_L of scFv-3DX and a 3' NotI site. The two PCR products were fused by overlap extension PCR producing the full-length anti-c-Myc light chain, V_L-3DX- $mC_L\kappa$. Similarly, the V_H domain sequence for anti-c-Myc was amplified from scFv-3DX using primers that added a 5' NdeI site and a sequence overlapping with the mFab/hFc heavy chain constant domains. At the same time, the mFab/hFc constant heavy chain domains were amplified with primers that introduced a 5' sequence overlap with the V_H of scFv-3DX and a 3' XhoI site. The two PCR products were combined by overlap extension PCR creating the full-length anti-c-Myc heavy chain, V_H-3DX- mC_H1-hFc. The full-length light chain and full-length heavy chain

products were cloned into the NcoI/NotI and NdeI/XhoI sites of pCOLA-Duet-cIgG, respectively to produce pCOLA-Duet-cIgG-3DX-mFab/hFc.

To generate the CAT-Ag reporter vectors, spTorA-JunLZ-FLAG, DNA, encoding the signal peptide of *E. coli* TorA (spTorA) fused to the N terminus of the c-Jun leucine zipper was amplified using pBAD18-spTorA-JunLZ-FLAG[88] as a template with 5' NheI and 3'HindIII restriction sites. The digested PCR product was cloned into pBAD24 that had been previously digested by NheI and HindIII yielding pBAD24-spTorA-JunLZ-FLAG. The gene for chloramphenicol acetyl transferase (CAT) was PCR-amplified from pACYC-Duet with a 5' XbaI site and downstream DNA coding for a flexible linker (GTSAAAG) flanked by SalI and SpeI restriction sites. The GCN4(7P14P) gene, encoding a double proline mutant of the bZIP domain of transcription factor Gcn4 that reduces its propensity for homodimerization, was amplified from pBAD33-GCN4(7P14P)-Bla[88] inserting the same flexible linker sequence at the 5' end and a 3'HindIII restriction site. The genes for CAT and GCN4(7P14P) were fused by overlap extension PCR. The overlap extension PCR product was digested by XbaI and HindIII and ligated into XbaI-HindIII digested pBAD24- spTorA-JunLZ-FLAG yielding pBAD24-spTorA-CAT- GCN4(7P14P). Genes for HAG peptide and c-Myc epitope tag (EQKLISEEDL) were constructed by annealing complementary oligonucleotides. HAG and c-Myc were cloned in the place of GCN4(7P14P) after digestion of pBAD24-spTorA-CAT- GCN4(7P14P) with SpeI and HindIII yielding plasmids pBAD24-spTorA-CAT- HAG and pBAD24-spTorA-CAT- c-Myc.

Selective growth assays. Chemically competent SHuffle cells were transformed with pCOLA-Duet encoding antibody expression and pBAD24-spTorA-CAT-Ag plasmids, spread on Lysogeny Broth (LB)-Agar plates supplemented with 25 μg/ml spectinomycin (Spec), 25 μg/ml kanamycin (Kan), and 50 μg ampicillin (Amp), and

cultured overnight at 37°C. The next day, 3 mL LB with 25 μg/ml spectinomycin, 25 μg/ml kanamycin, and 50 μg ampicillin was inoculated with three freshly transformed colonies and incubated at 30°C for 12-18 h. Cells carrying the pCOLA-Duet and pBAD24-spTorA-CAT-Ag plasmids were normalized to a cell density of A_{600}=2.5 ($2.5x10^9$ cells/mL) as measured by a spectrophotometer. Cells were then serially diluted ten-fold in LB medium typically. 5 μl of each dilution was spotted on selective induction plates with 25 μg/ml spectinomycin, 25 μg/ml kanamycin, and 50 μg/ml ampicillin, 1 M IPTG, 0.2% arabinose, and varying concentrations of chloramphenicol. The plates were then incubated at 30°C for 24-48 h.

Library construction. The first anti-Gcn4 library was generated by random mutagenesis of the first three residues of CDR-H3 using the NDT codon (NDT3). The resulting library encoded anti-Gcn4 heavy chain CDR-H3 variants of the form XXXDY, where X can be any of the 12 amino acids encoded by the NDT codon (X = G, V, L, I, C, S, R, H, D, N, F, or Y). The NDT codon degeneracy (12 codons/12 amino acids) theoretically results in no codon bias at the randomized positions and zero probability of the occurrence of a premature stop codon. Also, the balanced mix of amino acids encoded by the NDT codon is representative of the chemical and structural diversity within the entire group. Finally, smaller number of possible members requires fewer transformants for full library coverage. Random mutagenesis of the CDR-H3 was achieved by amplifying the entire pCOLA-Duet-cIgG-aGcn4(GFA)-mFab/hFc plasmid by inverse PCR with a reverse primer encoded the three randomized codons within CDR-H3. The resulting linear PCR product was circularized by blunt end ligation producing the plasmid library pCOLA-Duet-cIgG-aGcn4(XXXDY). The circularized product was used to transform electrocompetent DH5alpha cells. The transformed cells were cultured overnight in 100 mL LB and 50 μg/ml kanamycin. Plasmid DNA was purified by maxiprep from the overnight culture

for selection experiments. A second library (NNK3) was created in a nearly identical manner with the only change being that the first three residues of CDR-H3 were randomized using the NNK codon instead of the NDT codon.

To create the NDT4 library, the first three residues of CDR-H3 of the anti-GCN4(GFA) were replaced with 4 randomized residues by mutagenesis PCR featuring a reverse primer that encodes 4 amino acids, each with the NDT codon. The PCR product, V_H-aGcn4(XXXXDY), was fused to the constant domains of the mFab/hFc heavy chain (mC_H1-hFc) to generate a full-length heavy chain product. The heavy chain product was ligated into the NdeI/XhoI site of pCOLA-Duet-cIgG-aGcn4 yielding pCOLA-Duet-cIgG-aGcn4(XXXXDY). The ligation product was used to transform electrocompetent DH5alpha cells. The transformed cells were cultured overnight in 100 mL LB and 50 μg/ml kanamycin. Plasmid DNA was purified by maxiprep from the overnight culture for selection experiments.

Library selection. To perform library selections, electrocompetent SHuffle T7 cells carrying the pBAD24-spTorA-CAT-Gcn4 reporter plasmid were transformed with the purified anti-Gcn4 mFab/hFc cyclonal libraries. Transformants were incubated in SOC media at 37 C for 1 hr without antibiotics and then cultured overnight in LB supplemented with 100 μg/ml Carb, 50 μg/ml Kan, and 0.2% glucose. The next day, overnight cells were normalized to A_{600} = 2.5 and serially diluted to 10^{-3}, 10^{-4}, and 10^{-5}. A total volume of 225 μl of each dilution was plated on LB-agar supplemented with 15-30 μg/ml Cm 0.2% Arabinose and 1 mM IPTG and cultured at 30°C for 72 hrs. At the same time, cells transformed with anti-Gcn4(GFA) and pBAD24-spTorA-CAT-Gcn4 were treated in an identical manner as library cells and used as a negative control. Clones that appeared on selective plates were picked at random and resistance to Cm was verified by selective spot plating. Plasmid DNA was isolated from positive clones and sequenced.

Expression of cytoplasmic IgGs. A single colony of SHuffle T7 Express transformed with one of the pCOLA-Duet-cIgG expression vectors was used to inoculate 2 ml Lysogeny Broth (10 g/L 1 tryptone, 5 g/L yeast extract, 5 g/L NaCl and NaOH to pH 7.2) supplemented with 50 µg/mL kanamycin and 25 µg/mL spectinomycin, and grown overnight at 30 °C. The next day, 5 ml of fresh LB supplemented with 50 µg/mL kanamycin was inoculated 1/100 with the overnight culture and cells were grown at 30 °C until reaching an absorbance at 600 nm (A_{600}) of 0.7. At this point, cyclonal expression from the pCOLA-Duet-cIgG vector was induced by addition of 0.1 mM isopropyl β-D-thiogalactopyranoside, after which cells were incubated an additional 16 h at RT or 30 °C. Cells were harvested by centrifugation before preparation of lysates.

Preparation of soluble cell extracts. Cells expressing recombinant proteins were harvested by centrifugation (4,000 x g, 4°C) and resuspended in PBS and 5 mM EDTA. Cells were lysed in an ice-water bath by sonication using a Branson sonifier 450 (Duty cycle 30% Output control 3) using four repetitions of 30 s each. The insoluble fraction was removed by centrifugation (21,000g, 4°C) and the supernatant collected as the soluble fraction.

Enzyme-linked immunosorbent assay (ELISA). Costar 96-well ELISA plates (Corning) were coated overnight at 4°C with 50 µl of 10 µg/ml GST-Gcn4, in 0.05 M sodium carbonate buffer (pH 9.6). The antigen GST-Gcn4 was expressed in *E. coli* T7 express cells and purified by standard nickel-charged affinity resin (Ni-NTA) purification. After blocking with 3% (w/v) milk in PBST (PBSTM) for 1–3 h at room temperature, the plates were washed four times with PBS buffer and incubated with serially diluted soluble fractions of crude cell lysates for 1 h at room temperature. IgG-containing samples were quantified by the Bradford assay and an equivalent amount of total protein (typically 8–64 mg) was applied to the plate. After washing four times

with the same buffer, 50 µl of 1:5,000-diluted rabbit anti-human IgG (Fc) antibody–HRP conjugate (Pierce) antibodies in PBSTM was added to each well for 1 h. The 96 well Plates were then washed six times with PBST. After the final wash, 200 µl SigmaFAST™ OPD solution (Sigma-Aldrich) was added and incubated within each well in the dark for 30 min. The HRP reaction was then terminated by the addition of 50 µl 3 M H_2SO_4 to the wells. Following reaction quenching, the absorbance of each well was measured at 492 nm. To develop plates with TMB, 50 µl 1-Step™ Ultra TMB-ELISA Substrate Solution (Thermofisher Scientific) was added and incubated within each well for 15 min. The absorbance of each well was measured at 652 nm and 370 nm.

Acknowledgements

We thank Dr. Mehmet Berkmen at New England Biolabs and Dr. Andreas Plückthun for kindly providing plasmids encoding genes for this study. We also thank Matt Chang for technical support in performing library selections and selective spot plating. We also thank Xiaolu Zheng for help in generating the NNK library.

CHAPTER 4

AN *IN VIVO* SPLIT-PROTEIN REPORTER FOR ANTIBODY:ANTIGEN INTERACTIONS

Introduction

In Chapter 3, we showed that microbial based genetic selections are viable options for isolation of antibodies from large combinatorial libraries. The goal of genetic selection strategies for antibody isolation is to couple fitness to intracellular reactivity between an antibody and its target. Techniques of this nature are attractive as they offer advantages over both display and traditional methods because they (1) do not require purification or elaborate preparation of the antigen and (2) greatly reduce the resources, expertise, and equipment required to successfully isolate and engineer antibodies. However, while we were successful in isolating full-length antibodies using our CAT selection, that strategy is potentially limited to smaller antigens. Therefore, in this chapter we developed a selection that can be applied to a more diverse set of targets.

The protein-fragment complementation assay (PCA), a strategy originally designed for studying protein-protein interactions (PPIs) [148, 166, 167], has been modified for the purpose of engineering antibody:antigen interactions. PCA strategies involve a reporter protein that is dissected into two inactive fragments. The two fragments are expressed as fusions to either an antigen of interest or its corresponding antibody. The activity of the reporter is restored when the antigen:antibody interaction brings the two fragments close enough to non-covalently reassemble into a native-like structure (**Figure. 4.1**). Although, several reporter proteins have been adapted for PCA including GFP, YFP, Luciferase, and β-galactosidase[168], PCAs designed for engineering binding interactions have most often leveraged murine Dihydrofolate reductase (mDHFR) or β-lactamase within the context of an *E. coli* survival

selection[86, 87, 169]. *E. coli* based PCAs using both enzymes have been used successfully to isolate antigen specific antibodies from naïve libraries [85, 149].

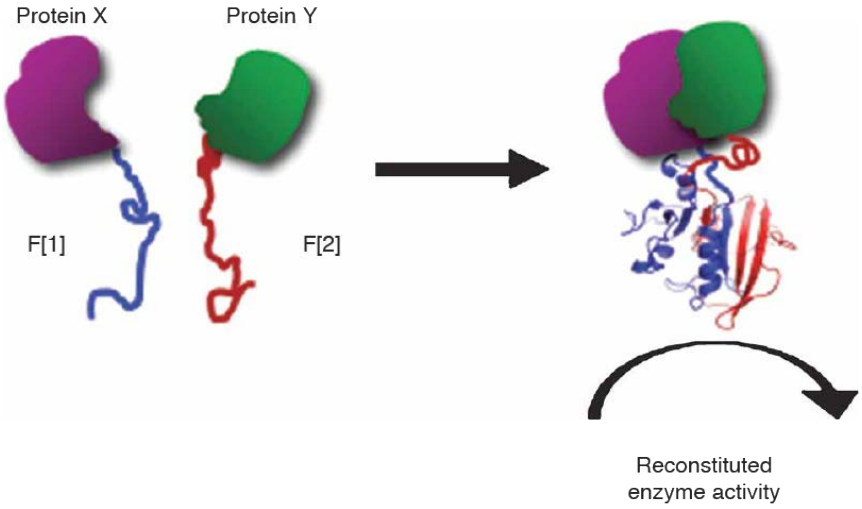

Figure 4.1 Principle of the protein fragment complementation assay. A reporter protein is expressed as two inactive polypeptide fragments F1 and F2. The fragments are then fused genetically to proteins of interest (X and Y) that potentially interact. If X and Y interact the fused fragments are brought into close enough contact to reconstitute enzymatic activity. Figure taken from Remy[170].

While there have been reports of isolating functional antibody fragments by survival selection, no study to date has described a genetic selection for specific full-length IgG antibody binding. This is partly because full-length IgG expression in *E. coli* had only been achieved by exporting the light and heavy chain polypeptide subunits to the periplasm where disulfide bonds can readily form. This requirement does not permit the use of cytoplasmic based reporters and would complicate implementation of a selection based on periplasmic reporters. However, recently we overcame this hurdle by proving that full-length monoclonal IgG antibodies (cyclonals) can in fact be expressed within the cytoplasm of bacteria engineered to permit cytoplasmic disulfide bonding. This finding opens up the possibility that a cytoplasmic reporter could be used to develop a selection for specific antibody:antigen binding.

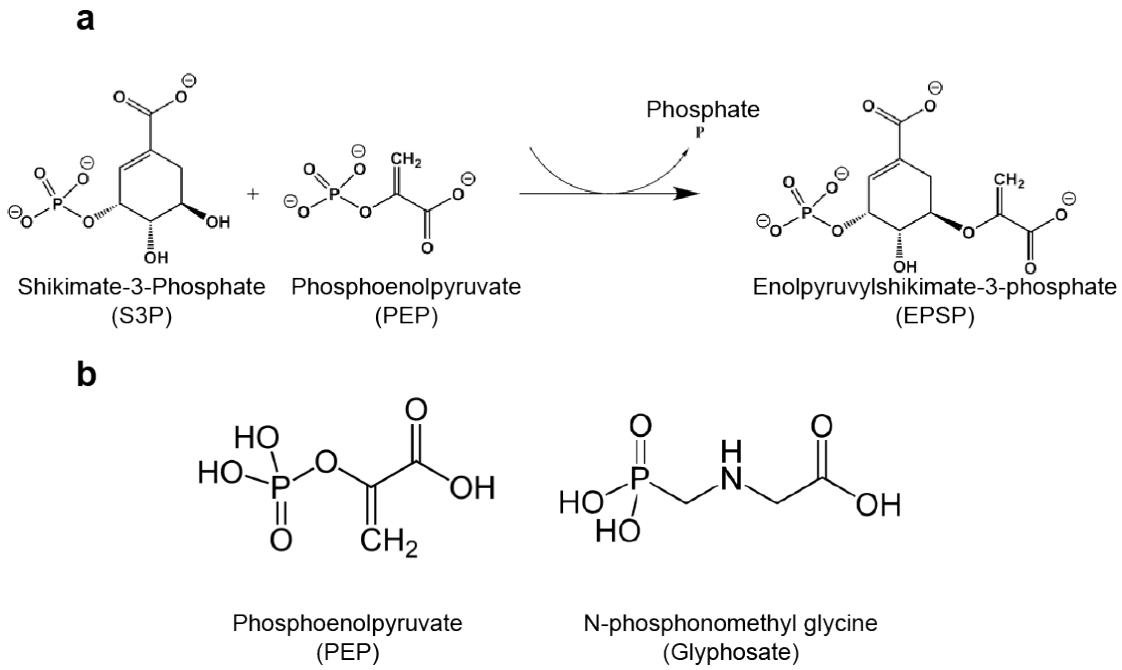

Figure 4.2 Enzyme catalyzed synthesis of EPSP. (a) The synthesis of 5-enolpyruvyl-shikimate-3-phophate (EPSP) is catalyzed by the product of the *aroA* gene. EPSP synthase facilitates the conversion of shikimate-3-phosphate (S3P) and phosphoenolpyruvate (PEP) generating EPSP and releasing a phosphate (b) Chemical structure of EPSPS substrate PEP and competitive inhibitor glyphosate N-phosphonomethylglycine.

In this study, we developed a genetic selection for reporting the binding of a full-length antibody to its target antigen within the cytoplasm of engineered bacterial cells based upon functional complementation of 5-Enol-pyruvl-shikimate-3-phosphate synthase (EPSPS). EPSPS is an enzyme produced natively in many plants, fungi, and other microorganisms that catalyzes the synthesis of 5-enol-pyruvl-shikimate-3-phosphate (EPSP) from shikimate-3-phosphate (S3P) and phosphoenolpyruvate (PEP) [171-174](**Figure 4.2a**). EPSP is an important precursor to the aromatic amino acids phenylalanine, tyrosine, and tryptophan[175]. *E. coli* lacking a functional copy of the *aroA* gene, the native gene that codes for the EPSPS, are auxotrophic with respect to aromatic amino acids and thus do not grow on minimal media[175].

Glyphosate (N-phosphonomethylglycine), a competitive inhibitor of EPSPS, is

broadly effective against plants, bacteria, and most organisms that utilize the shikimate pathway [176-178] (**Figure 4.2b**). It is the active ingredient of the herbicide Roundup (Monsanto) which is widely used in agriculture. As a result, several groups investigated protein fragment complementation as a means to engineer glyphosate tolerance in valuable crops while preempting lateral gene transfer of glyphosate resistance to other unwanted plants [179-181]. *E. coli* is often used as model system in several of these studies to test glyphosate resistance. For example, *Synechocystis* sp. PCC6803 DnaE split intein was shown to reconstitute a glyphosate tolerant version of *S. typhimurium* EPSPS from split fragments and confer growth on minimal media supplemented with glyphosate to an *E. coli aroA* knockout strain [179]. In another study, Dai et al. identified potential split sites within *E. coli* EPSPS using computational prediction methods to predict stable circular permutation mutants and then tested the ability of the most stable mutants to confer survival on *aroA* deficient cells cultured on minimal media[180]. Predicted split sites were confirmed by demonstrating that the two complementary fragments created by dissection at any one of the given sites restored growth on minimal media if the fragments were fused to homodimerizing leucine zippers[180].

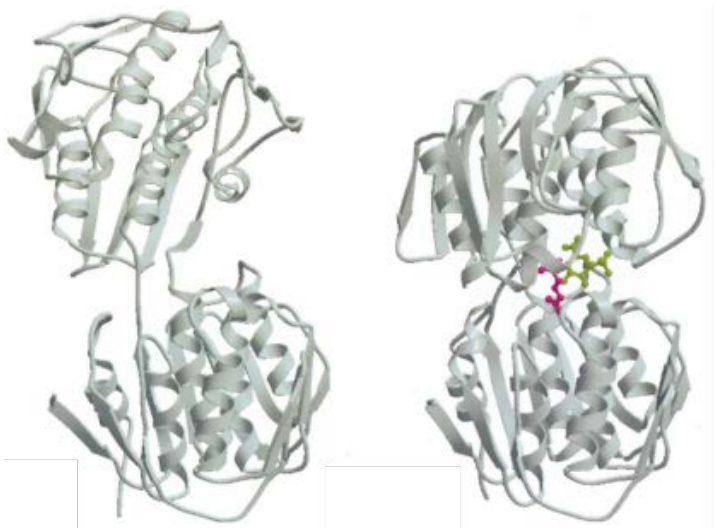

Figure 4.3 Structure of EPSPS synthase in its open and closed conformations. (a) Three-dimensional representation of the crystal structure of the EPSPS in its "open" conformation (i.e. without bound ligands). Cartoon shows the two distinct globular domains of EPSPS that are composed entirely of αβ-type folding units (b) "Closed" conformation of EPSPS in a complex with one of its substrates S3P (yellow) and competitive inhibitor glyphosate (magenta) represented as "ball-and-stick" models. Figure taken from Schönbrunn[172].

Here, we implemented a PCA in which EPSPS is dissected into two inactive fragments, one of which is fused to a full-length antibody and the second fused to its target antigen. The antibody:antigen interaction facilitates association of the two fragments thereby reconstituting the activity of EPSPS *in vivo*. The reassembled EPSPS enzyme confers growth on minimal media as well as resistance to glyphosate. Using this strategy we are able to distinguish between Δ*aroA* cells coexpressing specific and non-specific cyclonal:antigen binding pairs. We demonstrate with three cognate antibody:antigen pairs that only SHuffle Δ*aroA* cells expressing a specific pair exhibit robust growth on minimal media. This allows us to distinguish those cells from those coexpressing a non-interacting pair by observing a simple phenotype. Glyphosate supplementation of the minimal media resulted in an increase of the stringency of the PCA further allowing discrimination between interacting and non-interacting cases. Using the EPSPS PCA, we were able to isolate cells harboring a

specific antibody:antigen pair from a mock library of cells that contained a 1000-fold excess of cells coexpressing a non-interacting antibody:antigen pair. With further development, our EPSPS PCA could become a powerful antibody engineering tool that because of its simplicity makes antibody development an option for virtually any standard molecular biology lab.

Results

The *aroA* gene is essential for growth of SHuffle T7 Express cells on minimal media. Wild-type *E. coli* cells express EPSPS endogenously which allows them to grow on minimal media [182, 183]. In order to use *in vivo* EPSP synthase activity as a fitness filter, we first generated *aroA* knockouts in the SHuffle strain background (SHuffle Δ*aroA*). SHuffle Δ*aroA* cells showed no detectable growth when cultured on M9 minimal media agar confirming previous studies that found that EPSP synthase was required for survival under these conditions (**Figure 4.4a**). Complementation with EPSP synthase, expressed from either pBAD34-EPSPS or pET21b-EPSPS, restored viability to SHuffle Δ*aroA* cells on M9 agar (**Figure 4.4a**). The high level of EPSPS expression from the T7 driven pET21b vector appears to be mildly toxic to the cells as they grow slightly less dense compared to those complemented with pBAD34-EPSPS. SHuffle Δ*aroA* cells expressing plasmid encoded EPSPS exhibited higher levels of resistance to the antimicrobial agent glyphosate when compared to the wild-type SHuffle strain. SHuffle Δ*aroA* cells complemented with the *aroA* gene were observed to grow on concentrations of glyphosate reaching as high as 5 mM while wild-type SHuffle cells failed to survive on M9 minimal agar supplemented with greater than 1mM glyphosate**.**

A previous study reported that complementary EPSPS fragments, one composed of residues 1-235 of *S. typhimurium* EPSPS and the other composed of residues 236-427 of *S. typhimurium* EPSPS, could complement *aroA* knockouts if

fused to interacting domains of a split intein. As inactivity of the fragments resulting from the genetic dissection of the full-length gene is paramount to a robust PCA selection, we sought to determine if *E. coli* EPSPS dissected into two analogous polypeptide fragments lacked EPSPS activity. Additionally, we sought to prove that the fragments would not spontaneously reassemble into functional EPSPS when coexpressed in SHuffle Δ*aroA* cells. Therefore, we constructed one vector for expressing the fragment consisting of residues 1-235 of *E. coli* EPSPS ($EPSPS^{N235}$), and a second vector for expressing the fragment composed of residues 236-427 of EPSP synthase ($EPSPS^{C236}$). Neither the expression of the fragments by themselves nor the coexpression of both EPSPS fragments conferred survival upon SHuffle Δ*aroA* cells when cultured on minimal media (**Figure 4.4a**).

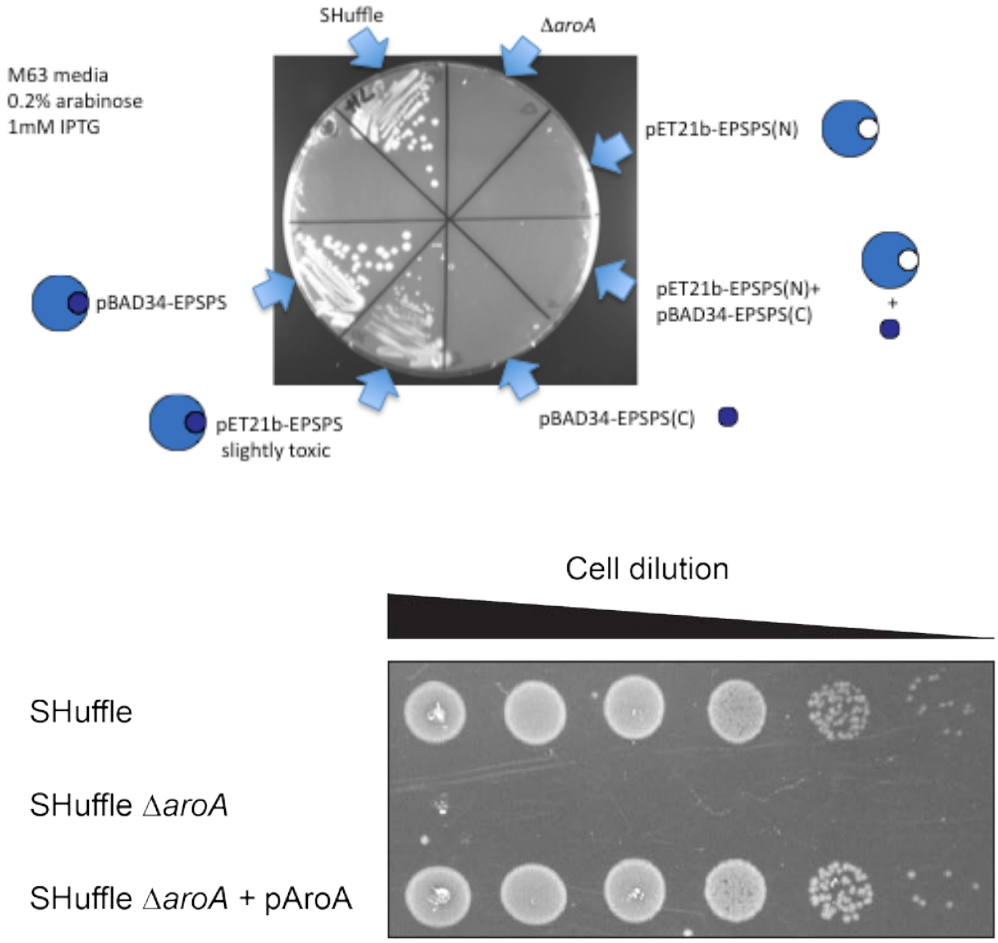

Figure 4.4 Complementation of EPSP synthase enzyme in SHuffle T7 express cells. (a) SHuffle T7 Express (SHuffle) or SHuffle T7 Express with the *aroA* deleted (Δ*aroA*) expressing the full-length EPSP synthase enzyme (EPSPS), the N terminal EPSP synthase fragment ($EPSPS^{N235}$), the C terminal EPSP synthase split fragment ($EPSPS^{C236}$), or both split fragments ($EPSPS^{N235}$ + $EPSPS^{C236}$) were streaked and cultured on M9 minimal media agar. Proteins were expressed from either the pBAD34 (arabinose inducible) vector or pET21b (b) Selective spot plating of serially diluted SHuffle T7 express (SHuffle), SHuffle T7 express Δ*aroA* (SHuffle Δ*aroA*) cells, and SHuffle T7 Express Δ*aroA* cells carrying the pBAD24-EPSPS (SHuffle Δ*aroA* + pAroA). SHuffle T7 express was plated as a positive control while SHuffle T7 express Δ*aroA* cells without a plasmid were plated as a negative control.

EPSP synthase activity reconstituted with basic leucine zipper interactions. Having demonstrated that the previously reported EPSPS fragments $EPSPS^{N235}$ and $EPSPS^{C236}$ do not possess EPSPS activity, we sought to confirm that fusing the

fragments to a known interacting pair would result in functional complementation of EPSPS in the SHuffle Δ*aroA* strain background. As an initial test of this concept, we chose to fuse the EPSPS fragments to the basic region leucine zipper (bZIP) domains of c-Fos (FosLZ) and c-Jun (JunLZ) (**Figure 4.5a)**. The interaction between leucine zipper domains is strong and well-characterized [184-186] and is often used as a model interaction to validate protein-protein interaction reporters and PCAs [88, 187, 188]. SHuffle Δ*aroA* cells expressing FosLZ- EPSPS^{N235} (FosLZ fused to N terminally EPSPS^{N235}) and JunLZ-EPSPS^{C236} (JunLZ domain fused to the C terminus of EPSPS^{C236}) showed a selective advantage over cells that coexpressed the unfused fragments when plated on M9 minimal media agar (**Figure 4.5b**). While EPSPS complementation facilitated by the FosLZ:JunLZ interaction resulted in restoration of cell viability, SHuffle Δ*aroA* cells expressing FosLZ:JunLZ assembled EPSP synthase are less viable than wild-type SHuffle T7 Express cells (**Figure 4.5b**).

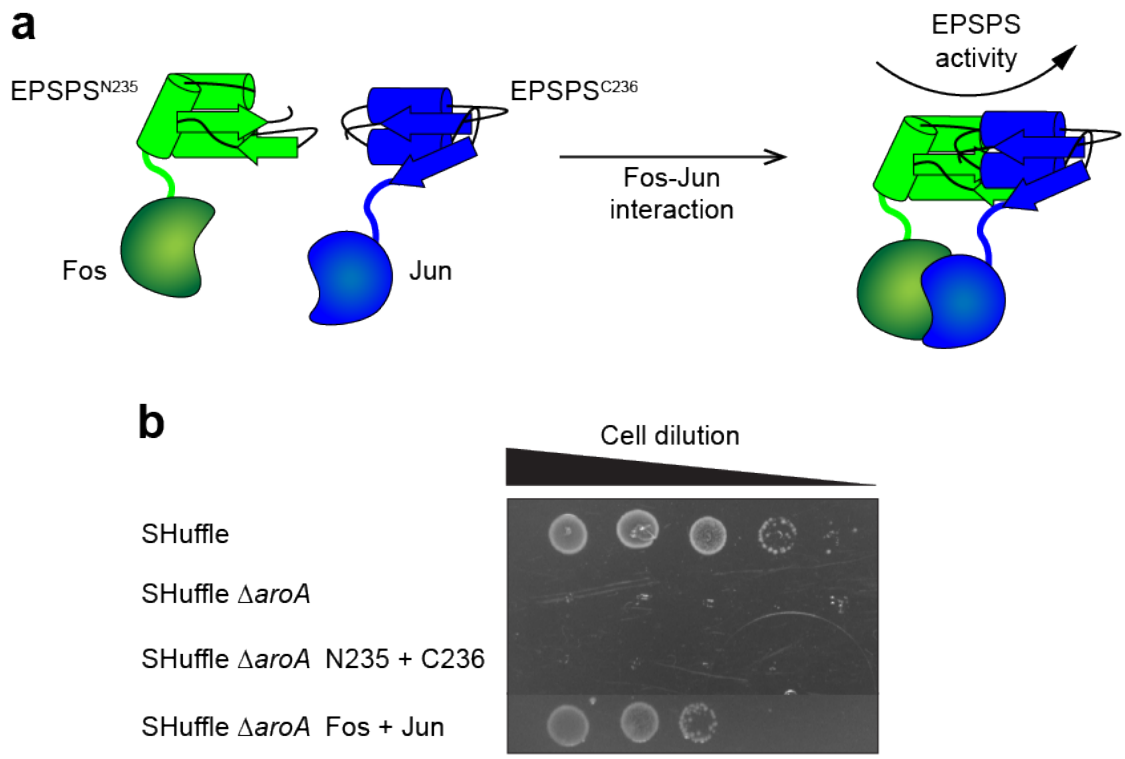

Figure 4.5 FosLZ-JunLZ mediated reconstitution of split EPSP synthase fragments. (a) Schematic representation of FosLZ:JunLZ oligomerization mediated reactivation of EPSPS. FosLZ is fused to the N terminus of an EPSPS fragment composed of residues 1-235 ($EPSPS^{N235}$) by means of a flexible linker $(Ala(Ser)_3(Asn)_{10})$ and coexpressed with JunLZ fused to the C terminus of the complementary EPSPS fragment composed of residues 236-427 ($EPSPS^{C236}$). The interaction between FosLZ and JunLZ leucine zippers bring the fragments within a functional radius within which they can form an active enzyme (b) Selective spot plating of serially diluted SHuffle Δ*aroA* cells carrying plasmids pET21b- $EPSPS^{N235}$ and pBAD34- $EPSPS^{C236}$ (N235 + C236) encoding the two complementary EPSPS fragments unfused, or SHuffle Δ*aroA* cells transformed with pET21b- FosLZ-$EPSPS^{N235}$ and pBAD34- $EPSPS^{C236}$-JunLZ, coding for FosLZ-$EPSPS^{N235}$ and $EPSPS^{C236}$-JunLZ interacting hybrid protein pair (SHuffle Δ*aroA* Fos+ Jun). Additional controls plated were empty SHuffle and SHuffle Δ*aroA* cells.

Rational design and characterization of a functional cyclonal-EPSPS fusion for PCA. Following the observation that the EPSP synthase-based PCA faithfully reports FosLZ:JunLZ heterodimerization, we set forth to determine whether this system could be adapted to identify antibody:antigen binding pairs. The requisite folding and assembly processes required for the correct biosynthesis of a functional cyclonal

presents several challenges. Cyclonals are tetrameric and require stable disulfide bond formation for their proper assembly and function. Therefore, one of the most crucial design considerations is the location of the EPSPS fragment in its fusion with the cyclonal.

There are four conceivable positions where an EPSP synthase fragment may be fused to a cyclonal of interest. These include the amino and carboxyl terminus of the light chain and the amino and carboxyl terminus of the heavy chain. The position of the EPSPS fusion must meet three critical criteria (**Figure 4.7**): (1) Allow for correct assembly of the IgG tetramer via disulfide bonding (2) Not interfere with antigen binding, and (3) Enable the split fragments to reassemble upon antigen:cyclonal interaction. Fusion to the N terminus of either cyclonal chain could potentially interfere with antigen binding since the binding pocket (formed by the six CDR loops) is structurally adjacent to the N terminus of both chains. However, these N terminal fusions should not interfere with heavy chain-heavy chain assembly (e.g. disulfide bonding) as the heavy chain cysteines within the hinge region (C226 and C229) should be completely free to participate in disulfide bonding. The C terminus of the light chain is distal to the antigen binding surface at N terminus of the cyclonal. Therefore EPSPS fusions to the C terminus of the light chain should also avoid interference with antigen recognition. Fusion to the C terminus of the heavy chain, however, would most likely position the fused EPSPS fragment too far from the antigen binding surface to functionally reconstitute enzymatic activity without the use of a long linker. Therefore, fusing an EPSPS fragment C terminally to the cyclonal light chain struck the best balance between positioning the fusion as close as possible to the antigen binding region while having minimal interference with binding and full-length cyclonal assembly. One possible disadvantage to fusing an EPSPS fragment to the C terminus of the light chain would be interference with heavy chain/light chain

assembly as the final cysteine at the C terminus of light chain participates in interchain disulfide bonding with C220 of the heavy chain. Nevertheless, a C terminal fusion to the light chain still represents the most rational option.

To determine if cyclonal-EPSPS fusions retained binding activity, we constructed a vector that coded for the expression of the $EPSPS^{N235}$ fragment genetically fused to the C terminus of the anti-MBP mFab/hFc cyclonal light chain (IgL-aMBP-$EPSPS^{N235}$). The gene coding for the full-length anti-MBP mFab/hFc heavy chain (IgH-aMBP) was cloned into the same cistron to generate a bicistronic expression vector. The cyclonal- $EPSPS^{N235}$ fusion was then expressed in SHuffle Δ*aroA* cells Next, the binding activity of the crude lysate prepared from these cells was measured by ELISA (**Figure 4.6**). Soluble lysate containing anti-MBP-$EPSPS^{N235}$ showed 20-fold greater binding activity against MBP when compared with lysate containing anti-HAG- $EPSPS^{N235}$, a non-specific cyclonal-EPSPS fusion.

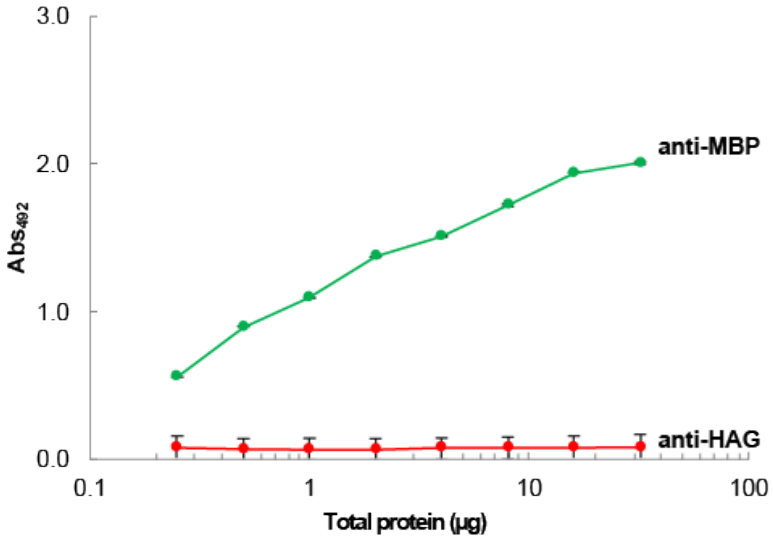

Figure 4.6 Characterization of cyclonal-EPSPS fusions. Binding activity of soluble cell extract containing the anti-MBP cyclonal-EPSPS fusion was measured by ELISA. Extracts were normalized by total protein content. EPSPS^{N235} is genetically fused to the C terminus of the light chain. The anti-MBP cyclonal-EPSPS fusion was expressed from pMAZ360-cIgG-aMBP-mFab/hFc(L)-EPSPS^{N235} in SHuffle Δ*aroA* cells. Anti-HAG IgG expressed from pMAZ360-cIgG-aHAG-mFab/hFc in SHuffle Δ*aroA* cells was used as a negative control.

Protein fragment complementation of EPSPS reports antibody:antigen binding. Having demonstrated that the anti-MBP cyclonal-EPSPS fusion retains binding activity, we sought to prove that EPSPS complementation could report antigen binding *in vivo*. The gene for MBP, the target antigen, was fused to the complementary fragment of EPSPS^{N235}, EPSPS^{C236}. SHuffle Δ*aroA* coexpressing the anti-MBP cyclonal- EPSPS^{N235}:MBP- EPSPS^{C236} PCA pair were tested for EPSPS complementation on M9 minimal agar plates supplemented with arabinose and IPTG for induction of protein expression. EPSPS complementation facilitated by antigen:cyclonal binding restored viability to SHuffle Δ*aroA* cells even when diluted 10,000 fold (**Figure 4.7**). The binding of anti-MBP:MBP appears comparable to that of FosLZ:JunLZ as reported by the EPSPS PCA system. No detectable growth was observed when anti-MBP- EPSPS^{N235} was co-expressed with a non-specific antigen,

JunLZ, further establishing the specificity of the assay (**Figure 4.7**).

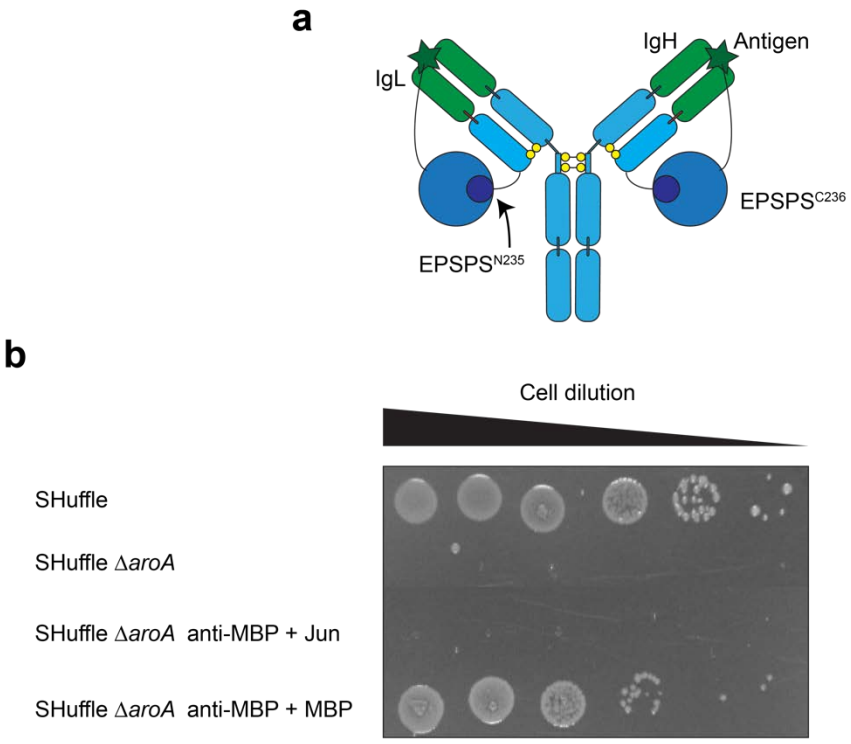

Figure 4.7 Split EPSP synthase selection for antibody:antigen interactions. (a) Schematic representation of EPSP synthase PCA based selection for antibody:antigen binding. The cyclonal light chain is fused to the N terminus of the EPSPS^{N235} fragment (residues 1-235) by means of a flexible linker (Ala(Ser)$_3$(Asn)$_{10}$) and coexpressed with a protein antigen fused to the C terminus of the complementary EPSPS fragment, EPSPS^{C236} (residues 236-427).The interaction between a specific antibody:antigen pair facilitates reconstitution of EPSPS activity and confers growth on minimal media (b) Spot plating of serially diluted SHuffle Δ*aroA* cells carrying plasmids pMAZ360-cIgG-aMBP-mFab/hFc(LC)-LN10-EPSPS(N)235 and pBAD34-EPSPS^{C236}- MBP (anti-MBP + MBP) encoding the matching antibody-antigen pair, or SHuffle Δ*aroA* cells transformed with pMAZ360-cIgG-aMBP-mFab/hFc(LC)-LN10-EPSPS(N)235 and pBAD34- EPSPS^{C236}-JunLZ, coding for a non-specific pair (SHuffle Δ*aroA* anti-MBP + Jun). SHuffle and SHuffle Δ*aroA* cells were plated as negative controls.

Having confirmed that the anti-MBP cyclonal:MBP pair enabled growth of SHuffle Δ*aroA* cells in the split EPSPS-based PCA, we aimed to prove that this assay is robust and applicable to a wide-range of cyclonal:antigen pairs. Replacing the anti-MBP cyclonal:MBP pair with two different cognate pairs, namely anti-HAG:HAG and Humira (anti-TNFα):TNFα yielded a similar growth advantage on minimal media

when compared with non-binding pairs. Furthermore, we also investigated supplementing the minimal media agar with the EPSP synthase inhibitor glyphosate as a means of applying additional selective pressure within the context of the EPSPS PCA. We found that cells expressing strongly interacting cyclonal:antigen pairs were in fact resistant to glyphosate up to at least 0.2 mM (200 μM) (**Figure 4.8**).

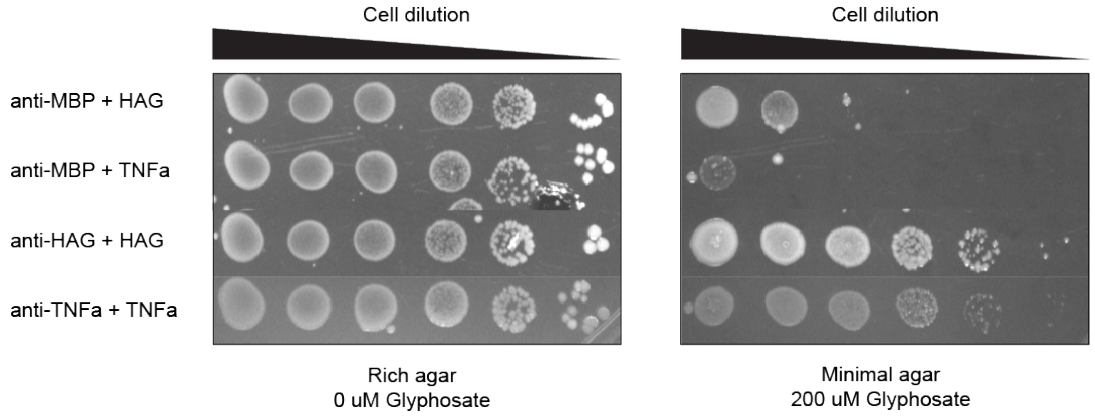

Figure 4.8 Extension of EPSPS PCA selection to therapeutic antibodies Selective spot plating of serially diluted SHuffle Δ*aroA* cells carrying plasmids coding for the anti-HAG-mFab/hFc-EPSPS^{N235} and EPSPS^{C236}-HAG antibody-antigen pair (anti-HAG + HAG), pMAZ360-cIgG-aHAG-mFab/hFc(LC)-LN10-EPSPS(N)235 and pBAD34-EPSPS^{C236}- HAG, and SHuffle Δ*aroA* cells transformed with pMAZ360-cIgG-Humira(LC)-LN10-EPSPS^{N235} and pBAD34- EPSPS^{C236}-TNFα, encoding the matching Humira -EPSPS^{N235} and EPSPS^{C236}- TNFα antibody-antigen pair (anti-TNFa + TNFa). SHuffle Δ*aroA* cells transformed with plasmids coding for mismatched pairs anti-MBP-mFab/hFc-EPSPS^{N235} and EPSPS^{C236}-HAG (anti-MBP + HAG) or anti-MBP-mFab/hFc-EPSPS^{N235} and EPSPS^{C236}- TNFα, (anti-MBP + TNFα) served as negative controls.

EPSPS PCA facilitates the isolation of cognate cyclonal:antigen pair from a mock library. Our preliminary results prove that the EPSPS PCA reliably reports antibody:antigen binding *in vivo* within SHuffle Δ*aroA*. However, our ultimate objective is to apply the strategy to isolating specific cyclonal:antigen pairs from diverse libraries, thereby enabling the rapid discovery of highly specific antibodies. Toward this goal, we designed a mock library experiment to test if cells expressing

matching cyclonal:antigen pairs could be selected from a pool of cells in which non-interacting pairs are overrepresented. Cells carrying split-EPSPS PCA plasmids for expressing anti-MBP- $EPSPS^{N235}$ and $EPSPS^{C236}$-MBP, and cells expressing anti-MBP- $EPSPS^{N235}$ and $EPSPS^{C236}$-JunLZ were mixed at a ratio of 1:1000. The cell mixture was cultured on minimal media and colonies picked at random were analyzed for the identity of the antigen ($EPSPS^{C236}$ fusion partner). The cell mixture was cultured on Lysogeny broth (LB) agar in parallel as a control for the mock library. Analysis of 26 randomly selected colonies revealed that each carried the cognate pair when the mock library was selected on M9 minimal agar. In contrast, none of the 26 colonies selected from the LB agar control plate harbored the specific anti-MBP:MBP pair, which suggests that selection for viability on minimal media favors the matched cyclonal:antigen pair. A second trial of the same experiment revealed similar results in which ~77% (20/26) of colonies picked from the minimal media plate contained the interacting pair whereas none of the colonies analyzed from the LB plate carried that pair (**Figure 4.9**).

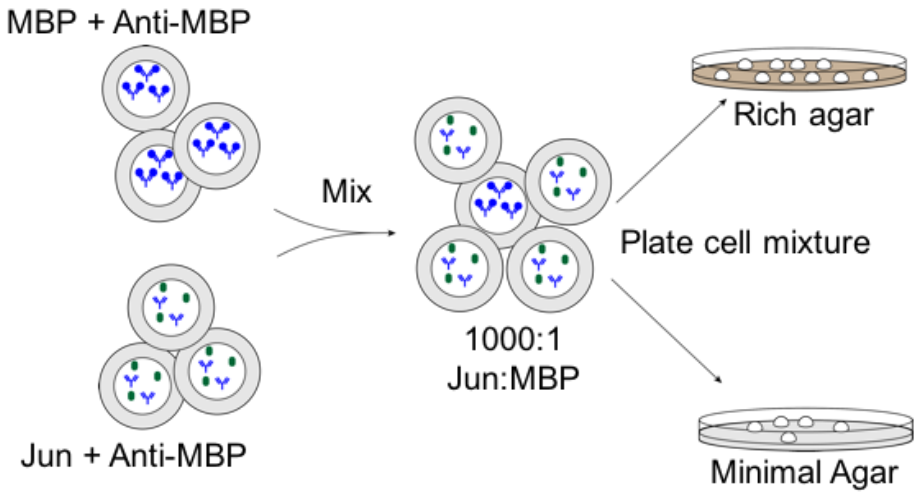

Trial No.	Jun cells : MBP cells	Matched pairs on Rich Agar	Matched pairs on Minimal Agar
1	1000:1	0/26	26/26
2	1000:1	0/26	20/26

Figure 4.9 Isolation of cognate antibody:antigen interaction from mock library using EPSPS PCA selection. (a) SHuffle Δ*aroA* cells were transformed with the cognate plasmid pair, pMAZ360-cIgG-aMBP-mFab/hFc(LC)-LN10-EPSPS^{N235} and pBAD34-EPSPS^{C236}- MBP, or a non-specific pair pMAZ360-cIgG-aMBP-mFab/hFc(LC)-LN10-EPSPS^{N235} and pBAD34-EPSPS^{C236}- JunLZ. Cells were normalized by A_{600} and mixed at a 1:1000 matched pair:unmatched pair ratio to make the mock library. The mock library was then plated on M9 minimal media agar supplemented with arabinose (0.4% w/v) and IPTG (1mM). The mock library was also plated on LB agar supplemented with arabinose (0.4% w/v) and IPTG (1mM) as a control. Single colonies were analyzed for the presence of either EPSPS^{C236}- JunLZ or EPSPS^{C236}- MBP gene by PCR. (b) Number of occurrences of each antigen after PCR analysis of single colonies. 26 colonies were analyzed from control and selection plates.

Discussion

We have successfully developed a survival selection that reports specific binding of full-length IgG antibodies to their target antigens within the cytoplasm engineered bacterial cells. Our results constitute the first example of a simple selection in which bacterial cells are used to report such interactions between full-length IgG antibodies and their antigens *in vivo*. While several laboratories have developed survival selections as a means to both report and identify specific binding between an

antigen and antibody fragments, none of these strategies to date have been applied to full-length IgGs. To achieve this milestone, we developed a version of the protein fragment complementation assay in which cell viability is predicated on EPSPS activity that in turn relies upon the specific intracellular interaction of a full-length IgG and its cognate antigen. This adaptation of the assay is made possible through the use of the redox engineered *E. coli* SHuffle strain which we showed in previous work permits the expression of active and correctly assembled IgG antibodies within its cytoplasm.

We first confirmed that EPSPS activity, essential for growth on minimal media agar, is a selectable phenotype for the *E. coli* SHuffle strain as cells with a genomic deletion of the *aroA* gene were not viable unless its product EPSPS was complemented exogenously from a plasmid. Essentiality of EPSPS for growth on minimal media was previously shown for wild-type *E. coli* cells, and had not been confirmed in redox-engineered cells. Through further experiments, we validated EPSPS as a suitable PCA reporter by showing that cells expressing inactive EPSPS fragments as fusions to the strongly interacting leucine zipper pair FosLZ and JunLZ, possess a selective advantage over those cells expressing the fragments alone or as fusions to non-interacting protein pairs. Interestingly, while EPSPS PCAs have been shown to report homodimerization between leucine zippers and interactions between split inteins, this is the first study describing the use of an EPSPS PCA to report heterodimeric interactions in bacteria.

The PCA was then adapted for use with cyclonals by first rationally designing a cyclonal fusion to the N terminal fragment of EPSPS via the C terminus light chain. First, we confirmed that the first cyclonal fusion, anti-MBP-EPSPS^{N235}, retained MBP binding activity. Next, we further extended our variation on the EPSPS PCA by showing that our model IgG:antigen case, anti-MBP:MBP, restores cell growth to

Shuffle Δ*aroA* cells on M9 minimal media. Though we conceptualized our fusion constructs by rational design and achieved positive results, we did not test all possible orientations. An empirical approach may reveal more optimal designs. It would be prudent to test alternate designs in the future.

Two additional IgG:antigen pairs were shown to facilitate reconstitution of functional EPSPS and restore growth to Shuffle Δ*aroA* cells on minimal media. Importantly, it is significant that complementation was demonstrated using a diverse collection of antigens derived from very different sources. Our results show that the EPSPS PCA is compatible with a peptide antigen derived from a viral coat protein (HAG), a native *E. coli* protein (MBP), and a therapeutically relevant human derived antigen (TNFα). In addition, the Humira:TNFα and anti-HAG:HAG pairs conferred tolerance to glyphosate upon SHuffle Δ*aroA* cells. This is crucial as glyphosate resistance will likely play an important role as we develop the assay for cyclonal selection and affinity maturation. The selective pressure provided by glyphosate would be integral in implementing any directed evolution strategy to engineer the biophysical properties of an antibody of interest. Additionally, we demonstrated a proof-of-concept selection by enriching cells expressing the anti-MBP:MBP pair from a mock library in which cells expressing non-interacting pairs were 1000 times more abundant. The selection represented a ~700 fold enrichment of the anti-MBP:MBP expressing cells in one step.

Our work has explored the molecular versatility of the EPSPS PCA. Several studies have exploited EPSPS PCAs for the purposes of engineering glyphosate resistance, however, none as of yet has explored the possibility of using it as a tool to report binding interactions. Notably all previous studies involving an EPSPS PCA were more focused on studying properties of the EPSPS enzyme itself and not protein-protein interactions as we have done here. The archive of information accumulated as

a result of nearly four decades of studies focused solely on EPSPS includes structural, kinetic, biochemical, and phylogenic data which could be leveraged in the future to improve and refine the PCA.

To date all other *E. coli* based isolation strategies have involved IgG export to the periplasm, fluorescently conjugated antigens, fluorescence-activated cell sorting, and/or panning on immobilized antigen [92, 93, 95]. Our EPSPS PCA represents the simplest protocol for identifying IgG:antigen binding as it only requires transformation, protein expression, and cell culture on selective media, which are all standard techniques performed by molecular and cellular biologists. We are able to report antibody reactivity without special *ex vivo* preparation of the antigen, rigorous washing or panning steps, laborious technical methods, or specialized equipment. We believe that our study is the first step on the way to a technique that would expand access to antibody development technology.

Materials and Methods

Plasmid construction. All cloning was performed using standard techniques. To construct vectors for the expression of EPSP synthase, total DNA was extracted from SHuffle T7 express using a DNeasy® Blood and Tissue kit (Qiagen). The full-length *aroA* gene was then amplified using the purified genomic DNA as a template by PCR using primers that added a 5' NdeI restriction site and a HindIII restriction site at the 3' end. The product was then ligated with pET21b using the NdeI and HindIII restriction sites to generate pET21b-EPSPS. To construct the pBAD34-EPSPS vector, the *aroA* gene was amplified with flanking NcoI and SphI restriction sites and then inserted into the NcoI/SphI site of pBAD34. The pBAD24-EPSPS (pAroA) vector was created similarly by cloning *aroA* into the NcoI/SphI site of pBAD24.

A DNA sequence for the N terminal split fragment of EPSPS homologous to the one reported by Chen et al. composed of EPSPS residues 1-235 ($EPSPS^{N235}$) was

generated by amplifying from the start codon to nucleotide 705 (nucleotides 1-705) of the *aroA* gene. The resulting product was cloned into the NdeI/HindIII site of pET21b creating pET21b- EPSPS^{N235}. Nucleotides 706-1281 of *aroA* were PCR amplified to create the gene for the C terminal fragment of EPSPS (EPSPS^{C236}), which is composed by residues 236-427 of EPSPS, and ligated between NcoI and SphI restriction sites of pBAD34 resulting in the expression vector pBAD34-EPSPS^{C236} .

In order to produce the sequence for a MBP fusion to EPSPS^{C236}, DNA encoding EPSPS residues 236-427 was amplified from pAroA inserting a NcoI site at the 5' end and a sequence overlap coding for part of a flexible linker at the 3' end of the PCR product. The MBP gene was amplified from pMAL-c5X (NEB) with primers that added an overlap to the 5' of MBP and a 3' SalI site. EPSPS^{C236} coding sequence was fused to 5' end of MBP by overlap extension PCR creating a genetic fusion of two genes with the overlap coding for a flexible linker, ASSSNNNNNNNNNN (LN10), followed by a KpnI site resulting in a gene that codes for EPSPS^{C236}-LN10-MBP. The EPSPS^{C236}-LN10-MBP fusion was cloned into the NcoI/SalI site of pBAD34 to create pBAD34-EPSPS^{C236}- MBP. The HAG peptide DNA insert was generated through annealing complementary oligonucleotides that encoded KpnI and SalI overhangs at the 5' and 3' ends respectively. The gene for human TNFα was PCR amplified using plasmid pBAD34-hsTNFa_EcOPT which encodes a codon optimized version of the gene. Both HAG and TNFα genes were cloned into the KpnI/SalI site of pBAD34-EPSPS^{C236}- MBP yielding pBAD34-EPSPS^{C236}- HAG and pBAD34-EPSPS^{C236}- hsTNFα, respectively.

To clone vectors for the expression of cyclonal-EPSPS ^{N235} fragment fusions, the anti-HAG and anti-MBP mFab/hFc light chain genes (IgL) were first amplified from pMAZ360-cIgG-aHAG-mFab/hFc and pMAZ360-cIgG-aMBP-mFab/hFc vectors. The light chain genes were then genetically fused via a LN10 linker to

EPSPS^{N235} by overlap extension creating IgL-LN10- EPSPS^{N235}. The anti-HAG mFab/hFc light chain- EPSPS^{N235} fusion was cloned into pMAZ360-cIgG-aHAG via the NdeI and HindIII sites creating pMAZ360-cIgG-aHAG-mFab/hFc(LC)-LN10-EPSPS^{N235}. The anti-aMBP mFab/hFc light chain- EPSPS^{N235} fusion was ligated into the NdeI/HindIII site of pMAZ360-cIgG-aMBP-mFab/hFc thereby generating the vector pMAZ360-cIgG-aMBP-mFab/hFc(LC)-LN10-EPSPS^{N235}. Genes encoding the heavy and light chains of the anti-TNFα antibody Humira were amplified from pETDuet-cIgG-aTNF. DNA for N terminal fragment of EPSPS was amplified by PCR using pBAD34-EPSPS as the template. The light chain was genetically fused to EPSPS^{N235} by overlap extension PCR. The light chain Humira-LN10- EPSPS^{N235} gene was cloned into cyclonal expression vector pMAZ360-cIgG between the NdeI and HindIII restriction sites in order to make an intermediate product pMAZ360-IgL-Humira-LN10- EPSPS^{N235}. The plasmid pMAZ360-cIgG-Humira(LC)-LN10- EPSPS-^{N235} was produced by ligating the Humira heavy chain sequence into the NheI/XhoI site of pMAZ360-IgL-Humira-LN10- EPSPS^{N235}.

Selective growth assays. For initial determination of *in vivo* EPSP synthase activity, SHuffle Δ*aroA* cells harboring control vectors, vectors for expression of EPSP synthase, EPSP synthase fragments, or EPSPS PCA fusions were grown overnight in Lysogeny broth (LB) medium supplemented with 100 µg/ml carbenicillin for pET21 or 34 µg/ml pBAD34 vectors at 30 C. Cells from overnight culture were harvested by centrifugation and approximately 10^9 cells of each strain were washed using M9 minimal medium by centrifugation at 16, 000xg to remove traces of LB and then normalized to 2.5 (A_{600}). The cells were serially diluted 10-fold in M9 media. A volume of 5 µl of cells from each dilution were cultured on solid M9 minimal Agar containing 1 mM IPTG, 0.4% Arabinose, and 0-5 mM glyphosate at 30ºC for 72-96 h. Images of selection plates were produced using the GelDoc or the ChemiDoc XRS+

molecular imager.

Protein expression. SHuffle T7 Express cells carrying plasmids form cyclonal-EPSPS^{N235} expression were cultured in LB media supplemented with 100 µg/ml ampicillin at 30°C overnight. Overnights were subcultured in 3-5 mL LB with 100 µg/ml ampicillin at 30°C to mid-log phase (0.6-0.8 A_{600}). Protein expression was induced with 1 mM IPTG at 30°C for 12-18 h.

Enzyme-linked immunosorbent assay (ELISA). Costar 96-well ELISA plates (Corning) were coated overnight at 4°C with 50 µl of 4µg/ml 1 MBP5 (New England Biolabs), in 0.05 M sodium carbonate buffer (pH 9.6). After blocking with 3% (w/v) milk in PBST (PBSTM) for 1–3 h at room temperature, the plates were washed four times with PBS buffer and incubated with serially diluted soluble fractions of crude cell lysates for 1 h at room temperature. IgG-containing samples were quantified by the Bradford assay and an equivalent amount of total protein (typically 8–64 mg) was applied to the plate. After washing four times with the same buffer, 50 µl of 1:5,000-diluted rabbit anti-human IgG (Fc) antibody–HRP conjugate (Pierce) antibodies in PBSTM was added to each well for 1 h. The 96 well Plates were washed six times with PBST. After the final wash, 200 µl SigmaFAST™ OPD solution (Sigma-Aldrich) was added and incubated within each well in the dark for 30 min. The HRP reaction was then terminated by the addition of 50 µl 3 M H_2SO4 to the wells. Following reaction quenching, the absorbance of each well was measured at 492 nm.

Protein analysis. Cells expressing recombinant proteins were harvested by centrifugation (4,000g, 4°C) and resuspended in PBS, Halt protease inhibitor, and 5 mM EDTA. Cells were lysed by sonication on ice using a Branson sonifier 450 (Duty cycle 30% Output control 3) using four repetitions of 30 sec each. The insoluble fraction was removed by centrifugation (21,000g, 4°C) and the supernatant collected as the soluble fraction.

Mock library selection. SHuffle Δ*aroA* transformed with pMAZ360-cIgG-aMBP-EPSPS^{N235} and pBAD34-EPSPS^{C336}-JunLZ or pMAZ360-cIgG-aMBP-EPSPS^{N235} and pBAD34-EPSPS^{C336}-MBP were cultured overnight in 5 mL LB supplemented with ampicillin (100 µg/ml), chloramphenicol (34 µg/mL), and spectinomycin (25 µg/ml) at 30°C. SHuffle cells were harvested by centrifugation and the LB media was decanted. Cells were then washed twice with minimal media to remove traces of LB. Cells from overnight culture were normalized to A_{600} = 2.5 in M9 minimal media. SHuffle Δ*aroA* harboring pMAZ360-cIgG-aMBP-EPSPS^{N235} and pBAD34-EPSPS^{C336}-MBP were diluted 10-fold with normalized SHuffle Δ*aroA* cells carrying the pMAZ360-cIgG-aMBP-EPSPS^{N235} and pBAD34-EPSPS^{C336}-JunLZ plasmid in minimal media.

Acknowledgements

I thank Dr. Matthew DeLisa and Dr. Mehmet Berkmen at New England Biolabs for conceptualizing the split-EPSPS PCA strategy for cyclonal engineering. Vectors pBAD34, pBAD34-hs hsTNFa_EcOPT, pETDuet-cIgG-aTNF were kindly provided by Dr. Na Ke of New England Biolabs. We also thank Dr. Na Ke also of New England Biolabs who engineered the SHuffle T7 Express Δ*aroA* strain used for all split-EPSPS PCA experiments and helped perform the FosLZ:JunLZ experiments. I thank Cristen Peterson who performed preliminary experiments with full length EPSPS to validate the initial approach. I also thank Daniel Tien of his indispensable role in developing the split-EPSPS assay.

CHAPTER 5

PROSPECTUS FOR BACTERIA-ENABLED CYCLONAL ENGINEERING

Introduction

Shortening the process and development time for monoclonal antibodies has long been a goal of antibody engineers. Additionally, greater control of discovery, affinity maturation, and engineering of mAb properties has been desired. Data presented in the previous chapters demonstrate that we have made progress toward these goals. We have proved that we can rapidly produce and engineer both antigen and effector activity using cyclonal technology. We also showed that selecting high affinity full-length antibodies from combinatorial libraries using simple *E. coli*-based survival assays is possible. Our focus in the near future will be on improving the efficiency of production in SHuffle cells and adaption of the cyclonal technology to select antibodies against diverse antigens in an attempt to completely bypass immunization. In this chapter experimental designs aimed at addressing these challenges will be proposed.

Discussion

Improvements on cyclonal expression system. Previous studies have found that placing antibody light and heavy chains under the control of separate promoters can greatly enhance full-length antibody assembly in *E. coli* by balancing the expression of the heavy and light chains[94]. Our current bicistronic constructs place expression of the HC and the LC under the control of the same promoter. Expression data we have collected so far suggest that the total expression of heavy chain is not optimally balanced with total light chain expression as we observe a large excess of monomeric light chain when cyclonals are expressed within the cytoplasm of SHuffle. We hypothesize that this imbalance is a result of the second gene in the cistron being transcribed less efficiently than the first. As such, we could apply this strategy to our

system in an attempt to improve the assembly efficiency of heavy and light chains into full-length antibodies. We will first clone dual promoter constructs using several diverse promoters. We will then clone HC and LC sequences such that each is under the control of its own promoter. These constructs will be used to transform SHuffle cells. IgGs will be expressed cytoplasmically in SHuffle cells and assembly will be assayed by western blot. The assembly efficiency will be compared to that of the same IgG expressed from the original bicistronic construct. Assembly efficiency of IgGs expressed in SHuffle cells from separate cistron and bicistronic constructs will also be evaluated by Coomassie staining after resolution of Protein A-purified IgG samples by SDS-PAGE. The Coomassie stained gels will be analyzed by densitometry to compare the assembly efficiency in the different experimental cases.

Promoter engineering could also be combined with other available strategies to enhance full-length IgG expression in our system. Engineering the translation initiation region, 5' untranslated region (UTR) engineering, ribosome binding site (RBS) engineering, and strain engineering, have all been used successfully to increase IgG production in periplasmic systems. Any of these strategies could also be applied in SHuffle [94, 189-191].

Affinity maturation of selected cyclonals. Interestingly, The CDR-H3 of the GTK clone selected in Chapter 3 departs from the observed preferences for anti-GCN4 binders reported in previous works and appears to have the weakest affinity for GCN4 as measured by ELISA. This provides an opportunity to explore the application of the CAT-Ag selection to antibody affinity maturation. Clone GTK is specific for GCN4 but has low affinity and therefore is a good candidate to use as a starting point for affinity maturation in a second round of selection. To test this, we could generate a second round cyclonal library by error prone PCR mutagenesis of the GTK cyclonal or by targeting another CDR, most likely CDR-L3, for mutagenesis. The library would

then be selected at a higher concentration range of Cm (30-50 μg/ml). If a higher affinity variant of GTK can be selected this would be yet another step in proving the utility of the CAT-Ag selection strategy.

Reprogramming antigen specificity of an existing antibody toward a new antigen. We have demonstrated that the CAT reporter can select for antibody antigen binding within SHuffle cells. To further show the utility of the CAT-Ag reporter strategy, we will attempt to select and evolve an antibody against a new antigen. We identified two criteria to select a suitable antigen-(1) the antigen should be small (<10 kDa) and (2) the antigen should be similar to antigen for which we already possess a specific antibody. We chose criterion (2) hypothesizing that we would have a better chance of finding an antigen specific antibody if we selected a library generated from a well-characterized antibody against an antigen that is similar to the cognate antigen of the well-characterized antibody. The two criteria led us to select the basic leucine zipper domain FosLZ as our target as it is homologous to Gcn4LZ, an antigen for which we have a cyclonal, and it is relatively small (~8 kDa).

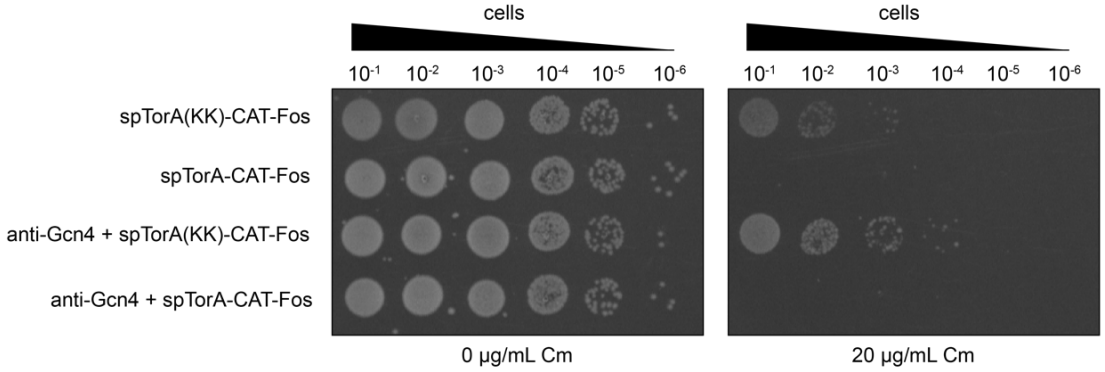

Figure 5.1 Characterization of CAT-FosLZ antigen for library selection. Selective plating of SHuffle cells with plasmids for CAT-Fos (spTorA-CAT-Fos) and CAT-Fos fusions with a defective Tat signal peptide that impedes translocation (spTorA(KK)-CAT-Fos) are indicated. SHuffle cells were serially diluted in LB media and 5 μl was plated on LB-agar supplemented with 0 or 20 μg/ml chloramphenicol, 0.4 % arabinose, and 1mM IPTG.

In order to determine if Fos is a suitable antigen, we constructed two CAT-Fos fusions, one with a functional Tat export signal (spTorA-CAT-Fos) and the other with a defective Tat export signal (spTorA (KK)-CAT-Fos). SHuffle T7 express cells were transformed with these constructs alone or co-transformed with the anti-Gcn4 antibody. Cells expressing CAT-Fos preceded by a functional export signal were not resistant to chloramphenicol (**Figure 5.1**). Coexpressing the anti-Gcn4 antibody was not sufficient to give chloramphenicol resistance, as presumably it cannot retain spTorA-CAT-Fos within the cytoplasm. However, when CAT-Fos is retained within the cytoplasm due to a defective Tat export signal peptide (spTorA(KK)), SHuffle cells were resistant to chloramphenicol (**Figure 5.1**). These results support moving forward with Fos as a target antigen. We have also constructed a similar CAT-Ag reporter fusion using the leucine zipper domain of c-Jun (JunLZ). While we have not confirmed its compatibility with the CAT reporter system, we anticipate that the CAT-JunLZ reporter will behave similar to the other leucine zippers.

The randomized 3-residue and 4-residue libraries we constructed in Chapter 3 could be selected for JunLZ and FosLZ binders. In addition, der Maur et al. reported successfully selecting JunLZ binders from a library with encoding 6 randomized residues within CDR-H3 [133]. We could use the CAT selection system to perform a similar selection. Therefore, we have designed library construction strategies to generate cyclonals with 5 and 6-residues randomized within CDR-H3. We would use the NDT degenerate codon as we selected a greater number of positive hits from the NDT library when compared with the NNK library despite the NNK library being much larger. We would select these libraries in parallel with the 3-residue and 4-residue CDR-H3 libraries against both FosLZ and JunLZ. A successful specificity switch to one or both of the antigens would further validate the CAT-Ag selection for antibody engineering applications.

Construction of a naïve cyclonal library. Attempting to select for more diverse antigens would almost certainly require an IgG library much more diverse that the CDR-H3 libraries we have previously proposed. In order to construct a large naïve cyclonal library, we would use the scFv Tomlinson I and J libraries, which were constructed using stable human V_H and V_L frameworks [192, 193]. In addition to these libraries, we also possess a separate naïve scFv library created in the lab of Dr. Pierre Martineau[194] that has been optimized for expression in *E. coli*. We would amplify the V_H and V_L genes from these libraries by PCR and genetically fuse the amplified V_H and V_L sequences with human constant heavy chain and light chain domains, respectively. We would then analyze the diversity of the newly created IgG library by sequencing. Finally, we would clone this library into vectors for selection with the EPSPS and CAT selection systems.

Selection from a naïve library. The compatibility of globular antigens with the CAT selection has yet to be determined. However, we showed that the EPSPS PCA can report binding between cyclonals and antigens ranging from the HAG peptide to MBP (~43 kDa). As such, we will test the EPSPS PCA against larger antigens that may not be compatible with the CAT-Ag selection.

To demonstrate the utility of the EPSPS PCA described in Chapter 4, we would select an IgG against a clinically relevant antigen, namely, the extracellular domain of the B-cell surface protein CD20. CD20 is an integral membrane phosphor-protein that is expressed on the surface of ~90% of all B-cell lymphomas and is not found on any other cell type, making it an excellent target for immunotherapy [195]. As a result, the “blockbuster” anti-CD20 antibody Rituximab (Rituxan) has been widely used to treat non-Hodgkin’s lymphoma and leukemia since its approval in 1997. Last year, Genentech won FDA approval of a new mAb, Obinutuzumab (Gazyva), which also targets CD20. This indicates that CD20 continues to be a

relevant antigen for monoclonal antibody development.

The extracellular loop of CD20 (exCD20) is the epitope for all currently available anti-CD20 antibodies[195]. Therefore, we would select our library against this epitope. Soluble expression of exCD20 in *E. coli* has been reported[196]. Therefore, we would co-transform the IgG libraries generated above with a vector encoding an exCD20-EPSPS fusion. We would select the library on M9 minimal media. The growth phenotype of selected cells would then be confirmed by back transforming DNA from the selected clones into fresh SHuffle cells. Once confirmed, we would express the selected IgGs and measure exCD20 binding activity by ELISA.

To further improve the binding affinity of the selected IgGs against exCD20, we would perform additional rounds of selection. This would be accomplished by generating a new library based upon the selected IgG clones by random mutagenesis of $V_{H \text{ and }} V_L$ genes or by DNA shuffling [70, 71]. We would then select the new library at increasing levels of glyphosate to select for IgG mutants that exhibit higher affinity for exCD20 as compared to the parent. We would also determine binding kinetics of the selected IgG clones by surface plasmon resonance (SPR).

Recently, there has been a great effort to develop broadly neutralizing antibodies (bnAbs) against viral pathogens. Broadly neutralizing antibodies (bnAbs) are those that can neutralize many different viral serotypes. Of particular interest are those against increasing virulent influenza strains that could be used to protect the population in the event of a pandemic. Recent studies have found that these broadly neutralizing antibodies recognize a conserved epitope in stem region of HA region near the fusion peptide [197, 198]. These antibodies, termed anti-fusogenic antibodies, inhibit the membrane fusion event vital for host cell infection. Interestingly, production of anti-fusogenic antibodies was elicited in mice by immunization with a mutant version of green fluorescent protein (GFP), which was engineered to mimic the

structure of the stem region of the influenza A virus[199]. We propose using this same protein to select broadly neutralizing antibodies against the influenza virus. We would synthesize DNA to encode a GFPHAmut-EPSPS fusion and co-transform this construct and the naive IgG libraries into SHuffle. We could then select for anti-viral antibodies as described for exCD20.

Summation

E. coli has proved to be a useful platform for producing and engineering antibodies. Plückthun and Skerra showed that *E. coli* possessed the capacity to produce specific antibody fragments[62]. The Winter lab demonstrated that bacteria and engineered bacteriophage could be used to screen large libraries for specific antibodies[74]. Yansura and colleagues at Genentech proved that full-length monoclonal antibodies could be expressed in *E. coli*[94]. Building upon the work by the Yansura group, Georgiou and coworkers developed an *E. coli*-based screen for isolating full-length IgG antibodies from combinatorial libraries[93]. Each advance further supplemented the toolkit available to develop antibodies crucial to research and the treatment of disease. Our work has similarly contributed to this growing body of techniques by adding a simple system that could potentially be used from discovery to final production without requiring immunization, or a complementary organism (e.g. phage, myeloma cells), antigen purification, or additional equipment (e.g. flow cytometer). The rapid production offered by the cyclonal platform could prove advantageous in the future for producing antibodies in response to epidemics as antibody therapies are often used as front-line treatments. Our work opens up the possibility that antibody development could be carried out in one system thereby allowing reliable affinity reagents to reach researchers more quickly and more cost-effectively for critical experiments. Finally, with further development we envision our system being a transformative platform for discovery and engineering of antibodies for

use in life-saving therapies.

REFERENCES

1. Lehninger, A.L., D.L. Nelson, and M.M. Cox, *Lehninger principles of biochemistry*. 6th ed. 2013, New York: W.H. Freeman.
2. Murphy, K., et al., *Janeway's immunobiology*. 8th ed. 2012, New York: Garland Science. xix, 868 p.
3. Weiner, L.M., J.C. Murray, and C.W. Shuptrine, *Antibody-based immunotherapy of cancer.* Cell, 2012. **148**(6): p. 1081-1084.
4. Nezlin, R.S., *The immunoglobulins : structure and function*. 1998, San Diego: Academic Press. xiii, 269 p.
5. Jung, S.T., et al., *Aglycosylated IgG variants expressed in bacteria that selectively bind FcgammaRI potentiate tumor cell killing by monocyte-dendritic cells.* Proc Natl Acad Sci U S A, 2010. **107**(2): p. 604-9.
6. Lobato, M.N. and T.H. Rabbitts, *Intracellular antibodies and challenges facing their use as therapeutic agents.* Trends in molecular medicine, 2003. **9**(9): p. 390-396.
7. Elgundi, Z., et al., *The state-of-play and future of antibody therapeutics.* Advanced Drug Delivery Reviews, 2016.
8. Robinson, M.-P., et al., *Efficient expression of full-length antibodies in the cytoplasm of engineered bacteria.* Nature Communications, 2015. **6**: p. 8072.
9. Berkmen, M., *Production of disulfide-bonded proteins in Escherichia coli.* Protein expression and purification, 2012. **82**(1): p. 240-251.
10. Sevier, C.S. and C.A. Kaiser, *Formation and transfer of disulphide bonds in living cells.* Nature reviews. Molecular cell biology, 2002. **3**(11): p. 836-847.
11. Ritz, D. and J. Beckwith, *Roles of thiol-redox pathways in bacteria.* Annual review of microbiology, 2001. **55**: p. 21-48.
12. Nakamoto, H. and J.C. Bardwell, *Catalysis of disulfide bond formation and isomerization in the Escherichia coli periplasm.* Biochimica et biophysica acta, 2004. **1694**(1-3): p. 111-119.
13. Kadokura, H. and J. Beckwith, *Mechanisms of oxidative protein folding in the bacterial cell envelope.* Antioxidants & redox signaling, 2010. **13**(8): p. 1231-1246.
14. Bardwell, J., K. McGovern, and J. Beckwith, *Identification of a protein required for disulfide bond formation in vivo.* Cell, 1991. **67**(3): p. 581-589.
15. Jander, G., N.L. Martin, and J. Beckwith, *Two cysteines in each periplasmic domain of the membrane protein DsbB are required for its function in protein disulfide bond formation.* The EMBO journal, 1994. **13**(21): p. 5121-5127.
16. Missiakas, D., C. Georgopoulos, and S. Raina, *Identification and characterization of the Escherichia coli gene dsbB, whose product is involved in the formation of disulfide bonds in vivo.* Proceedings of the National Academy of Sciences of the United States of America, 1993. **90**(15): p. 7084-7088.

17. Bardwell, J.C., et al., *A pathway for disulfide bond formation in vivo.* Proceedings of the National Academy of Sciences of the United States of America, 1993. **90**(3): p. 1038-1042.
18. Bader, M., et al., *Oxidative protein folding is driven by the electron transport system.* Cell, 1999. **98**(2): p. 217-227.
19. Bader, M., et al., *Reconstitution of a protein disulfide catalytic system.* The Journal of biological chemistry, 1998. **273**(17): p. 10302-10307.
20. Kadokura, H., et al., *Snapshots of DsbA in action: detection of proteins in the process of oxidative folding.* Science (New York, N.Y.), 2004. **303**(5657): p. 534-537.
21. Missiakas, D., C. Georgopoulos, and S. Raina, *The Escherichia coli dsbC (xprA) gene encodes a periplasmic protein involved in disulfide bond formation.* The EMBO journal, 1994. **13**(8): p. 2013-2020.
22. Rietsch, A., et al., *An in vivo pathway for disulfide bond isomerization in Escherichia coli.* Proceedings of the National Academy of Sciences of the United States of America, 1996. **93**(23): p. 13048-13053.
23. Missiakas, D., F. Schwager, and S. Raina, *Identification and characterization of a new disulfide isomerase-like protein (DsbD) in Escherichia coli.* The EMBO journal, 1995. **14**(14): p. 3415-3424.
24. Rietsch, A., et al., *Reduction of the periplasmic disulfide bond isomerase, DsbC, occurs by passage of electrons from cytoplasmic thioredoxin.* Journal of bacteriology, 1997. **179**(21): p. 6602-6608.
25. Prinz, W.A., et al., *The role of the thioredoxin and glutaredoxin pathways in reducing protein disulfide bonds in the Escherichia coli cytoplasm.* The Journal of biological chemistry, 1997. **272**(25): p. 15661-15667.
26. Stewart, E.J., F. Aslund, and J. Beckwith, *Disulfide bond formation in the Escherichia coli cytoplasm: an in vivo role reversal for the thioredoxins.* The EMBO journal, 1998. **17**(19): p. 5543-5550.
27. Faulkner, M.J., et al., *Functional plasticity of a peroxidase allows evolution of diverse disulfide-reducing pathways.* Proceedings of the National Academy of Sciences of the United States of America, 2008. **105**(18): p. 6735-6740.
28. Miranda-Vizuete, A., et al., *Cloning, expression, and characterization of a novel Escherichia coli thioredoxin.* The Journal of biological chemistry, 1997. **272**(49): p. 30841-30847.
29. Holmgren, A., *Thioredoxin and glutaredoxin systems.* The Journal of biological chemistry, 1989. **264**(24): p. 13963-13966.
30. Zheng, M., F. Aslund, and G. Storz, *Activation of the OxyR transcription factor by reversible disulfide bond formation.* Science (New York, N.Y.), 1998. **279**(5357): p. 1718-1721.
31. Derman, A.I., et al., *Mutations that allow disulfide bond formation in the cytoplasm of Escherichia coli.* Science (New York, N.Y.), 1993. **262**(5140): p. 1744-1747.
32. Ortenberg, R., et al., *Interactions of glutaredoxins, ribonucleotide reductase, and components of the DNA replication system of Escherichia coli.*

Proceedings of the National Academy of Sciences of the United States of America, 2004. **101**(19): p. 7439-7444.
33. Ritz, D., et al., *Conversion of a peroxiredoxin into a disulfide reductase by a triplet repeat expansion.* Science (New York, N.Y.), 2001. **294**(5540): p. 158-160.
34. Yamamoto, Y., et al., *Mutant AhpC peroxiredoxins suppress thiol-disulfide redox deficiencies and acquire deglutathionylating activity.* Molecular cell, 2008. **29**(1): p. 36-45.
35. Bessette, P.H., et al., *Efficient folding of proteins with multiple disulfide bonds in the Escherichia coli cytoplasm.* Proceedings of the National Academy of Sciences of the United States of America, 1999. **96**(24): p. 13703-13708.
36. Hatahet, F., et al., *Disruption of reducing pathways is not essential for efficient disulfide bond formation in the cytoplasm of E. coli.* Microbial cell factories, 2010. **9**: p. 67.
37. Nguyen, V.D., et al., *Pre-expression of a sulfhydryl oxidase significantly increases the yields of eukaryotic disulfide bond containing proteins expressed in the cytoplasm of E.coli.* Microbial cell factories, 2011. **10**: p. 1.
38. Hatahet, F. and L.W. Ruddock, *Topological plasticity of enzymes involved in disulfide bond formation allows catalysis in either the periplasm or the cytoplasm.* Journal of molecular biology, 2013. **425**(18): p. 3268-3276.
39. Waldmann, T.A., *Immunotherapy: past, present and future.* Nature medicine, 2003. **9**(3): p. 269-277.
40. Lachmann, P.J., *The use of antibodies in the prophylaxis and treatment of infections.* Emerging microbes & infections, 2012. **1**(8).
41. Keller, M.A. and E.R. Stiehm, *Passive immunity in prevention and treatment of infectious diseases.* Clinical microbiology reviews, 2000. **13**(4): p. 602-614.
42. Miller, R.A., et al., *Treatment of B-cell lymphoma with monoclonal anti-idiotype antibody.* The New England journal of medicine, 1982. **306**(9): p. 517-522.
43. Aggarwal, R.S., *What's fueling the biotech engine-2012 to 2013.* Nature biotechnology, 2014. **32**(1): p. 32-39.
44. Ecker, D.M., S.D. Jones, and H.L. Levine, *The therapeutic monoclonal antibody market.* mAbs, 2015. **7**(1): p. 9-14.
45. Weiner, L.M., R. Surana, and S. Wang, *Monoclonal antibodies: versatile platforms for cancer immunotherapy.* Nature reviews. Immunology, 2010. **10**(5): p. 317-327.
46. Oflazoglu, E. and L.P. Audoly, *Evolution of anti-CD20 monoclonal antibody therapeutics in oncology.* mAbs, 2010. **2**(1): p. 14-19.
47. Chan, A.C. and P.J. Carter, *Therapeutic antibodies for autoimmunity and inflammation.* Nature reviews. Immunology, 2010. **10**(5): p. 301-316.
48. Yamada, T., *Therapeutic monoclonal antibodies.* The Keio journal of medicine, 2011. **60**(2): p. 37-46.
49. Reichert, J.M., *Antibodies to watch in 2017.* mAbs, 2017. **9**(2): p. 167-181.

50. Coombs, R.R., A.E. Mourant, and R.R. Race, *A new test for the detection of weak and incomplete Rh agglutinins.* British journal of experimental pathology, 1945. **26**: p. 255-266.
51. Yalow, R.S. and S.A. Berson, *Immunoassay of endogenous plasma insulin in man.* The Journal of clinical investigation, 1960. **39**: p. 1157-1175.
52. Engvall, E. and P. Perlmann, *Enzyme-linked immunosorbent assay (ELISA). Quantitative assay of immunoglobulin G.* Immunochemistry, 1971. **8**(9): p. 871-874.
53. Köhler, G. and C. Milstein, *Continuous cultures of fused cells secreting antibody of predefined specificity.* Nature, 1975. **256**(5517): p. 495-497.
54. Joyce, J.G. and J. ter Meulen, *Pushing the envelope on HIV-1 neutralization.* Nature biotechnology, 2010. **28**(9): p. 929-931.
55. Maynard, J. and G. Georgiou, *Antibody engineering.* Annual review of biomedical engineering, 2000. **2**: p. 339-376.
56. Li, J., et al., *Human antibodies for immunotherapy development generated via a human B cell hybridoma technology.* Proceedings of the National Academy of Sciences of the United States of America, 2006. **103**(10): p. 3557-3562.
57. Chames, P., et al., *Therapeutic antibodies: successes, limitations and hopes for the future.* British Journal of Pharmacology, 2009. **157**(2): p. 220-233.
58. Green, L.L., et al., *Antigen-specific human monoclonal antibodies from mice engineered with human Ig heavy and light chain YACs.* Nature genetics, 1994. **7**(1): p. 13-21.
59. Lonberg, N., *Human antibodies from transgenic animals.* Nature biotechnology, 2005.
60. Lonberg, N., et al., *Antigen-specific human antibodies from mice comprising four distinct genetic modifications.* Nature, 1994. **368**(6474): p. 856-859.
61. Bowers, P.M., et al., *Coupling mammalian cell surface display with somatic hypermutation for the discovery and maturation of human antibodies.* Proceedings of the National Academy of Sciences, 2011. **108**(51): p. 20455-20460.
62. Skerra, A. and A. Pluckthun, *Assembly of a functional immunoglobulin Fv fragment in Escherichia coli.* Science, 1988. **240**(4855): p. 1038-41.
63. Huston, J.S., et al., *Protein engineering of antibody binding sites: recovery of specific activity in an anti-digoxin single-chain Fv analogue produced in Escherichia coli.* Proceedings of the National Academy of Sciences of the United States of America, 1988. **85**(16): p. 5879-5883.
64. Carter, P., et al., *High level Escherichia coli expression and production of a bivalent humanized antibody fragment.* Nature Biotechnology, 1992. **10**(2): p. 163-167.
65. Skerra, A., *A general vector, pASK84, for cloning, bacterial production, and single-step purification of antibody F ab fragments.* Gene, 1994.
66. Holliger, P. and P.J. Hudson, *Engineered antibody fragments and the rise of single domains.* Nature biotechnology, 2005. **23**(9): p. 1126-1136.
67. Bradbury, A.R. and J.D. Marks, *Antibodies from phage antibody libraries.* Journal of immunological methods, 2004. **290**(1-2): p. 29-49.

68. Benhar, I., *Design of synthetic antibody libraries.* Expert opinion on biological therapy, 2007. **7**(5): p. 763-779.
69. Barbas, C.F., et al., *In vitro evolution of a neutralizing human antibody to human immunodeficiency virus type 1 to enhance affinity and broaden strain cross-reactivity.* Proceedings of the National Academy of Sciences of the United States of America, 1994. **91**(9): p. 3809-3813.
70. Harvey, B.R., et al., *Anchored periplasmic expression, a versatile technology for the isolation of high-affinity antibodies from Escherichia coli-expressed libraries.* Proceedings of the National Academy of Sciences of the United States of America, 2004. **101**(25): p. 9193-9198.
71. Boder, E.T., K.S. Midelfort, and K.D. Wittrup, *Directed evolution of antibody fragments with monovalent femtomolar antigen-binding affinity.* Proceedings of the National Academy of Sciences of the United States of America, 2000. **97**(20): p. 10701-10705.
72. Sblattero, D. and A. Bradbury, *Exploiting recombination in single bacteria to make large phage antibody libraries.* Nature biotechnology, 2000. **18**(1): p. 75-80.
73. Bradbury, A.R., et al., *Beyond natural antibodies: the power of in vitro display technologies.* Nature biotechnology, 2011. **29**(3): p. 245-254.
74. McCafferty, J., et al., *Phage antibodies: filamentous phage displaying antibody variable domains.* Nature, 1990. **348**(6301): p. 552-554.
75. Barbas, C.F., et al., *Assembly of combinatorial antibody libraries on phage surfaces: the gene III site.* Proceedings of the National Academy of Sciences of the United States of America, 1991. **88**(18): p. 7978-7982.
76. Hoogenboom, H.R., *Selecting and screening recombinant antibody libraries.* Nature biotechnology, 2005. **23**(9): p. 1105-1116.
77. Hanes, J. and A. Plückthun, *In vitro selection and evolution of functional proteins by using ribosome display.* Proceedings of the National Academy of Sciences of the United States of America, 1997. **94**(10): p. 4937-4942.
78. Hanes, J., et al., *Ribosome display efficiently selects and evolves high-affinity antibodies in vitro from immune libraries.* Proceedings of the National Academy of Sciences of the United States of America, 1998. **95**(24): p. 14130-14135.
79. Hanes, J., et al., *Picomolar affinity antibodies from a fully synthetic naive library selected and evolved by ribosome display.* Nature biotechnology, 2000. **18**(12): p. 1287-1292.
80. Tsuji, S., et al., *Hishot display--a new combinatorial display for obtaining target-recognizing peptides.* PloS one, 2013. **8**(12).
81. Boder, E.T. and K.D. Wittrup, *Yeast surface display for screening combinatorial polypeptide libraries.* Nature biotechnology, 1997. **15**(6): p. 553-557.
82. Boder, E.T., M. Raeeszadeh-Sarmazdeh, and J.V. Price, *Engineering antibodies by yeast display.* Archives of biochemistry and biophysics, 2012. **526**(2): p. 99-106.

83. Karlsson, A.J., et al., *Engineering antibody fitness and function using membrane-anchored display of correctly folded proteins.* Journal of molecular biology, 2012. **416**(1): p. 94-107.
84. Chen, G., et al., *Isolation of high-affinity ligand-binding proteins by periplasmic expression with cytometric screening (PECS).* Nature Biotechnology, 2001. **19**(6): p. 537-542.
85. Löfdahl, P.A.A., et al., *Selection of TNF-alpha binding affibody molecules using a beta-lactamase protein fragment complementation assay.* New biotechnology, 2009. **26**(5): p. 251-259.
86. Mössner, E., H. Koch, and A. Plückthun, *Fast selection of antibodies without antigen purification: adaptation of the protein fragment complementation assay to select antigen-antibody pairs.* Journal of molecular biology, 2001. **308**(2): p. 115-122.
87. Secco, P., et al., *Antibody library selection by the {beta}-lactamase protein fragment complementation assay.* Protein engineering, design & selection : PEDS, 2009. **22**(3): p. 149-158.
88. Waraho, D. and M.P. DeLisa, *Versatile selection technology for intracellular protein–protein interactions mediated by a unique bacterial hitchhiker transport mechanism.* Proceedings of the National Academy of Sciences, 2009. **106**(10): p. 3692-3697.
89. Waraho-Zhmayev, D., et al., *Optimizing recombinant antibodies for intracellular function using hitchhiker-mediated survival selection.* Protein Engineering, Design and Selection, 2014. **27**(10): p. 351-358.
90. Speck, J., et al., *TAT hitchhiker selection expanded to folding helpers, multimeric interactions and combinations with protein fragment complementation.* Protein engineering, design & selection : PEDS, 2013. **26**(3): p. 225-242.
91. Nelson, A.L. and J.M. Reichert, *Development trends for therapeutic antibody fragments.* Nature biotechnology, 2009. **27**(4): p. 331-337.
92. Mazor, Y., et al., *Selection of full-length IgGs by tandem display on filamentous phage particles and Escherichia coli fluorescence-activated cell sorting screening.* The FEBS journal, 2010. **277**(10): p. 2291-2303.
93. Mazor, Y., et al., *Isolation of engineered, full-length antibodies from libraries expressed in Escherichia coli.* Nature biotechnology, 2007. **25**(5): p. 563-565.
94. Simmons, L.C., et al., *Expression of full-length immunoglobulins in Escherichia coli: rapid and efficient production of aglycosylated antibodies.* Journal of immunological methods, 2002. **263**(1-2): p. 133-147.
95. Lombana, T.N., et al., *Optimizing antibody expression by using the naturally occurring framework diversity in a live bacterial antibody display system.* Scientific reports, 2015. **5**: p. 17488.
96. Bradbury, A. and A. Plückthun, *Reproducibility: Standardize antibodies used in research.* Nature, 2015. **518**(7537): p. 27-29.
97. Reichert, J.M., *Marketed therapeutic antibodies compendium.* MAbs, 2012. **4**(3): p. 413-5.

98. Li, F., et al., *Cell culture processes for monoclonal antibody production.* MAbs, 2010. **2**(5): p. 466-79.
99. Zhou, C., et al., *Development of a novel mammalian cell surface antibody display platform.* MAbs, 2010. **2**(5): p. 508-18.
100. Beerli, R.R., et al., *Isolation of human monoclonal antibodies by mammalian cell display.* Proc Natl Acad Sci U S A, 2008. **105**(38): p. 14336-41.
101. Chartrain, M. and L. Chu, *Development and production of commercial therapeutic monoclonal antibodies in Mammalian cell expression systems: an overview of the current upstream technologies.* Curr Pharm Biotechnol, 2008. **9**(6): p. 447-67.
102. Farid, S.S., *Process economics of industrial monoclonal antibody manufacture.* J Chromatogr B Analyt Technol Biomed Life Sci, 2007. **848**(1): p. 8-18.
103. Yin, G., et al., *Aglycosylated antibodies and antibody fragments produced in a scalable in vitro transcription-translation system.* MAbs, 2012. **4**(2).
104. Mayfield, S.P., S.E. Franklin, and R.A. Lerner, *Expression and assembly of a fully active antibody in algae.* Proc Natl Acad Sci U S A, 2003. **100**(2): p. 438-42.
105. Palmberger, D., et al., *Insect cells for antibody production: evaluation of an efficient alternative.* J Biotechnol, 2011. **153**(3-4): p. 160-6.
106. Orzaez, D., A. Granell, and M.A. Blazquez, *Manufacturing antibodies in the plant cell.* Biotechnol J, 2009. **4**(12): p. 1712-24.
107. Johansson, D.X., et al., *Efficient expression of recombinant human monoclonal antibodies in Drosophila S2 cells.* J Immunol Methods, 2007. **318**(1-2): p. 37-46.
108. Kadokura, H., F. Katzen, and J. Beckwith, *Protein disulfide bond formation in prokaryotes.* Annu Rev Biochem, 2003. **72**: p. 111-35.
109. Lobstein, J., et al., *SHuffle, a novel Escherichia coli protein expression strain capable of correctly folding disulfide bonded proteins in its cytoplasm.* Microb Cell Fact, 2012. **11**: p. 56.
110. Shibui, T. and K. Nagahari, *Secretion of a functional Fab fragment in Escherichia coli and the influence of culture conditions.* Appl Microbiol Biotechnol, 1992. **37**(3): p. 352-7.
111. Skerra, A., I. Pfitzinger, and A. Pluckthun, *The functional expression of antibody Fv fragments in Escherichia coli: improved vectors and a generally applicable purification technique.* Bio/technology, 1991. **9**(3): p. 273-8.
112. Jendeberg, L., et al., *Engineering of Fc(1) and Fc(3) from human immunoglobulin G to analyse subclass specificity for staphylococcal protein A.* J Immunol Methods, 1997. **201**(1): p. 25-34.
113. Sonoda, H., et al., *Cytoplasmic production of soluble and functional single-chain Fv-Fc fusion protein in Escherichia coli.* Biochemical Engineering …, 2011.
114. Jurado, P., et al., *Production of functional single-chain Fv antibodies in the cytoplasm of Escherichia coli.* J Mol Biol, 2002. **320**(1): p. 1-10.

115. Levy, R., et al., *Production of Correctly Folded Fab Antibody Fragment in the Cytoplasm of Escherichia coli trxB gor Mutants via the Coexpression of Molecular Chaperones.* Protein Expression and Purification, 2001. **23**(2): p. 338-347.
116. Venturi, M., C. Seifert, and C. Hunte, *High level production of functional antibody Fab fragments in an oxidizing bacterial cytoplasm.* Journal of molecular biology, 2002. **315**(1): p. 1-8.
117. Hakim, R. and I. Benhar, *"Inclonals": IgGs and IgG-enzyme fusion proteins produced in an E. coli expression-refolding system.* mAbs, 2009. **1**(3): p. 281-287.
118. Cabilly, S., et al., *Generation of antibody activity from immunoglobulin polypeptide chains produced in Escherichia coli.* Proceedings of the National Academy of Sciences of the United States of America, 1984. **81**(11): p. 3273-3277.
119. Boss, M.A., et al., *Assembly of functional antibodies from immunoglobulin heavy and light chains synthesised in E. coli.* Nucleic Acids Res, 1984. **12**(9): p. 3791-806.
120. Alder, N.N. and S.M. Theg, *Energy use by biological protein transport pathways.* Trends Biochem Sci, 2003. **28**(8): p. 442-51.
121. Stanley, N.R., et al., *Escherichia coli strains blocked in Tat-dependent protein export exhibit pleiotropic defects in the cell envelope.* J Bacteriol, 2001. **183**(1): p. 139-44.
122. Ravetch, J.V. and S. Bolland, *IgG Fc receptors.* Annu Rev Immunol, 2001. **19**: p. 275-90.
123. Jefferis, R., J. Lund, and J.D. Pound, *IgG-Fc-mediated effector functions: molecular definition of interaction sites for effector ligands and the role of glycosylation.* Immunol Rev, 1998. **163**: p. 59-76.
124. Jefferis, R., *Recombinant antibody therapeutics: the impact of glycosylation on mechanisms of action.* Trends Pharmacol Sci, 2009. **30**(7): p. 356-62.
125. Sazinsky, S.L., et al., *Aglycosylated immunoglobulin G1 variants productively engage activating Fc receptors.* Proc Natl Acad Sci U S A, 2008. **105**(51): p. 20167-72.
126. Jung, S.T., et al., *Effective Phagocytosis of Low Her2 Tumor Cell Lines with Engineered, Aglycosylated IgG Displaying High FcgammaRIIa Affinity and Selectivity.* ACS Chem Biol, 2012.
127. Braakman, I. and N.J. Bulleid, *Protein folding and modification in the mammalian endoplasmic reticulum.* Annu Rev Biochem, 2011. **80**: p. 71-99.
128. Yuan, S., et al., *The role of thioredoxin and disulfide isomerase in the expression of the snake venom thrombin-like enzyme calobin in Escherichia coli BL21 (DE3).* Protein Expr Purif, 2004. **38**(1): p. 51-60.
129. Clark, M., *Antibody humanization: a case of the 'Emperor's new clothes'?* Immunol Today, 2000. **21**(8): p. 397-402.
130. Boulianne, G.L., N. Hozumi, and M.J. Shulman, *Production of functional chimaeric mouse/human antibody.* Nature, 1984. **312**(5995): p. 643-6.

131. Morrison, S.L., et al., *Chimeric human antibody molecules: mouse antigen-binding domains with human constant region domains.* Proc Natl Acad Sci U S A, 1984. **81**(21): p. 6851-5.
132. Koch, H., et al., *Direct selection of antibodies from complex libraries with the protein fragment complementation assay.* J Mol Biol, 2006. **357**(2): p. 427-41.
133. der Maur, A.A., et al., *Direct in vivo screening of intrabody libraries constructed on a highly stable single-chain framework.* J Biol Chem, 2002. **277**(47): p. 45075-85.
134. Jermutus, L., et al., *Tailoring in vitro evolution for protein affinity or stability.* Proc Natl Acad Sci U S A, 2001. **98**(1): p. 75-80.
135. Jefferis, R., *Glycosylation of recombinant antibody therapeutics.* Biotechnol Prog, 2005. **21**(1): p. 11-6.
136. Schaefer, J.V. and A. Pluckthun, *Transfer of engineered biophysical properties between different antibody formats and expression systems.* Protein Eng Des Sel, 2012. **25**(10): p. 485-506.
137. van Stelten, J., et al., *Effects of antibiotics and a proto-oncogene homolog on destruction of protein translocator SecY.* Science, 2009. **325**(5941): p. 753-6.
138. Chan, C.E., et al., *Optimized expression of full-length IgG1 antibody in a common E. coli strain.* PLoS One, 2010. **5**(4): p. e10261.
139. Makino, T., et al., *Comprehensive engineering of Escherichia coli for enhanced expression of IgG antibodies.* Metab Eng, 2011. **13**(2): p. 241-51.
140. Better, M., et al., *Escherichia coli secretion of an active chimeric antibody fragment.* Science, 1988. **240**(4855): p. 1041-3.
141. Kearney, J.F., et al., *A new mouse myeloma cell line that has lost immunoglobulin expression but permits the construction of antibody-secreting hybrid cell lines.* J Immunol, 1979. **123**(4): p. 1548-50.
142. Kabat, E.A., et al., *Sequences of proteins of immunological interest* 1992. **1**.
143. Chen, G., et al., *In vitro scanning saturation mutagenesis of all the specificity determining residues in an antibody binding site.* Protein Eng, 1999. **12**(4): p. 349-56.
144. Spadiut, O., et al., *Microbials for the production of monoclonal antibodies and antibody fragments.* Trends in biotechnology, 2014. **32**(1): p. 54-60.
145. Rakestraw, J.A., et al., *Secretion-and-capture cell-surface display for selection of target-binding proteins.* Protein engineering, design & selection : PEDS, 2011. **24**(6): p. 525-530.
146. Rhiel, L., et al., *REAL-Select: full-length antibody display and library screening by surface capture on yeast cells.* PloS one, 2014. **9**(12).
147. Rocco, M.A., D. Waraho-Zhmayev, and M.P. DeLisa, *Twin-arginine translocase mutations that suppress folding quality control and permit export of misfolded substrate proteins.* Proceedings of the National Academy of Sciences of the United States of America, 2012. **109**(33): p. 13392-13397.
148. Remy, I., I.A. Wilson, and S.W. Michnick, *Erythropoietin receptor activation by a ligand-induced conformation change.* Science, 1999. **283**(5404): p. 990-993.

149. Koch, H., et al., *Direct selection of antibodies from complex libraries with the protein fragment complementation assay.* Journal of molecular biology, 2006. **357**(2): p. 427-441.
150. Löfdahl, P.-A.A. and P.-A.A. Nygren, *Affinity maturation of a TNFalpha-binding affibody molecule by Darwinian survival selection.* Biotechnology and applied biochemistry, 2010. **55**(3): p. 111-120.
151. Shaw, W.V., *The enzymatic acetylation of chloramphenicol by extracts of R factor-resistant Escherichia coli.* The Journal of biological chemistry, 1967. **242**(4): p. 687-693.
152. Röttig, A. and A. Steinbüchel, *Acyltransferases in bacteria.* Microbiology and molecular biology reviews : MMBR, 2013. **77**(2): p. 277-321.
153. Biswas, T., et al., *The structural basis for substrate versatility of chloramphenicol acetyltransferase CATI.* Protein science : a publication of the Protein Society, 2012. **21**(4): p. 520-530.
154. Fujiwara, K., et al., *A Single-Chain Antibody/Epitope System for Functional Analysis of Protein−Protein Interactions†.* Biochemistry, 2002. **41**(42): p. 12729-12738.
155. der Maur, A.A., et al., *Direct in vivo screening of intrabody libraries constructed on a highly stable single-chain framework.* The Journal of biological chemistry, 2002. **277**(47): p. 45075-45085.
156. Cristóbal, S., et al., *Competition between Sec- and TAT-dependent protein translocation in Escherichia coli.* The EMBO journal, 1999. **18**(11): p. 2982-2990.
157. DeLisa, M.P., D. Tullman, and G. Georgiou, *Folding quality control in the export of proteins by the bacterial twin-arginine translocation pathway.* Proceedings of the National Academy of Sciences of the United States of America, 2003. **100**(10): p. 6115-6120.
158. Rodrigue, A., et al., *Co-translocation of a periplasmic enzyme complex by a hitchhiker mechanism through the bacterial tat pathway.* The Journal of biological chemistry, 1999. **274**(19): p. 13223-13228.
159. Mahon, C.M., et al., *Comprehensive Interrogation of a Minimalist Synthetic CDR-H3 Library and Its Ability to Generate Antibodies with Therapeutic Potential.* Journal of Molecular Biology, 2013. **425**(10): p. 1712-1730.
160. Chothia, C. and A.M. Lesk, *Canonical structures for the hypervariable regions of immunoglobulins.* Journal of molecular biology, 1987. **196**(4): p. 901-917.
161. Chothia, C., et al., *Domain association in immunoglobulin molecules. The packing of variable domains.* Journal of molecular biology, 1985. **186**(3): p. 651-663.
162. Padlan, E.A., *Anatomy of the antibody molecule.* Molecular immunology, 1994. **31**(3): p. 169-217.
163. Kabat, E.A., et al., *Sequences of proteins of immunological interest.* Sequences of proteins of immunological interest, 1992.
164. Lee, H.-C., et al., *An engineered genetic selection for ternary protein complexes inspired by a natural three-component hitchhiker mechanism.* Scientific Reports, 2014. **4**(1): p. 7570.

165. Guzman, L.M., et al., *Tight regulation, modulation, and high-level expression by vectors containing the arabinose PBAD promoter.* Journal of bacteriology, 1995. **177**(14): p. 4121-4130.
166. Pelletier, J.N., F.X. Campbell-Valois, and S.W. Michnick, *Oligomerization domain-directed reassembly of active dihydrofolate reductase from rationally designed fragments.* Proceedings of the National Academy of Sciences, 1998. **95**(21): p. 12141-12146.
167. Tarassov, K., et al., *An in vivo map of the yeast protein interactome.* …, 2008.
168. Remy, I. and S.W. Michnick, *Application of protein-fragment complementation assays in cell biology.* BioTechniques, 2007. **42**(2).
169. Amstutz, P., et al., *Rapid selection of specific MAP kinase-binders from designed ankyrin repeat protein libraries.* Protein Engineering, Design and Selection, 2006. **19**(5): p. 219-229.
170. Remy, I., F.X. Campbell-Valois, and S.W. Michnick, *Detection of protein-protein interactions using a simple survival protein-fragment complementation assay based on the enzyme dihydrofolate reductase.* Nature protocols, 2007. **2**(9): p. 2120-2125.
171. Priestman, M.A., et al., *Interaction of phosphonate analogues of the tetrahedral reaction intermediate with 5-enolpyruvylshikimate-3-phosphate synthase in atomic detail.* Biochemistry, 2005. **44**(9): p. 3241-3248.
172. Schönbrunn, E., et al., *Interaction of the herbicide glyphosate with its target enzyme 5-enolpyruvylshikimate 3-phosphate synthase in atomic detail.* Proceedings of the National Academy of Sciences of the United States of America, 2001. **98**(4): p. 1376-1380.
173. Stallings, W.C., et al., *Structure and topological symmetry of the glyphosate target 5-enolpyruvylshikimate-3-phosphate synthase: a distinctive protein fold.* Proceedings of the National Academy of Sciences, 1991. **88**(11): p. 5046-5050.
174. Eschenburg, S., et al., *How the mutation glycine96 to alanine confers glyphosate insensitivity to 5-enolpyruvyl shikimate-3-phosphate synthase from Escherichia coli.* Planta, 2002. **216**(1): p. 129-135.
175. Rogers, S.G., et al., *Amplification of the aroA gene from Escherichia coli results in tolerance to the herbicide glyphosate.* Applied and environmental microbiology, 1983. **46**(1): p. 37-43.
176. Roberts, F., et al., *Evidence for the shikimate pathway in apicomplexan parasites.* Nature, 1998. **393**(6687): p. 801-805.
177. Zhou, M., et al., *Identification of a Glyphosate-Resistant Mutant of Rice 5-Enolpyruvylshikimate 3-Phosphate Synthase Using a Directed Evolution Strategy.* Plant Physiology, 2006. **140**(1): p. 184-195.
178. Schulz, A., D. Sost, and N. Amrhein, *Insensitivity of 5-enolpyruvylshikimic acid-3-phosphate synthase to glyphosate confers resistance to this herbicide in a strain of Aerobacter aerogenes.* Archives of microbiology, 1984.
179. Chen, L., S. Pradhan, and T.C. Evans, *Herbicide resistance from a divided EPSPS protein: the split Synechocystis DnaE intein as an in vivo affinity domain.* Gene, 2001. **263**(1-2): p. 39-48.

180. Dai, X., M. Zhu, and Y.-P. Wang, *Circular permutation of E. coli EPSP synthase: increased inhibitor resistance, improved catalytic activity, and an indicator for protein fragment complementation.* Chemical Communications, 2013. **50**(15): p. 1830-1832.
181. Dun, B.-Q., et al., *Reconstitution of Glyphosate Resistance from a Split 5-Enolpyruvyl Shikimate-3-Phosphate Synthase Gene in Escherichia coli and Transgenic Tobacco.* Applied and Environmental Microbiology, 2007. **73**(24): p. 7997-8000.
182. Joyce, A.R., et al., *Experimental and computational assessment of conditionally essential genes in Escherichia coli.* Journal of bacteriology, 2006. **188**(23): p. 8259-8271.
183. Patrick, W.M., et al., *Multicopy suppression underpins metabolic evolvability.* Molecular biology and evolution, 2007. **24**(12): p. 2716-2722.
184. John, M., et al., *Two pairs of oppositely charged amino acids from Jun and Fos confer heterodimerization to GCN4 leucine zipper.* The Journal of biological chemistry, 1994. **269**(23): p. 16247-16253.
185. O'Shea, E.K., R. Rutkowski, and P.S. Kim, *Mechanism of specificity in the Fos-Jun oncoprotein heterodimer.* Cell, 1992. **68**(4): p. 699-708.
186. O'Shea, E.K., et al., *Preferential heterodimer formation by isolated leucine zippers from fos and jun.* Science (New York, N.Y.), 1989. **245**(4918): p. 646-648.
187. Wehrman, T., et al., *Protein-protein interactions monitored in mammalian cells via complementation of beta -lactamase enzyme fragments.* Proceedings of the National Academy of Sciences of the United States of America, 2002. **99**(6): p. 3469-3474.
188. Pelletier, J.N., et al., *An in vivo library-versus-library selection of optimized protein-protein interactions.* Nature biotechnology, 1999. **17**(7): p. 683-690.
189. Makino, T., et al., *Comprehensive engineering of Escherichia coli for enhanced expression of IgG antibodies.* Metabolic Engineering, 2011. **13**(2): p. 241-251.
190. Lee, Y., D. Lee, and K. Jeong, *Enhanced production of human full-length immunoglobulin G1 in the periplasm of Escherichia coli.* Applied Microbiology and Biotechnology, 2014. **98**(3): p. 1237-1246.
191. Simmons, L.C. and D.G. Yansura, *Translational level is a critical factor for the secretion of heterologous proteins in Escherichia coli.* Nature biotechnology, 1996. **14**(5): p. 629-634.
192. Griffiths, A.D., et al., *Isolation of high affinity human antibodies directly from large synthetic repertoires.* The EMBO journal, 1994. **13**(14): p. 3245-3260.
193. Nissim, A., et al., *Antibody fragments from a 'single pot' phage display library as immunochemical reagents.* The EMBO journal, 1994. **13**(3): p. 692-698.
194. Philibert, P., et al., *A focused antibody library for selecting scFvs expressed at high levels in the cytoplasm.* BMC Biotechnology, 2007. **7**(1): p. 1-17.
195. Teeling, J.L., et al., *The biological activity of human CD20 monoclonal antibodies is linked to unique epitopes on CD20.* Journal of immunology (Baltimore, Md. : 1950), 2006. **177**(1): p. 362-371.

196. Habibi Anbouhi, M., et al., *Functional recombinant extra membrane loop of human CD20, an alternative of the full length CD20 antigen.* Iranian biomedical journal, 2012. **16**(3): p. 121-126.
197. Sui, J., et al., *Structural and functional bases for broad-spectrum neutralization of avian and human influenza A viruses.* Nature structural & molecular biology, 2009. **16**(3): p. 265-273.
198. Ekiert, D.C., et al., *Antibody recognition of a highly conserved influenza virus epitope.* Science (New York, N.Y.), 2009. **324**(5924): p. 246-251.
199. Inoue, Y., et al., *Induction of anti-influenza immunity by modified green fluorescent protein (GFP) carrying hemagglutinin-derived epitope structure.* The Journal of biological chemistry, 2013. **288**(7): p. 4981-4990.